Vapor-Liquid Equilibrium and Thermodynamic Property Estimation of CO_2 - alkanolamines - water System using Molecular Modeling and Validation with Experiments

A Thesis Submitted in Partial Fulfillment

of the Award of the Degree

Of

MASTER OF TECHNOLOGY (Research)

In

CHEMICAL ENGINEERING

By

SHIVANI

(610CH305)

Under the guidance of

Prof. MADHUSREE KUNDU

Chemical Engineering Department

National Institute of Technology

Rourkela 769008

JUNE 2013

Dedication

To my Parents

Department of Chemical Engineering

National Institute of Technology

Rourkela 769008 (ORISSA)

CERTIFICATE

This is to certify that the thesis entitled "**Vapor-Liquid Equilibrium and Thermodynamic Property Estimation of (CO_2 - alkanolamines - water) System using Molecular Modeling and Validation with Experiments**", being submitted by **Shivani** for the award of **Master of Technology by Research** is a record of bonafide research carried out by her at the Chemical Engineering Department, National Institute of Technology, Rourkela, under my guidance and supervision. The matter embodies original work done by her under my supervision.

Prof. Madhusree Kundu

Department of Chemical Engineering

National Institute of Technology, Rourkela

ACKNOWLEDGEMENT

I take this opportunity to express my respect and sincere gratitude to my thesis supervisor, Prof. Madhusree Kundu, for giving me an opportunity to work under her supervision for my M.Tech (Research) degree at the National Institute of Technology, Rourkela. I am indebted to Prof. Madhusree Kundu for her valuable guidance and for instilling in me a relentless quest for perfection. Some of her remarkable qualities, such as her depth of perception and her lucid presentation, perhaps the best I have come across so far, will always continue to inspire me. The experience of working with her, I strongly believe, will have far-reaching influence in my future life.

I would like offer my thanks to Prof. R. K. Singh, HOD of our department for his guidance and support during his tenure.

And grateful acknowledgement is made to members of Masters Scrutiny Committee (MSC) and all the staff and faculty members of Chemical Engineering Department, National Institute of Technology, Rourkela for their consistent encouragement and support.

I am also thankful for all the support that I had received from Mr. Gaurav Kumar as my senior. I also would like to thank all my friends who encouraged me in every aspect during the project.

I am indebted to F. Eckert and A. Klamt, COSMOtherm, Version C2.1, Release 01.10; COSMOlogic GmbH & Co. KG, Leverkusen, Germany, 2009 and Sonali Ghosh from Aspara Innovations for their support in the completion of my thesis.

Finally, I am forever indebted to my parents for their understanding, endless patience and encouragement from the beginning.

SHIVANI

National Institute of Technology, Rourkela

ABSTRACT

The study of phase equilibrium thermodynamics of (CO_2 + alkanolamine + H_2O) system is of immense significance in the context of energy efficient capture of CO_2, the most alarming green- house gas in the atmosphere. Among the various methodologies available so far absorption in alkanolamine solvent is currently in use. However, alkanolamines as solvent have certain drawbacks such as solvent loss due to volatility and high regeneration costs due to the high water content, which has driven researchers for new and alternative technologies. Recently room temperature ionic liquids (ILs'); called green solvents are emerging as promising candidates to capture CO_2 due to their wide liquid range, low melting point, tunable properties, negligible vapor pressure, high CO_2 solubility and reasonable thermal stability. But it is difficult to realize practically owing to its high viscous and high cost, which left us so far with the alkanolamine-CO_2 technology. There is a rejuvenation of interest for newer alkanolamine formulation. In view of this, present thesis aimed towards the generation of new vapor-liquid equilibrium data on ($EAE + CO_2 + H_2O$) system along with the generation of density data on aqueous ($EAE + AMP$) and ($EAE + MDEA$) blends. The physicochemical data are considered to be a very important contribution towards the design database of gas treating process.

A priori prediction of the thermodynamic behavior of mixtures is industrially important problem. Engineers and scientists usually refer excess Gibbs energy models for vapor- liquid equilibria calculations such as WILSON, NRTL, UNIQUAC, and UNIFAC. In order to describe the thermodynamics for mixtures, these methods compute the activity coefficient of the compounds using the information on binary interaction parameters that are derived from experimental results. Thus these models have limited applicability in thermodynamics properties and VLE prediction for the new systems that have no experimental data. For solution of this problem, Solvation thermodynamics models based on computational quantum mechanics, such as the Conductor – like Screening Model (COSMO), provide a good alternative to traditional group-contribution and activity coefficient methods for predicting thermodynamic phase behavior. The major molecule-specific COSMO model is based on surface charge density sigma profile, which is computed by quantum mechanics using DFT/TZVP (density functional theory/triple zeta polarized valence) approach. Present work

also aims for molecular simulation of thermodynamic properties of aqueous EAE solutions. Phase equilibrium of ($EAE + H_2O$) and ($EAE + CO_2 + H_2O$) solutions were simulated using COSMOtherm software (based on COSMO and COSMO-RS; a variant of the dielectric continuum solvation model).

CONTENTS

LIST OF FIGURES

LIST OF TABLES

ABBREVIATIONS

CO_2	Carbon Dioxide
COS	Carbonyl Sulphide
H_2S	Hydrogen Sulphide
PZ	Piperazine
2-PE	2-Piperidineethanol
AHPD	2-Amino-2-Hydroxymethyl-1, 3-Propanediol
MEA	Monoethanolamine
DEA	Diethanolamine
MDEA	N-Methyl-Diethanolamine
DIPA	Diisopropanolamine
MAE	2-Methyl- Amino ethanol
EAE	2-Ethyl- Amino ethanol
AMP	2- amino- 2- methyl - 1- propanol
DGA	2-(2-Aminoethoxy) Ethanol
DIPA	Diisopropanolamine
TEA	Triethanolamine
TSP	Trisodium Phosphate
ILs'	Ionic Liquids
COSMO	Conductor – like Screening Model
COSMO-RS	Conductor – like Screening Model for Real Solvent
AM1	Austin Model 1
PBE	Perdew-Burke-Ernzerhof
BP	Becke-Perdew
TZVP	Triple Zeta Polarized Valence
SVP	Split Valence Plus Polarization Function
DFT	Density Functional Theory
MM	Molecular Mechanics
SE	Semi-Empirical
MD	Molecular Dynamics

QM	Quantum Mechanics
LDA	Local Density Approximation
CGTO	Contracted Gaussian Type Orbital
SCRF	Self-Consistent Reaction Field Models
VLE	Vapor liquid equilibrium

NOMENCLATURE

μ	Chemical potential
f	Fugacity
ΔG , dG	Gibbs free energy
H	Planck' s constant
V	Force functioning on a particle
Ψ	Wave perform
∇^2	Operator describes the behavior of the wave perform with position
E	State energy of the particle or the system
m	Mass of the particle being delineate
E^T	Electronic energy depends on kinetic energy from electronic motion
E^V	Potential energy of electron nuclear attraction and repulsion of nuclei pairs
E^J	Electronic repulsion
E^{XC}	Exchange correlation terms which will take into consideration the non-counted electronic interaction
P	Electronic density
$\emptyset_i$	i-th molecular orbital
$C_{\mu i}$	Molecular expansion coefficient
X_μ	μ-th atomic orbital also known as arbitrary basis function
n	Number of atomic orbitals
σ	Charge density
ε	Dielectric screening constant for the solute
E	Total electrostatic field from the solute and polarized charges
σ^*	Ideal screening charge density
E_{misfit}	Electrostatic interaction energy
a_{eff}	Effective area of contact between two solute molecules

	surface segments
$\sigma,\ \sigma'$	Surface screening charge densities for solute molecules
$\mu_{S\,(\sigma)}$	Sigma potential
$P^{Xi}(\sigma)$	Sigma profile of compound X
$n_i\,(\sigma)$	Number of divided segments that has surface charge density (σ)
$A_i\,(\sigma)$	Segments surface area that has charge density σ
A_i	Area of the whole surface cavity that is embedded is the medium
P_s	Sigma profile of the whole mixture
σ_i	Surface charge density
$\tau_{vdW}\,,\tau'_{vdW}$	Van der Waals interaction parameter
E_{HB}	Hydrogen bonding energy
c_{HB}	Adjustable parameter used for hydrogen bond strength
σ_{HB}	Adjustable parameter for hydrogen bonding threshold
σ_{donor}	Screening charge density for hydrogen bond donor surface area
$\sigma_{acceptor}$	Screening charge density for hydrogen bond acceptor surface area
E_{gas}^{Xi}	Total energy of the molecule in the gas phase computed by quantum mechanics
E_{COSMO}^{Xi}	Total COSMO energy of the molecule in solution computed by solvation model using quantum mechanics
E_{vdW}^{Xi}	Van der Waals energy of the molecule
μ_{gas}^{Xi}	Chemical potential of pure compound in ideal gas
k	Boltzmann constant
T	Temperature in K
γ_S^{Xi}	Activity coefficients of the compound i as predicted by COSMOtherm.
μ_S^{Xi}	Chemical potential in the Solvent S
μ_{Xi}^{Xi}	Chemical potential of the pure compound

R	Ideal gas constant
P^{tot}	Total pressure of the mixture
P_{vap}^{Xi}	Vapor pressure of pure compound i
X_i	Mole fractions in the liquid phase
y_i	Mole fractions in the gas phase
P_{CO_2}	Equilibrium pressure
P_t	Total pressure of cell
P_v	Vapor pressure
V_{jk}^E	Excess molar volume for a binary solvent system
V^E	Excess molar volume
V_i^0	Molar volume of the pure fluids at the system temperature
V_m	Molar volume of the liquid mixture
M_i	Molar mass of pure component i
ρ_m	Measured liquid Density
x_i	Mole fraction of pure component i

Chapter 1

Introduction

INTRODUCTION

1.1 MOTIVATION

An acid gas stream is a stream of gas that contains significant amounts of acidic gases such as carbon dioxide (CO_2), carbonyl sulphide (COS), and hydrogen sulphide (H_2S). Removal of above acid gas impurities from gas streams is a very important operation for natural gas processing, oil refineries, ammonia manufacturing units, gasification of coal, and petrochemical plants. The process of removal of acid gases from gas streams is commonly referred as acid gas treating and also as gas sweetening. CO_2 being a green-house gas, its sequestration has drawn the attention of researcher community. In view of this, study of vapor-liquid equilibrium and thermodynamic property estimation of (CO_2 + alkanolamine + H_2O) system is of immense significance.

Among the different technologies available for CO_2 mitigation, capture of CO_2 by chemical absorption is the technology that is mature one and closed to get implemented commercially. Exploration of newer solvent has always been an agenda in gas trading. A recent range of alkanolamines including Piperazine (PZ), 2-piperidineethanol (2-PE), 2-amino-2-hydroxymethyl-1, 3-propanediol (AHPD), 2-methyl-amino ethanol (MAE) and 2-ethyl-amino ethanol (EAE) have been proposed for CO_2 capture.

The priori prediction of the thermodynamic behavior of mixtures is industrially important problem. Engineers and scientists usually refer to excess Gibbs energy models for vapor- liquid equilibria calculations such as WILSON (Wilson, 1964), NRTL (Renon and Prausnitz, 1968), UNIQUAC (Abrams and Prausnitz, 1975), UNIFAC (Fredenslund et al, 1975). In order to describe the thermodynamics for mixtures, these methods compute the activity coefficient of the compounds using the information on binary interaction parameters that are derived from experimental results. Thus these models have limited applicability in thermodynamic properties and Vapor liquid equilibrium (VLE) prediction for the new systems that have no experimental data. For solution of this problem, Solvation thermodynamics models based on computational quantum mechanics, such as the Conductor – like Screening Model (COSMO) (Klamt and Schuurmaan, 1993), provide a good

alternative to traditional group-contribution and activity coefficient methods for predicting thermodynamic phase behavior. The major molecule-specific COSMO model is based on surface charge density sigma profile, which is computed by quantum mechanics using Density functional theory/Triple zeta polarized valence (DFT/TZVP) approach. Klamt (1995) proposed a completely new perspective in liquid-phase thermodynamics. Klamt developed a Conductor – like Screening Model for Real Solvent (COSMO-RS), which can be used to determine the chemical potential of any species in any mixture from quantum chemical calculation and statistical thermodynamics.

In the aforesaid perspective, present thesis aimed towards the generation of new vapor-liquid equilibrium (VLE) data for aqueous 2-ethyl-amino ethanol (EAE) solutions. This thesis also aims for molecular simulation of thermodynamic properties of aqueous alkanolamine solutions with a special mention to EAE. VLE of CO_2 in aqueous EAE solutions were simulated using COSMO and compared with our own experimental data. Density of aqueous blends of EAE+MDEA and EAE+AMP were generated in this work keeping in view of the immense significance of physicochemical properties in design of gas treating processes.

1.2 OVERVIEW OF CO_2 REMOVAL PROCESS

A wide range of separation techniques have been developed for the removal of acid gases: absorption into physical or chemical solvents (Astarita, 1983; Danckwerts, 1970), adsorption on activated carbon (Kapoor and Yang, 1989; Kohl and Riesenfield, 1985; Astarita, 1983), cryogenic distillation (Astarita, 1983), membrane separation process (Davis, 1992; Weber and Bowman, 1986; Schell, 1983), absorption in ionic liquids (Camper et al., 2008; Ahmady et al., 2011) and salts of tertiary amino acids promoted with reactive amines (Wagner et al., 2009; Weiland and Hatcher, 2011). Among these, most widely practiced techniques for the removal of CO_2, absorption into physical solvents or chemical solvents, and hybrid solvents (blends of chemical and physical solvents) are the major ones.

1.2.1 Major Alkanolamines

Today approximately 90% of the acid gas treating processes uses alkanolamine solvents for the CO_2 removal because of the versatility and ability of these solvents to remove acid gases

to very low levels. Alkanolamines are divided into three major categories; primary, secondary and tertiary. The most commonly used alkanolamines are the primary amine monoethanolamine (MEA), the secondary amines diethanolamine (DEA), and diisopropanolamine (DIPA) and the tertiary amine N-methyl-diethanolamine (MDEA). One important class of amines is the steric ally hindered amines, e.g., 2- amino- 2- methyl - 1- propanol (AMP), 2-methyl-amino ethanol (MAE) and 2-ethyl-amino ethanol (EAE).

1.2.2 Characteristics of solvents

The water solubility of alkanolamine solvents is a function of the molecular structure. The larger the number of hydroxyl groups, the higher is the water solubility of the solvent and lower the vapor pressure of the alkanolamine. The presence of more aliphatic groups tends to raise hydrocarbon solubility and lower water solubility (Butwell et al., 1982).The amine group in the solvent molecules provides the basicity. The stoichiometric loading of primary and secondary alkanolamines is 0.5 moles of CO_2 per mole of alkanolamine (Kundu, M., Mandal, B.P. and Bandyopadhyay, S.S., 2003). On reaction with CO_2 they form stable carbamate apart from the formation of bicarbonate. Unlike the primary and secondary alkanolamines, the CO_2 absorption into MDEA can reach 1 mole CO_2 per mole of amine. While the high CO_2 loading in MDEA is very attractive, the low rates of absorption of CO_2 in tertiary alkanolamines may limit their use because of the high cost of MDEA relative to MEA and DEA. Aqueous solutions of tertiary alkanolamines promote the hydrolysis of CO_2 to form bicarbonate and protonated alkanolamine. Alkanolamine promoted hydrolysis reactions is much slower than the direct reaction of primary and secondary amines with CO_2 and therefore kinetic selectivity of tertiary amines towards CO_2 is poor. MDEA is kinetically selective for H_2S in the presence of CO_2. The heat of reaction associated with the formation of bicarbonate ion is much lower than that associated with carbamate formation (Kundu, M., 2004). Thus regeneration cost for tertiary amines are lower than for primary and secondary amines. Sterically hindered amines, e.g., 2- amino- 2- methyl - 1- propanol (AMP), 2-methyl amino ethanol (MAE) and 2- ethyl- amino ethanol (EAE), are said to approach the stoichiometric loading of 1 mole CO_2 per mole of amine combined with the absorption rate characteristic of primary and secondary amines. This high loading is obtained by destabilizing the carbamate due to the presence of bulky substituent next to the nitrogen atom of the amine group. Sterically hindered amines have the advantage of exhibiting highly

reversible kinetics with CO_2 and thus requiring less energy for regeneration. Besides saving energy and capital in gas treating processes significantly, the hindered amines have much better stability than conventional amines, since hindered amines have low degradation.

1.3 MOLECULAR MODELLING

Molecular modelling encompasses all theoretical methods and computational techniques, which are used to model the behavior of molecules. Molecular simulation based on quantum mechanics calculation is attractive alternative to conventional engineering modeling techniques. Molecular simulation strategies give an intermediate layer between direct experimental measurements and engineering models (as shown in Figure (1.1)). Molecular simulation method can provide results applicable over wider ranges of process conditions because of the fewer approximations that are made during computation. The prediction of thermodynamic property starts with quantum theory and solvation model. Firstly, the Schrodinger equation is solved by using Density Functional Theory (DFT) with an appropriate basis set, and then the COSMO model is applied to predict the sigma profile. COSMO for real solvent proposed by (Klamt, 1995) can be used to determine the chemical potential of any species in any mixture from quantum mechanical calculations. The extension to real solvent (RS) is a statistical thermodynamic approach based on the results of quantum chemical calculations. In COSMO calculations, the solute molecules are assumed to be in a virtual conductor environment, where the solute molecule induces a polarization charge density $\boldsymbol{\sigma}$ on the interface between the molecule and the conductor, that is, on the molecular surface. These charges act back on the solute and generate a more polarized electron density than in vacuum. During the quantum chemical self-consistency cycle, the solute molecule is thus converged to its energetically optimal state in a conductor with respect to electron density, and the molecular geometry can be optimized using conventional methods for calculations in vacuum. Although time consuming, one advantage of this procedure is that the quantum chemical calculations have to be performed just once for each molecule of interest. The calculation of multi component phase equilibria needs a wide variety of simulation and still a target to be achieved.

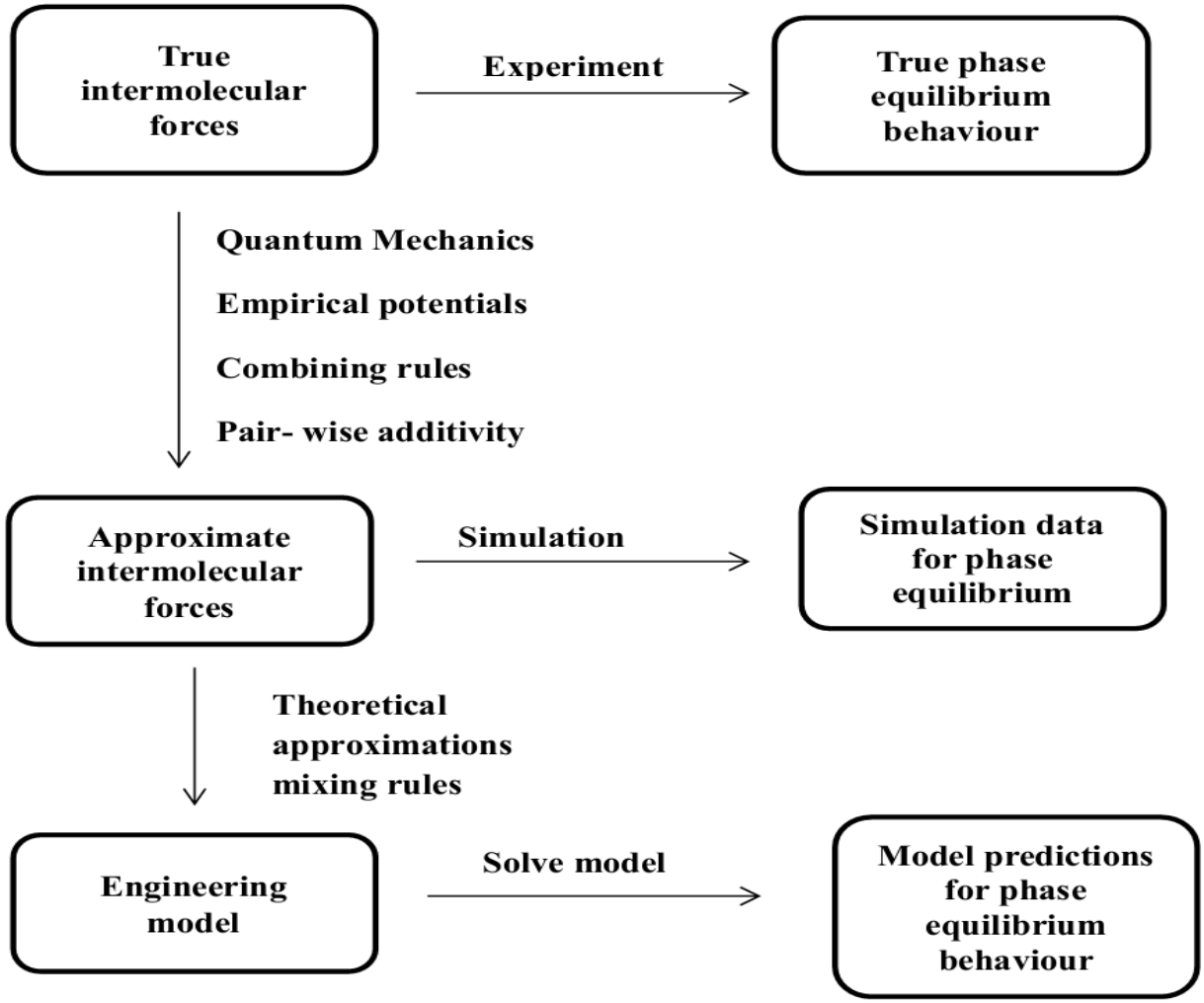

Figure 1.1: Relationships between engineering and molecular simulation-based predictions of phase equilibria.

1.4 OBJECTIVES OF THE PRESENT WORK

EAE is a very recently proposed alkanolamine, which have drawn attention to the researchers to get acceptance as a potential solvent for CO_2 removal. In view of this, following are the objectives of the present thesis:

- Generation of new VLE data of CO_2 over 2-ethyl-amino ethanol (EAE) solutions.
- Evaluation of thermodynamic properties of aqueous solutions of MEA, DEA, MDEA, MAE, EAE and AMP solutions using COSMO.
- Evaluation of thermodynamic properties of $(CO_2 + EAE + H_2O)$ system.

- Simulation of VLE of CO_2 in aqueous single alkanolamine solution of EAE using COSMO and validation using the experimental data.
- Generation of new density data of $(EAE + MDEA + H_2O)$ and $(EAE + AMP + H_2O)$ system.

1.5 THESIS ORGANIZATION

The thesis is organized into the following chapters:

- **Chapter 1** presents the background, objective, and outline of the thesis.
- **Chapter 2** presents a brief overview of basic chemistry of CO_2- alkanolamines system with thermodynamics of alkanolamines water system. It also presents perspective of the present work so far VLE and density data generation is concerned.
- **Chapter 3** covers molecular modeling theory, computational procedure and applicability of COSMO-RS.
- **Chapter 4** covers the COSMO-RS (Conductor like screening model for real solvents) prediction of thermodynamic properties of binary alkanolamine systems: $(MEA + H_2O)$, $(MDEA + H_2O)$, $(AMP + H_2O)$, $(MAE + H_2O)$, and $(EAE + H_2O)$.
- **Chapter 5** reports the experimental results on VLE of $(CO_2 + EAE + H_2O)$ system. COSMO predictions of VLE and thermodynamic properties of $(CO_2 + EAE + H_2O)$ system.
- **Chapter 6** is devoted to density data generation of $2-\text{ethyl}-\text{amino ethanol (EAE)} + \text{N}-\text{methyl}-\text{diethanolamine (MDEA)}$ and $2-\text{ethyl}-\text{amino ethanol (EAE)} + 2-\text{amino}-2-\text{methyl}-1-$ propanol (AMP) systems and their correlation with Redlich-Kister equation.
- **Chapter 7** In an ending note chapter 7 Concludes the thesis with future recommendations.

REFERENCES

- Abrams D. S. and Prausnitz J. M., "Statistical thermodynamics of liquid mixtures: A new expression for the excess Gibbs energy of partly or completely miscible systems", American Institute of Chemical Engineers Journal; 21, 116–128, 1975.
- Ahmady, A., Hashim, M.A. and Aroua, M.K., "Absorption of carbon dioxide in the aqueous mixtures of methyldiethanolamine with three types of imidazolium-based ionic liquids", Fluid Phase Equilibria; 309, 76-82, 2011.
- Astarita, G., Savage. D.W. and Bisio, A., "Gas treating with chemical solvents", John Wiley and Sons, New York; 1983.
- Butwell, K. F., Kubek, D. J. and Sigmund, P. W., "Alkanolamine treating", Hydrocarbon Process; 61, 108-116, 1982.
- Camper, D., Bara, J. E., Gin, D.L. and Nobel, R.D., "Room-Temperature Ionic Liquid-Amine Solutions: Tunable Solvents for Efficient and Reversible Capture of CO_2", Industrial and Engineering Chemistry Research; 47, 8496–8498, 2008.
- Danckwerts, P.V. "Gas Liquid Reactions", MacGraw- Hill, New York; 1970.
- Davis, A., "The separation of carbon dioxide from methane by facilitated transport in liquid membranes", Ph.D. Dissertation. University of California, Santa Barbara; 1992.
- Fredenslund, A., Jones, R. L. and Prausnitz, J. M., "Group-contribution estimation of activity coefficients in non-ideal liquid mixtures", American Institute of Chemical Engineers Journal; 21, 1086, 1975.
- Kapoor, A., and Yang, R.T., "Kinetic separation of methane-carbon dioxide mixture by absorption on molecular sieve carbon", Chemical Engineering Science; 44, 1723-1733, 1989.
- Klamt, A. and Schüürmann, G., "COSMO: A New Approach to Dielectric Screening in Solvents with Explicit Expression for the Screening Energy and its Gradients", Journal of the Chemical Society, Perkin Trans; 2, 799-805, 1993.
- Klamt, A., "Conductor like screening model for real solvents: A new approach to the quantitative calculation of solvation phenomena", The Journal of Physical Chemistry; 99, 2224-2235, 1995.

- Kohl, A.L., and Riesenfeld, F.C., "Gas Purification", 4th ed., Gulf publishing Company, Houston; 1985.
- Kundu, M., "Vapour - Liquid Equilibrium of Carbon Dioxide in Aqueous Alkanolamines", P.hd. Thesis. Indian Institute of Technology, Kharagpur; January 2004.
- Kundu, M., Mandal, B.P. and Bandyopadhyay, S.S., "Vapor-Liquid Equilibrium of CO_2 in Aqueous Solutions of 2-Amino-2-methyl-1-propanol; 48, 789-796, 2003.
- Renon, H. and Prausnitz, J. M., "Local composition in thermodynamic excess functions for liquid mixtures", American Institute of Chemical Engineers Journal; 14, 135-144, 1968.
- Schell, W.J., "Membrane use/technology growing", Hydrocarbon Process; 62, 43-46, 1983.
- Wagner, R., Lichtfers, U. and Schuda, V., "Removal of Carbon Dioxide from Combustion Exhaust Gases", U.S. Patent Application, US 2009/0320682 A1, Dec 31, 2009.
- Weber, W.F. and Bowman, W., "Membranes replacing other separation technologies", Chemical Engineering Progress; 82, 23 – 28, 1986.
- Weiland, R. and Hatcher, N.A., " Post- combustion CO_2 capture with Amino-Acids Salts", Paper presented at SOGAT 2011, Abu Dubai, UAE, 2011.
- Wilson, G. M., "Vapour-Liquid Equilibrium. XI. A New Expression for the Excess Free Energy of Mixing", Journal of the American Chemical Society; 86, 127-130, 1964.

Chapter 2

Basic Chemistry and thermodynamics of (CO_2 + alkanolamine + water) system with recent contributions

BASIC CHEMISTRY AND THERMOYNAMICS OF (CO_2 + ALKANOLAMINE + WATER) SYSTEM WITH RECENT CONTRIBUTIONS

This chapter is an introduction to the basic chemistry of alkanolamines and thermodynamics of aqueous alkanolamines system. It provides a brief review of the chemical reactions in the CO_2 + alkanolamine + water systems and the relations between chemical potential, fugacity, activity coefficient and excess Gibbs energy functions, especially as they are related to weak electrolyte systems. Equilibrium thermodynamics is the combination of physical vapor - liquid equilibrium (VLE) of molecular species and chemical reaction equilibrium that typically occur in aqueous alkanolamine systems.

A review of previous work on thermodynamics and vapor-liquid equilibrium of CO_2 in (alkanolamine + water) system are presented in this chapter.

2.1 BASIC CHEMISTRY OF CO_2-AQUEOUS ALKANOLAMINES

Alkanolamines, which have two hydrogen atoms directly attached to a nitrogen atom, such as monoethanolamine (MEA) and 2-(2-aminoethoxy) ethanol (DGA), are called primary alkanolamines and are generally the most alkaline. Diethanolamine (DEA) and diisopropanolamine (DIPA) have one hydrogen atom directly attached to the nitrogen atom and are called secondary alkanolamines. Triethanolamine (TEA) and *N*-methyldiethanolamine (MDEA) represent completely substituted ammonia molecules with no hydrogen atom directly attached to the nitrogen atoms, and are called tertiary alkanolamines. The amine group present in the alkanolamine provides the basicity whereas the hydroxyl group increases the solubility, thus reducing the vapor pressure of aqueous alkanolamine solutions. A hindered amine, such as 2-amino 2-methylpropanol (AMP), 2-methyl amino ethanol (MAE) and 2- ethyl amino ethanol (EAE) is defined as a primary amine in which the amino-group is attached to a tertiary carbon atom, or a secondary amine in which the amino-group is attached to at least one secondary or tertiary carbon atom (Sartori and Savage, 1983). The development of a reaction mechanism is, of course, a prerequisite to the equilibrium /

rate modelling of CO_2 with amine systems. The principal reactions occurring when a solution of an alkanolamine is used to absorb CO_2 may be represented as follows.

2.1.1 CO_2-Alkanolamine Reactions

In the aqueous phase for the $(CO_2 + \text{alkanolamine} + H_2O)$ system the following chemical reactions are involved

$$H_2O \overset{k1}{\Leftrightarrow} H^+ + OH^- \text{(Ionization of water)} \quad (2.1)$$

$$CO_2 + H_2O \overset{k2}{\Leftrightarrow} HCO_3^- + H^+ \quad \text{(Hydration of carbon dioxide)} \quad (2.2)$$

$$HCO_3^- \overset{k3}{\Leftrightarrow} H^+ + CO_3^{2-} \text{(Bicarbonate dissociation)} \quad (2.3)$$

$$RR'NH^+ \overset{k4}{\Leftrightarrow} RR'N + H^+ \text{(Amine de-protonation for EAE)} \quad (2.4)$$

$$RR'NCOO^- \overset{k5}{\Leftrightarrow} RR'N + HCO_3^- \text{(Carbamate reversion for EAE)} \quad (2.5)$$

For EAE R, and R′ are C_2H_5 and CH_3CH_2OH. The equilibrium constants for reactions are in molarity (kmol.m^{-3}) scale.

2.2 THERMODYNAMIC PROPERTIES

The knowledge of thermodynamic properties and phase equilibria of CO_2 in pure and blended aqueous alkanolamines is crucial for the design of gas treating processes. In a multiphase, multi-component system, chemical equilibrium is established. When a system is out of equilibrium, mass transfer between the phases will try to establish a new equilibrium situation. The driving force for mass transfer is proportional to how far the system is from thermodynamic equilibrium. Thus the modelling of thermodynamic equilibrium is important also when we want to calculate the driving force for mass transfer. Accurate modelling of thermodynamic properties such as activity coefficient, excess Gibbs free energy, and excess enthalpy are of vital importance in VLE calculation.

2.2.1 Chemical Potential and Fugacity

Equilibrium between two phases was defined by using chemical potentials given by Gibbs. The chemical potential of a species must be stated same in the both phases

$$\mu^{\alpha} = \mu^{\beta} \tag{2.6}$$

This forms the backbone of equilibrium thermodynamics relating with the measurable quantities such as temperature and compositions. G.N. Lewis took the Gibbs – Duhem equation for a pure substance i and substitute it with ideal gas law for the partial volume term resulting the equation (2.7)

$$\mu^{i} - \mu_i^{o} = RT \ln \left(\frac{P}{P_o}\right) \tag{2.7}$$

Since the assumptions on equation (2.7) are too limiting for practical use, Lewis reformed the equation by replacing the pressure term with fugacity.

$$\mu^{i} - \mu_i^{o} = RT \ln \left(\frac{f_i}{f_o}\right) \tag{2.8}$$

Lewis further defines the fugacity ratio as activity.

$$\left(\frac{f_i}{f_o}\right) = \text{activity} = a_i \tag{2.9}$$

We can apply the equation (2.6) to obtain a new, completely general, expression of equilibrium for vapor- liquid equilibrium.

$$f_i^{\alpha} = f_i^{\beta} \tag{2.10}$$

2.2.2 Activity coefficient

The ideal solution fugacity and chemical potential are calculated from

$$f_i = x_i \times f_i^{o} \tag{2.11}$$

$$\mu_i = \mu_i^{o} + RT \ln x_i \tag{2.12}$$

We see that the fugacity of a component in the solution is a linear function of the mole fraction. The ideal solution is a conventional hypothetical state which no solution strictly follows. Real solutions are non-ideal solutions. In the non-ideal solution we can calculate the fugacity and chemical potential from

$$f_i = \gamma_i x_i \times f_i^o \tag{2.13}$$

$$\mu_i = \mu_i^o + RT \ln(\gamma_i x_i) \tag{2.14}$$

Where γ_i is the activity coefficient and is equal to 1 in case of ideal solutions. The relation between the chemical potential and the fugacity coefficient is given as,

$$\mu_i - \mu_i^{IG} = RT \ln(\varphi_i x_i) \tag{2.15}$$

Sometimes we need to calculate activity coefficients from relations for the fugacity coefficient. This will typically be the case when we use an equation of state to calculate the activity. We see that the activity coefficient with reference state pure solvent (symmetric) is given by

$$\gamma_i = \frac{\varphi_{i(T,P,x_i)}}{\varphi_{i,pure(T,P)}} \tag{2.16}$$

With a similar argumentation we can show that the activity coefficient with reference state at infinite dilution (unsymmetrical) can be calculated as

$$\gamma_i^{\infty} = \frac{\varphi_{i(T,P,x_i)}}{\varphi_{i(T,P,x_{i\to 0})}} \tag{2.17}$$

2.2.3 Chemical Equilibria

Discussion so far has concerned the thermodynamics of molecules between two phases. Chemical equilibrium is commonly expressed in two ways. The Gibbs free energy is minimized at equilibrium yielding

$$dG = \sum_{i=1}^{n} \mu_i \, dn_i = 0 \tag{2.18}$$

Where the chemical potential is expressed as

$$\mu_i = \mu_i^o + RT\ln(\gamma_i x_i) \quad (2.19)$$

A more common definition is the definition of the equilibrium constant

$$\prod_{i=1}^{n}(x_i\gamma_i)^{\nu_i} = -\frac{1}{RT}\left(\sum_{i=1}^{n}\nu_i\mu_i^0\right) = K = \exp\left(\frac{\Delta G^o}{RT}\right) \quad (2.20)$$

ΔG^o is calculated from $\mu^0$and is generally a function of temperature only. The equilibrium constant K will consequently be a function of temperature only, when defined reference state for all components are used. The activity coefficients in equation (2.19) can be calculated from liquid models like Margules, Van-Laar, Wilson, Clegg-Pitzer equation, NRTL, UNIQUAC, and UNIFAC. In the aforesaid liquid models, excess Gibbs energy is expressed as function of composition at a fixed temperature and pressure. If excess Gibbs energy is derived with respect to mole number of any i^{th} species at constant temperature, pressure and composition of other species apart from i^{th} species; results into the activity coefficient of i^{th} species. The excess Gibbs energy is defined as the Gibbs energy of a real solution, that is in excess of the Gibbs energy of an ideal solution at the same condition of temperature, pressure, and composition (Prausnitz et al., 1986). Excess Gibbs energy arises due to inequalities in inter-particle forces.

2.3 VAPOR-LIQUID EQUIBIRIUM

Among the various avenues available for efficient CO_2 removal, absorption in aqueous alkanolamine solutions is long proven and most effective so far. However, solvent loss and high regeneration costs of alkanolamines have driven researchers for new and alternative technologies. Recently room temperature ionic liquids (ILs'); are emerging as promising solvents to capture CO_2 due to their wide liquid range, low melting point, negligible vapor pressure, high CO_2 solubility and reasonable thermal stability. Sodium and Potassium salts of primary or tertiary amino acids promoted with reactive alkanolamines can be other alternative. Absorption of CO_2 in aqueous alkanolamine is very close to get implemented commercially; hence, in the present context we cannot deny the role of this technology. Alkanolamines including Piperazine (PZ), 2-piperidineethanol $(2-PE)$, 2-amino-2-hydroxymethyl-1, 3-propanediol (AHPD), 2-methyl-amino ethanol (MAE) and 2-ethyl-amino ethanol (EAE) have been recently proposed as possible potential solvents.

Equilibrium solubility of the acid gases in aqueous alkanolamine solutions determines the minimum recirculation rate of the solution to treat a specific sour gas stream and it determines the maximum concentration of acid gases which can be left in the regenerated solution in order to meet the product gas specification. This is a multi-component and multiphase equilibrium problem. Hence any data generated are needed to be correlated with a thermodynamic framework. But for a system where no experimental data is available so far, molecular modeling approach can predict the VLE of that system; it can also predict the thermodynamics of (alkanolamine + H_2O) system.

2.4 PREVIOUS WORK RELATED TO VLE, THERMODYNAMIC PROPEERTIES AND DENSITY OF AQUEOUS ALKANOLAMINE SYSTEM

Present study is aiming to highlight the recently proposed alkanolamines for CO_2 sequestration. Previous investigations related to PZ, MAE, AHPD solvents and their blends used in the recent past are included in this discussion. Some investigations related to ionic liquids, and Sodium and Potassium salts of primary or tertiary amino acids are also included in the present discussion. Previous work involving molecular modeling is abstracted in chapter 3 of the present thesis.

Kundu and Bandyopadhyay (2007) focused on thermodynamics and associated non ideal behavior of binary MEA + H_2O, DEA + H_2O, and MDEA + H_2O systems, which was required to predict the vapor-liquid equilibrium of acid gases such as CO_2 over aqueous alkanolamine solutions. They determined binary interaction parameters, made analytical prediction of infinite dilution activity coefficient; heats of solution at infinite dilution, the excess Gibbs free energy, and excess enthalpy for non-ideal alkanolamine-water systems. In an aim to establish MAE as a potential solvent for CO_2 removal, Kumar and Kundu (2012) generated and reported CO_2 solubility in N-methyl-2-ethanolamine aqueous solutions of concentrations (0.968, 1.574, 2.240 and 3.125 mol.kg^{-1} of solvent; 0.0676, 0.1052, 0.1427, and 0.1878 mass fractions of MAE) at temperatures (303.1, 313.1 and 323.1) K in the CO_2 pressure range of (1 to 350) kPa. Bougie and Iliuta (2010) measured and reported CO_2 solubility in aqueous mixtures of 2-amino-2-hydroxymethyl-1, 3-propanediol (AHPD) and piperazine (Pz) over a range of temperature from (288.15 to 333.15) K and for total amine concentrations up to 3.1

$kmol.m^{-3}$(0.37 mass fraction). The CO_2 partial pressure was kept within (0.21 to 2 637) kPa using a vapor-liquid equilibrium (VLE) apparatus based on a static-analytic method. Balsora and Mondal (2011) presented experimental results on CO_2 solubility in a new blend of Diethanolamine (DEA) and Trisodium phosphate (TSP) at temperatures ranging from (303.14 to 333.14) K and over the partial pressure range of (10.133 to 20.265) kPa. Total concentrations of aqueous (DEA + TSP) blends were kept as (1.0, 1.5, and 2.0) $mol.dm^{-3}$. Mole fractions of TSP varied in the range 0.02 to 0.20 in those blends. However, drawbacks such as solvent loss and high regeneration costs due to the high water content have driven the researchers in search of new technologies.

Recently room temperature ionic liquids (ILs'); called green solvents are emerging as promising candidates to capture CO_2 due to their wide liquid range, low melting point, tunable properties, negligible vapor pressure, high CO_2 solubility and reasonable thermal stability. Off late, the idea of mixing ILs and alkanolamines has been received great attention from the industries, since its advantages and capabilities in reducing the problem caused by the usage of conventional alkanolamines solutions are promising (Chinn et.al, 2009; Camper et.al, 2008; Zhang and Zhao, 2010). Xu et al. (2012) reported the solubility of CO_2 in aqueous mixture of a low viscous IL ($[C_2OHmim]$ $[N(CN)_2]$) and MEA at temperature 313.15K and 333.15K, over CO_2 partial pressure ranging from 100 to 1000 kPa and IL concentration varying from 5% to 30% . But it is difficult to realize industrialization owing to its high viscous and high cost, which left us so far with the alkanolamine-CO_2 technology. Weiland and Hatcher (2011) reported the performance of a CO_2 capture plant using Sodium-glycine (NaGly), MEA-promoted Potassium salt of dimethyl glycine (KDiMGly), piperazine-promoted KDiMGly, 30 wt.% MEA and Piperazine-promoted MDEA. The results revealed that "the regeneration energy required with piperazine-promoted KDiMGly was about 20% lower that for MEA in an identical plant and with 20 % lower solvent rates". Alvarez et al. (2008) reported densities of aqueous ternary mixtures of 2-ethyl-amino ethanol with MDEA and Triethanolamine from (298.15 to 323.15) K. The relative amine compositions were different than those considered in the present study for $(EAE + MDEA + H_2O)$ system.

REFERNCES

- Alvarez, E.; Gomez-Diaz, D.; Rubina, M. D. L. and Navaza, J. M., "Densities and Viscosities of Aqueous Ternary Mixtures of 2-(Methyl amino)ethanol and 2-(Ethyl amino)ethanol with Diethanolamine, Triethanolamine, N-Methyldiethanolamine, or 2-Amino-1-methyl-1-propanol from 298.15 to 323.15 K", Journal of Chemical and Engineering Data; 53, 318-321, 2008. 53.
- Balsora, H.K. and Mondal, M.K., "Solubility of CO_2 in an aqueous blend of diethanolamine and Trisodium Phosphate", Journal of Chemical and Engineering Data; 56, 4691-4695, 2011.
- Bougie, F. and Iliuta, M.C., "CO_2 Absorption into mixed aqueous solutions of 2-amino-2-hydroxymethyl-1, 3-propanediol and piperazine", Industrial and Engineering Chemistry Research; 49, 1150-1159, 2010.
- Camper, D., Bara, J. E., Gin, D.L. and Nobel, R.D., "Room-Temperature Ionic Liquid-Amine Solutions: Tunable Solvents for Efficient and Reversible Capture of CO_2", Industrial and Engineering Chemistry Research; 47, 8496–8498, 2008.
- Chinn, D.; Vu, D. Q.; Driver, M. S. and Boudreau, L. C., "CO_2 removal from gas using ionic liquid absorbents", US Patent, 7,527, 775 B2, 2009.
- Kumar, G. and Kundu,M., "Vapor-liquid equilibrium of CO_2 in aqueous solutions of N-methyl-2-ethanolamine", The Canadian journal of Chemical Engineering; 90, 627-630,2012.
- Kundu, M. and Bandyopadhyay, S.S., "Thermodynamics of alkanolamine and water system", Chemical Engineering Communication; 194, 1138-1159, 2007.
- Prausnitz, J. M., Lichtenthaler, R. N., and de Azevedo, E. G., "Molecular thermodynamics of fluid phase equilibria", Prentice-Hall Inc., Englewood Cliffs, N. J; 1986.
- Weiland, R. and Hatcher, N.A., " Post- combustion CO_2 capture with Amino-Acids Salts", Paper presented at SOGAT 2011, Abu Dubai, UAE, 2011.
- Xu, F,; Dong, H.; Zhang, X.; Gao, H.; Wang, Z.; Zhang, S. and Ren, B., "Solubilities of CO_2 in Aqueous Solutions of Ionic Liquid and Monoethanolamine", Innovations of Green Process Engineering for Sustainable Energy and Environment, in the

proceedings of American Institute of Chemical Engineers 12 annual meeting, Pittsburgh, PA; Oct 28-Nov 2, 2012.

- Zhao, Y.; Zhang, X.; Zeng, S.; Zhou, Q.; Dong, H.; Tian, X. and Zhang, S., "Density, Viscosity, and Performances of Carbon Dioxide Capture in 16 Absorbents of $\text{Amine} + \text{Ionic Liquid} + H_2O$, $\text{Ionic Liquid} + H_2O$, and $\text{Amine} + H_2O$ Systems", Journal of Chemical and Engineering Data; 55, 3513-3519, 2010.

Chapter 3

Molecular Modeling Theory, Computational Procedure and Applicability of COSMO

MOLECULAR MODELLING THEORY, COMPUTATIONAL PROCEDURE AND APPLICABILITY OF COSMO

For designing separation process, knowledge on phase equilibrium behavior is mandatory. Models based on modified Clegg-Pitzer equations, NRTL, UNIQUAC, UNIFAC are the most popular models currently in use. Those models find out activity coefficients of the compounds using the structural property information of pure components and binary interaction parameters between the components. Molecular simulation using conductor like screening model is a useful alternative to those models. Prediction of any thermodynamic property of solution starts with quantum theory and solvation model. First, the Schrodinger equation is resolved by Density Functional Theory (DFT) using an appropriate basis set, and then the conductor-like screening model (COSMO) model can be applied to predict the sigma profile and finally application of statistical thermodynamics to predict the thermodynamic properties of solution.

3.1 MOLECULAR MODELING AND Schrödinger EQUATION

There are five broad classes in molecular modeling calculations, which are as follows:

Molecular mechanics (MM): is based on a model of a molecule as a collection of balls (atoms) held together by springs (bonds). If the normal spring length, angle between them and energy required to stretch and bend the bonds are known, the geometry optimization of the molecule can be performed. Molecular geometry can be subjected to change until the lowest energy is found. MM is fast; the geometry of a large steroid molecule can be optimized within a few seconds.

Ab-initio calculations: Are based on Schrödinger equation. This method solves Schrödinger equation for a molecule and calculates the molecules energy and wave function. The wave function is a mathematical function that can be used to calculate electron distribution. The electron distribution can explain the polarity of a molecule for example. Schrödinger equation cannot be solved exactly for a molecule with more than one electron; hence, Ab initio methods are slow.

Semi-empirical (SE) calculations also use Schrödinger equation. However more approximations are used in it and very complicated integral that are solved in Ab initio methods are actually evaluated in SE calculations. The program draws on a kind of library of integrals that was compiled by finding the best fit of some calculated entity like geometry or energy to the experimental values. This plugging of experimental values in to a mathematical procedure to get the best calculated values is called Parameterization. It is the mixing of theory and experiment: that makes the method semi empirical. The abstraction of this method is that it is based on Schrödinger equation but parameterized with experimental values. SE calculations are slower than MM but faster than Ab initio method.

Density functional (DFT) calculations: Is also based on Schrödinger equation. However DFT does not calculate wave function but derives the electron distribution called density function directly. A functional is a mathematical entity related to function. This method is faster than Ab initio but slower than MM and SE.

Molecular dynamics (MD): Apply laws of motion to molecules.

Mechanics is the study of behavior of the bodies under the action of forces like gravity. MM is based on this very idea of classical physics. Molecules are made of nuclei and electrons, quantum chemistry/ mechanics deals with the motion of electrons under the influence of electromagnetic force exerted by nuclear charges. Development of quantum mechanics as a part of modern physics/ leads up to the Schrödinger equation followed by the birth of quantum chemistry with the application of Schrödinger equation to chemistry by HÜckel. The events that ensured the transition from classical to modern physics and quantum chemistry follows the sequence, the origin of quantum theory: black body radiation and photoelectric effect; radioactivity; relativity, the nuclear atom; the Bohr atom; the wave mechanical atom and Schrödinger equation. Quantum mechanics (QM) postulates that energy is quantized; absorbed and emitted in discrete packets (quanta) of magnitude $\boldsymbol{h\nu}$, where $\boldsymbol{h}$ **is Planck′s** constant and $\boldsymbol{\nu}$ is the frequency associated with the energy. QM evolved out of studies of black body radiation and photoelectric effect. Beside QM, radioactivity, relativity contributes in transition from classical physics to modern physics. The classical Rutherford nuclear atom suffered from the deficiency that Maxwell's electromagnetic theory demanded. The orbiting electrons here radiate away energy and swiftly fall into the nucleus. This

problem was addressed by Bohr's quantum atom, in which an electron could orbit stably if its angular momentum was an integral multiple of $\mathbf{h}/\mathbf{2\pi}$. However Bohr's model could work for hydrogen atom. The shortcoming of Bohr atom was overcome by Schrödinger's wave mechanical atom; this was based on a combination of classical wave theory and De Broglie postulate that any particle is associated with a wavelength $\boldsymbol{\lambda}/\boldsymbol{p}$, where **p is the momentum**.

Based on Broglie's theory Heisenberg and Max Born invented matrix mechanics in 1925 where they studied the behavior of subatomic particles by relating their properties to matrices. Later, Heisenberg developed the uncertainty principle which was based on wave particle duality and Broglie's theory, since this principle was based on the wavelength of electron and wave particle duality, the conclusion of the uncertainty principle stated that position and momentum of a particle cannot be determined at the same time. In 1927 Erwin Schrödinger developed the famous Schrödinger equation, which treated particle motion as a wave that is a function of position and time. After 1930 Ab Initio methods started to develop with Hartree Fock theory, in order to solve Schrödinger equation. In 1964 Pierre Hohenberg and Walter Kohn developed the Density Functional Theory (DFT), in which they were able to study the electronic structure of many body systems such as molecules. So far we were discussing the perspective of inception and development of Schrödinger equation, the most powerful proposition of modern physics, which embellished the quantum chemistry.

The first step in quantum computation starts with Schrödinger equation (3.1), since electrons have particle and wave-like character, Schrödinger's equation plays a vital role in describing the wave perform of a particle (Frisch, 1996; Griffiths, 2005; Szabo 1996). There are 2 types of Schrödinger equations; time-independent and time-dependent. Quantum computation in the present work is predicated on the idea that the forces acting on a particle don't rely upon time, so the time-independent differential equation is employed.

$$-\frac{\boldsymbol{h^2}}{\mathbf{2m}}\boldsymbol{\nabla^2\Psi} + \mathbf{V}\,\boldsymbol{\Psi} = \mathbf{E}\boldsymbol{\Psi} \qquad (3.1)$$

where **m** is that the mass of the particle being delineate, $\boldsymbol{h}$ is Planck' s constant, **V** describes the force functioning on a particle, $\boldsymbol{\Psi}$ is that the wave perform,$\boldsymbol{\nabla^2}$ the operator describes the behavior of the wave perform with position, and **E** is that the state energy of the particle or

the system. Equation (3.1) is that the most significant equation in physics. The answer to Schrödinger's equation is the wave function. Assuming there's an electron cornered in an exceedingly box, at first we all know its first position which can be entered into the equation. In finding Schrödinger equation, the wave perform provides the probability of the particle position in all area at any time within the future. (Note that the wave perform itself isn't probability; it's to be squared). Schrödinger's equation provides a perfect solution for a hydrogen atom because of its one electron spatial term. For many electron systems like molecules, equation (3.1) becomes extraordinarily tough to unravel and that is where ab initio methods such as density functional theory start to play a role.

3.2 DENSITY FUNCTIONAL THEORY

Density functional theory (DFT), calculates the electron probability density of the molecule then the molecular electronic energy is computed based on the accurate prediction of the electron probability density (Foresman, 1996; Levine, 2000)

$$E_o = E_V[\rho_o] \tag{3.2}$$

The most important part in our computation is solving the ground state energy of the molecule $E_o$which is dependent on energy functional E_V. Solution to equation (3.2) can be accomplished by implementing the electronic energy equation (equation (3.3)).

$$E = E^T + E^V + E^J + E^{XC} \tag{3.3}$$

In a molecule, electrons are in a random motion where they are interacting with each other and with the nuclei. Electronic energy depends on kinetic energy from electronic motion which is represented by E^T, potential energy of electron nuclear attraction and repulsion of nuclei pairs which is represented by E^V, electronic repulsion which is presented by E^J, and E^{XC} known as the exchange correlation terms which will take into consideration the non-counted electronic interaction. All terms in equation (3.3) are dependent on electronic density ρ. The electronic repulsion term represented in equation (3.4) is dependent on molecular geometry.

$$E^J = \frac{1}{2}\iint \rho\,(r_1)(\Delta\, r_{12})^{-1}\,\rho\,(r_2)\,dr_1 dr_2 \tag{3.4}$$

Electronic repulsion equation (equation (3.4)) is known as Coulomb self- interaction of electron density. Equation (3.4) is based on Coulomb's law, where electronic density is dependent upon r_1 and r_2, and charges are located in both volume elements ($dr_1$and dr_2). If we integrate over dr_2 we will get repulsion energy between charges and its distribution, to get the total repulsion energy E^J, we integrate over dr_1 and multiply by ½ to prevent double counting repulsion between charges.

E^T, $E^V$and E^J in equation (3.3) takes into consideration the symmetry of the wave function only; on the other hand exchange correlation term will take into consideration wave functional symmetry (note: anti symmetry wave function is based on Pauli exclusion principle that is two identical fermions cannot occupy the same quantum state and two identical particles will have half integer spin). E^{XC} in equations (3.5) and (3.6) below depends on electronic density distribution.

$$E^{XC}(\rho) = \int f(\rho_\alpha(r), \rho_\beta(r), \nabla\rho_\alpha(r), \nabla\rho_\beta(r))\, d^3\, r \tag{3.5}$$

$$E^{XC}(\rho) = E^X(\rho) + E^C(\rho) \tag{3.6}$$

Equation (3.5) is a function of alpha spin density and beta spin density where total electron density is in equation (3.7) below.

$$\rho = \rho\alpha + \rho\beta \tag{3.7}$$

E^{XC} can be defined as the sum of exchange and correlation term (equation (3.6)). Exchange energy formula in equation (3.6) will be the same as exchange energy in Hartree Fock theory, but the orbital is replaced by a Kohn-Sham orbital. The exchange term is represented in equation (3.8) below.

$$E^X_{LDA} = -\frac{3}{2}\left(\frac{3}{4\pi}\right)^{1/3} \int \rho^{4/3} d^3\, r \tag{3.8}$$

Equation (3.8) is known as local density approximation (LDA), where the exchange energy is calculated based on the assumption that the exchange energy of any electron is placed in an interacting homogenous electron gas, but equation (3.8) is inaccurate for a molecular system.

3.3 BASIS SET

DFT offers theoretical solution for electron density in a molecular system but it does not define its geometry or the electronic boundary. Therefore, the next step is to construct electronic boundaries by defining a basis set (Foresman, 1996; Szabo, 1996; Levine, 2000). A basis set is a collection of vectors that is used to specify the space where electron density is computed. The mathematical function in the basis set is a linear combination of one electron basis function centered on the atomic nuclei. Such a mathematical method is used to create molecular orbital.

$$\emptyset_i = \sum_{\mu=1}^{n} C_{\mu i} X_\mu \qquad (3.9)$$

Equation (3.9) is for an individual molecular orbital, where $\emptyset_i$ is the i-th molecular orbital, $C_{\mu i}$is the molecular expansion coefficient, $X_\mu$is the μ-th atomic orbital also known as arbitrary basis function, and n is the number of atomic orbitals. Gaussian functions are used in constructing molecular orbitals. A linear combination of Gaussian functions results in contracted Gaussian type orbital. In our quantum computation, the triple zeta polarized valence (TZVP) basis set was used. TZVP is based on the CGTO (contracted Gaussian type orbital) concept. The advantage of such a basis set is that it has three basic functions for each atomic orbital. If different size atoms are getting close, the TZVP basis set will allow the orbital to get bigger or smaller. Another advantage of TZVP is its polarized function that adds orbitals with angular momentum beyond the atomic limitations.

3.4 HISTORY OF SOLVATION MODELS

In 1920 Max Born developed a formula for the free energy of solvation of ions by assuming the ion is embedded in a solvent which is considered as a dielectric continuum medium (Klamt, 2005). Max Born's theory started the development of solvation models or self-consistent reaction field models (SCRF) as it is called by some literature. In 1936, Onsager developed a solvation model that is based on dipole moment; he assumed that the solute is inside a fixed spherical cavity with a fixed radius where the cavity is embedded in a dielectric continuum (solvent) (Foresman, 1996). The Onsager model concluded that the dipole of the molecule will induce a dipole in the continuum medium where an electric field supplied by

solvent dipole will react with the molecular dipole leading to stabilization of charges on the molecular surface. The Onsager model had two weaknesses: first was the assumption of a spherical cavity and constant radius; in fact the molecule is not spherical, and the second weakness was not accounting for multi pole moment and considering only dipole moment. Both of those weaknesses led to a large error in the sigma profile and dielectric constant values. Additionally, if the dipole moment of a molecule is zero, the Onsager model is not applicable (Figure (3.1) shows Onsager model cavity). In 1982, Tomasi developed another solvation model called Polarized Continuum Model (PCM) (Foresman, 1996). Tomasi's model considers the molecule is inside a cavity that is a union of atomic spheres and the polarization of the continuum is computed numerically by integration of the molecular surface segments. Figure (3.1) shows that the PCM cavity is closer to the molecular shape.

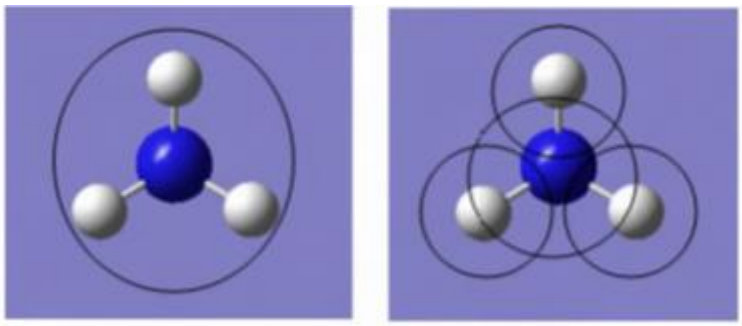

Figure 3.1: Onsager cavity and PCM

In 1992, Klamt and co-workers developed a new solvation model called Conductor like Screening Model (COSMO) (Klamt, 2005). Klamt's model included much modification on PCM and solved many problems that PCM and Onsager model failed to solve. In 2002, Sandler and co-workers developed a solvation model called COSMO-SAC, where group contribution solvation was added and activity coefficients from the solvation free energy of molecule in a solution were computed (Oldland, 2006; Sandler, 2002; Lin, 2004). In contrast, COSMO-RS calculates the chemical potential based on charge density of the conductor.

3.5 COSMO THEORY

The conductor-like screening model (COSMO) offers quantum chemistry calculation for molecules in a solution**.** In COSMO theory, the molecule which is a solute is placed inside a

cavity in a dielectric continuum medium the solvent. The molecule has dipole or higher level moment also its charges are distributed within its cavity.

According to COSMO theory molecular moment will induce solvent moment which in turn produces electric field that interacts with the molecular dipole leading to charge redistribution on the cavity surface. As a result polarization or screening charges will be located on molecular surface by COSMO model based on electrostatic interaction between the molecule and its continuum medium. A brief illustration of conductor like screening model is represented in Figure (3.2) (Oldland, 2006). Polarization or screening charges that are seen in Figure (3.2) can be calculated by equation (3.10) which is used by many solvation models.

$$4\pi\sigma = \frac{\varepsilon-1}{\varepsilon} E \bullet n \qquad (3.10)$$

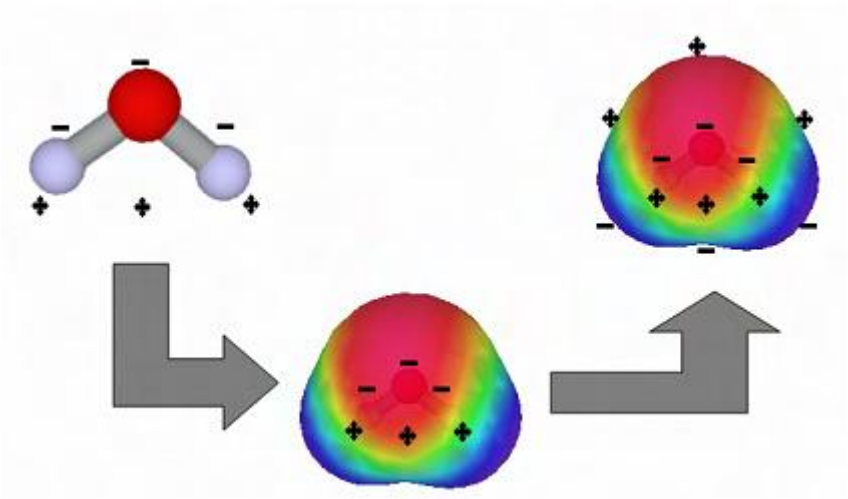

Figure: 3.2: An illustration of conductor like screening model process. In the top left of the picture molecule is in its original form. In the middle picture, the molecule is being placed inside a molecular shape cavity in a continuum medium. Top right pictures represents screening charges on the cavity surface due to electrostatic interaction between the molecule and its medium**.**

In equation (3.10) σ is the charge density, ε is the dielectric screening constant for the solute, E is the total electrostatic field from the solute and polarized charges and n is the normal vector pointing out from the cavity surface. Such an equation does not provide accurate

solution for large size molecules. In order to calculate screening charge density accurately for larger molecules, COSMO model provided much simpler formula in equation (3.11)

$\sigma = f(\varepsilon)\, \sigma^*$

$$f(\varepsilon) = \frac{\varepsilon - 1}{\varepsilon + 0.5} \tag{3.11}$$

According to COSMO, if charge distribution on cavity surface is known then ideal screening charge density (σ^*) can be calculated by equation (3.11). The number 0.5 in equation (3.11) was derived empirically based on dipole moment in spherical cavities.

3.6 COSMO-RS THEORY

The advanced model COSMO-RS, i.e., COSMO for realistic solvation, is a statistical thermodynamics theory based on COSMO polarization charge densities, which overcomes many of the limitations and theoretical shortcomings of dielectric continuum models. Due to its ability to treat mixtures at variable temperatures, it has become very popular in chemical engineering and in wide areas of physical and medicinal chemistry. COSMO-RS currently may be considered as the most accurate model for the prediction of solvation energies. As discussed earlier, in the COSMO model the solute which is inside a cavity is placed in a perfect conductor which is the solvent. Induced moment from the solute and back polarization from the medium will result in screening charges on the cavity surface with a total energy E_{cosmo}. In order to perform thermodynamics calculation, COSMO-RS theory is used, where the solute is considered as an ensemble of closely packed screened molecules, because of such packing character, the molecules are in close contact with each other. Hence, the conductor between surface areas of the solute molecules vanishes. Therefore; electrostatic interaction occurs between two different surface screening charge densities (σ and σ') with interaction energy E_{misfit}:

$$E_{misfit}(\sigma, \sigma') = a_{eff} \frac{\alpha'}{2} (\sigma + \sigma')^2 \tag{3.12}$$

Where a_{eff} is the effective area of contact between two solute molecules surface segments, α' is an interaction parameter that can be adjustable, σ and σ' are two different surface

screening charge densities for solute molecules that are in contact with each other, and E_{misfit} is the electrostatic interaction energy of two segments per unit area. In equation (3.12) $\sigma + \sigma'$ could equal to zero due to ideal contact between two effective surface areas in other word, E_{misfit} could be equal to zero when molecules screen each other out due to opposite polarity. Another molecular interaction energy used in COSMO-RS that depends on screening charge densities is the hydrogen bonding energy (E_{HB}):

$$E_{HB} = a_{eff} c_{HB} \min(0; \min(0; \sigma_{donor} + \sigma_{HB}) \max(0; \sigma_{acceptor} - \sigma_{HB})) \quad (3.13)$$

Where c_{HB} is an adjustable parameter used for hydrogen bond strength, σ_{HB} is the adjustable parameter for hydrogen bonding threshold, σ_{donor} is the screening charge density for hydrogen bond donor surface area, and $\sigma_{acceptor}$ is the screening charge density for hydrogen bond acceptor surface area. In equation (3.13) hydrogen bonding energy is computed based on close contact between molecules with strong opposite polarity, where the hydrogen bond donor segment have strong negative screening charge density and the hydrogen bond acceptor segment have strong positive screening charge density. In addition to molecular interaction energy that is dependent on screening charge density, COSMO-RS takes into consideration the van der waals energy:

$$E_{vdW} = a_{eff}(\tau_{vdW} + \tau'_{vdW}) \quad (3.14)$$

Equation (3.14) is highly dependent on the type of atomic element, where the computed van der waals interaction energy (E_{vdW}) is based on effective contact area and van der waals interaction parameter (τ and τ') of the element. If we look at equations (3.12) and (3.13) we find that the surface charge density (σ) is an important parameter; to calculate surface interaction energies in COSMO-RS is calculated as an average over larger areas:

$$\sigma_{i=} \frac{\sum_j \frac{q_j}{s_j + s_{av}} \exp\left(\frac{-d_{ij}^2}{r_{av}^2}\right)}{\sum_j \frac{s_j}{s_j + s_{av}} \exp\left(\frac{-d_{ij}^2}{r_{av}^2}\right)} \quad (3.15)$$

Where r_{av} is the average radius set at a value of 0.05 nm, s_{av} is the average area of circle with $r = r_{av}$, s_j is the area of thedifferent segment j that could contribute to $\sigma_i$and d_{ij} represents the distance between the two segments i and j. After surface charge density has been defined

for COMSO-RS, the surface charge interaction in an ensemble is based on the probability distribution of σ over the whole molecular surface in the system. Such probability distribution is called sigma profile:

$$P_s(\sigma) = \sum_{i=N} X_i P^{Xi}(\sigma) \tag{3.16}$$

Where P_s is the sigma profile of the whole mixture, X_i is the mole fraction of compound X, and $P^{Xi}(\sigma)$is the sigma profile of compound X, it is defined by equation (3.17):

$$P^{Xi}(\sigma) = \frac{n_i(\sigma)}{n_i} = \frac{A_i(\sigma)}{A_i} \tag{3.17}$$

$n_i(\sigma)$ is the number of divided segments that has surface charge density (σ), $A_i(\sigma)$ represents all segments surface area that has charge density σ and A_i is the area of the whole surface cavity that is embedded is the medium.

The next step in COSMO-RS is to determine how much the system in the ensemble likes the polarity of charge density σ. This can be done by implementing equation (3.18):

$$\mu_{S(\sigma)} = -\frac{RT}{\alpha_{eff}} \ln\left[\int P_{s(\sigma^*)} \exp\left(\frac{\alpha_{eff}}{RT}\left(\mu_S(\sigma^*) - E_{misfit}(\sigma,\sigma^*) - E_{HB}(\sigma,\sigma^*)\right)\right) d\sigma^*\right] \tag{3.18}$$

Where $\mu_{S(\sigma)}$ is called the sigma potential, equation (3.18) is dependent on temperature, composition, electrostatic interaction energies and sigma profile. Once the sigma potential is calculated, the chemical potential in the solvent S (μ_S^{Xi}) can be calculated by equation (3.19) which takes into consideration the different size of molecules in the system by adding a combinatorial term ($\mu_{C,S}^{Xi}$):

$$\mu_S^{Xi} = \mu_{C,S}^{Xi} + \int P^{Xi}(\sigma)\mu_S(\sigma)\, d\sigma \tag{3.19}$$

COSMO-RS takes into consideration the computation of chemical potential of pure compound in ideal gas (μ_{gas}^{Xi}):

$$\mu_{gas}^{Xi} = E_{gas}^{Xi} - E_{COSMO}^{Xi} - E_{vdW}^{Xi} + \omega_{ring} n_{ring}^{Xi} + n_{gas} RT \tag{3.20}$$

Where E_{gas}^{Xi} is the total energy of the molecule in the gas phase computed by quantum mechanics, E_{COSMO}^{Xi} is the total COSMO energy of the molecule in solution computed by solvation model using quantum mechanics, E_{vdW}^{Xi} is the vdW energy of the molecule and the rest of the terms in equation (3.20) are correction parameters for molecules with ring shape geometry. Once the chemical potential of pure compound has been computed in solution and ideal gas phase, vapor pressure of pure compound can be calculated by equation (3.21):

$$P_{vap(T)}^{xi} = exp\left(\frac{\mu_{Xi}^{Xi} - \mu_{gas}^{Xi}}{kT}\right) \quad (3.21)$$

Where $P_{vap(T)}^{Xi}$ the vapor pressure of pure compound (x_i), k is the Boltzmann constant, T is the temperature and μ_{xi}^{xi} is the pseudo-chemical potential of pure compound x_i in a liquid x_i. After vapor pressure of pure compound has been calculated, COSMO-RS can predict vapor liquid equilibrium based on the following equations:

$$\gamma_S^{Xi} = exp\left(\frac{\mu_S^{Xi} - \mu_{Xi}^{Xi}}{RT}\right) \quad 3.22)$$

$$P^{tot} = \sum_i P_{vap}^{Xi} x_i \gamma_s^{Xi} \quad (3.23)$$

$$y_{i=\frac{P_{vap}^{Xi} x_i \gamma_S^{Xi}}{P^{tot}}} \quad (3.24)$$

In above equations γ_S^{Xi} is the activity coefficient of pure compound x_i in solution which is considered the continuum medium according to COSMO model P^{tot} is total vapor pressure of the mixture that is used to predict the vapor liquid equilibrium diagram, x_i is the mole fraction of compounds in liquid phase and y_i is the mole fraction of compounds in gas phase. Hence vapor liquid equilibirium in COMSO-RS is based on vapor pressure and activity coefficients of pure compounds.

3.7 COMPUTATIONAL PROCEDURE

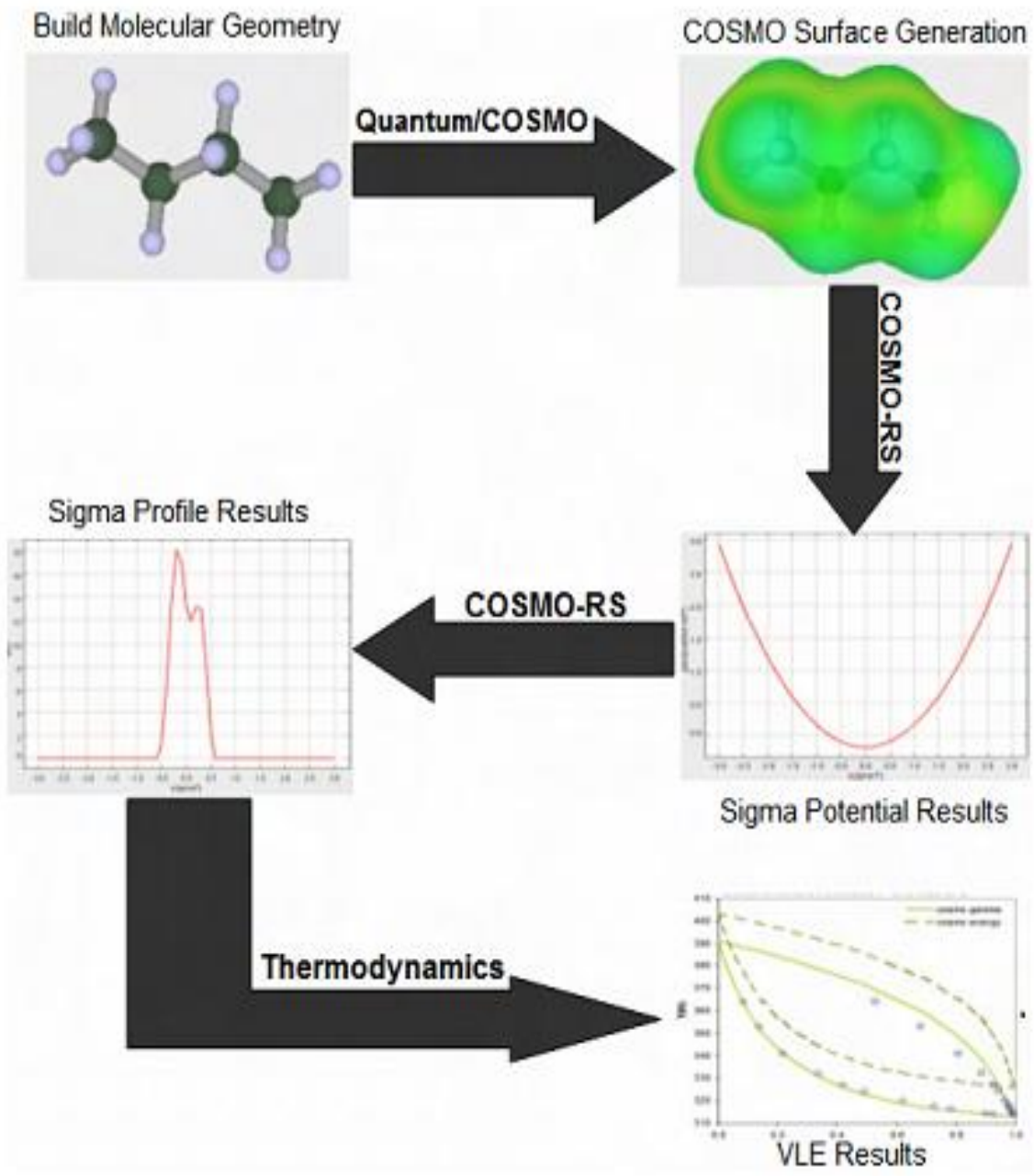

Figure 3.3: Overall summary of COSMO-RS computation. First, start the computation by building a molecule then perform a Quantum and COSMO calculations to generate COSMO surface. Second, generate sigma potential and sigma profile by COSMO-RS theory. Finally, perform thermodynamics calculation such as VLE by applying statistical thermodynamics.

We started our computation procedure by performing molecular geometry optimization using Quantum Mechanics, then we applied COSMO calculation to generate COSMO surface in order to calculate sigma potential and sigma profile by COSMO-RS to compute VLE and vapor pressure using statistical thermodynamics. An overall picture of computational procedure is represented in Figure (3.3).

Performing COSMO-RS computation to predict VLE and vapor pressure for any type of molecule requires generating three types of files: COSMO file, Energy file and VAP file. The COSMO and ENERGY files are generated by TURBOMOLE software while the VAP file is generated by COSMOtherm program package. Once these files are generated the COSMOtherm program can be used to perform thermodynamic calculations.

3.8 COSMO-RS APPLICATION

Originally COSMO-RS was developed mainly for the prediction of various kinds of partition coefficients (Klamt et.al., 2000). In 1998 it was applied to activity coefficients and complete vapor–liquid equilibria of binary mixtures by chemical engineers (Clausen, 2000; Arlt, 2000). Since then COSMO-RS has become very popular and is widely used in chemical engineering for all kinds of phase equilibrium predictions (vapor–liquid, liquid–liquid, and solid–liquid) and for the efficient screening of solvents and additives for chemical process optimization (Franke, 2002; Klamt et al., 2010). The strength of COSMO-RS as compared with other conventional chemical engineering tools, such as group contribution methods, is its broad homogeneous applicability from simple compounds toward complicated, multifunctional, or novel chemical compounds. Although developed and parameterized exclusively on neutral compounds, in 2002 COSMO-RS was proven to be able to treat ionic liquids as mixtures of anions and cations (Marsh, 2002; Diedenhofen, 2002). Since then ionic liquids have become an important application area of COSMO-RS in chemical engineering. Klamt et al. (2004) implemented the COSMO-RS method for the prediction of vapor-liquid equilibria for the mixtures of dimethylether (1) and propene (2) and of nitroethane (1) and propylene glycol monomethylether (1-methoxy-2-propanol) (2). Good quality predictions were achieved using experimental values for the pure compound vapor pressures and predicted activity coefficients for the mixture thermodynamics. The quantitative success combined with the relatively low computational and time requirements clearly demonstrated that COSMOtherm

was an efficient and reliable tool for the prediction of VLE data for typical industrial relevant mixtures. Tamal Banarjee (2006) predicted the phase equilibrium behavior and vapor pressure of ionic liquid system (phosphonium ionic liquids) using conductor like screening model. Ayman Gazawi (2007) emphasized on the VLE and vapor pressure predictions using Turbo mole software package version 5.8 with DFT/TZVP ab initio method for; sigma profile, ideal gas heat capacity and ideal gas absolute entropy computation of 71 pure compounds. Yamada et al. (2011) used density functional theory (DFT) calculations with the latest continuum solvation model (SMD/IEF-PCM) to determine the mechanism of CO_2 absorption into aqueous solutions of 2-amino-2-methyl-1-propanol (AMP). Possible absorption process reactions were investigated by transition-state optimization and intrinsic reaction coordinates (IRC). They also predicted that the carbamate readily decomposed by a reverse reaction rather than by hydrolysis. Mustapha et al. (2013) considered more than 2000 solvents comprising of four groups for study including the alkanolamine solvents (primary, secondary, tertiary, and sterically hindered alkanolamines and physical solvents), neutral solvents, mixed solvents and ionic liquids (ILs). They predicted the thermodynamic properties, such as Henry's constant, partition coefficient, solubility in water and vapor pressure of all the solvents using COSMO-RS model. Because of its ability to treat complex molecules not only in water but in any solvent and mixture, COSMO-RS is widely used in pharmaceutical and general life science research for solvent screening and formulation research in drug development (Klamt, 2008; Wichmann, 2010). Although the σ-based COSMO-RS picture of molecular interactions surely opens interesting options for the description of drug activity in drug design, it has not yet been widely used in that area. The environmental distribution of compounds had been one of the starting points for the development of COSMO and COSMO-RS, and remains to be an interesting and demanding application area of COSMO-RS (Niederer, 2007; Goss, 2009). Other application areas are fragrance, flavor, or other ingredient distribution in food, perfumes, or personal care products, additives in polymers, and many more (Klamt et al., 2001). Within the COSMOtherm software, a number of additional applications of COSMO-RS have been developed, including the prediction of dissociation constants in aqueous and non-aqueous solvents (Klamt et al., 2003; Eckert et al., 2009), the prediction of the free energy of molecules at liquid–liquid and liquid–vapor interfaces, and the prediction of the free energies and of the partitioning of solutes in polymers, micellar systems, and bio membranes (Klamt et

al., 2008). Furthermore, a set of QSAR descriptors, the so-called σ-moments, has been derived from the COSMO-RS theory, which can be used to regress almost any kind of partition property even in complex cases as blood–brain partitioning, soil sorption, adsorption to activated carbon, and many more.

REFERNCES

- Banerjee, T., "Ionic liquids- Phase equilibria and thermodynamic property predictions using molecular modelling and dynamics, and their validations with experiments", Ph.D. Thesis. Indian Institute of Technology, Kanpur; Nov 2006.
- Clausen I., "Experimental and theoretical analysis of the applicability of COSMO-RS for distribution coefficients", PhD Thesis. Technical University of Berlin, Berlin; 2000.
- Clausen, I. and Arlt, W., "A priori calculation of phase equilibria for the thermal process technology with COSMO-RS", Chemie Ingenieur Technik; 72, 727-733, 2000.
- Diedenhofen, M., Eckert, F. and Klamt, A., "Prediction of infinite dilution activity coefficients of organic compounds in ionic liquids using COSMO-RS", Journal of Chemical and Engineering Data; 48, 475-479, 2002.
- Eckert, F., Leito, I., Kaljurand, I., KÜtt, A., Klamt, A. and Diedenhofen, M., "Prediction of acidity in Acetonitrile solution with COSMO-RS", Journal of Computational Chemistry; 30, 799-810, 2009.
- Foresman, J.B. and Frisch, A.E., "Exploring Chemistry with Electronic Structure Methods", 2nd Ed., Pittsburgh: Gaussian, Inc., 1996.
- Franke, R., Krissmann, J. and Janowsky, R., "What should the process engineer of COSMO-RS expect?", Chemie Ingenieur Technik; 74, 85-89, 2002.
- Gazawi, A., "Evaluating COSMO-RS for vapour liquid equilibrium and TURBOMOLE for ideal gas properties", M.Sc. Thesis. The graduate faculty of the university of Akron; Dec 2007.
- Goss, K.U. and Arp, H.P.H., "Ambient gas / Particle partitioning. 3. Estimating partition coefficients of Apolar, Polar, and Ionizable organic compounds by their molecular structure", Environmental Science and Technology; 43, 1923-1929, 2009.
- Griffiths, D. J., "Introduction To Quantum Mechanics", 2nd Ed., Upper Saddle River, NJ: Pearson Prentice Hall; 2005.
- Klamt, A. and Eckert, F., "COSMO-RS: A novel and efficient method for the priori prediction of thermo physical data of liquids", Fluid Phase Equilibria; 172, 43-72, 2000.

- Klamt, A. and Eckert, F., "Prediction of vapor liquid equilibria using COSMOtherm", Fluid Phase Equilibria; 217, 53-57, 2004.
- Klamt, A. and Smith, B. J., "Challenge of drug solubility prediction" MannholdRaimund (ed.)- Molecular Drug Properties Measurement and Prediction, Weinheim: John Wiley & Sons; 283-311, 2008.
- Klamt, A., "COSMO-RS From Quantum Chemistry to Fluid Phase Thermodynamics and Drug Design", 1st Ed., Elsevier; 2005.
- Klamt, A., Arlt, W. and Eckert, F., "COSMO-RS: An alternative to simulation for calculating thermodynamic properties of liquid mixtures", Annual Reviews of Chemical and Biomolecular Engineering; 1, 101-122, 2010.
- Klamt, A., Eckert, F., Diedenhofen, M. and Beck, M.E., "First principles calculations of aqueous pKa values for organic and inorganic acids using COSMO-RS reveal an inconsistency in the slope of the pKa", The journal of Physical Chemistry A; 107, 9380-9386, 2003.
- Klamt, A., Huniar, U., Spycher, S. and Keldenich J., "COSMOmic: A mechanistic approach to the calculation of membrane−water partition coefficients and internal distributions within membranes and micelles", The journal of Physical Chemistry B; 112, 12148-12157, 2008.
- Levine, I.N., "Quantum Chemistry", 5th Ed., Upper Saddle River, NJ: Prentice Hall; 2000.
- Lin, S.T. and Sandler, S., "A Priori Phase Equilibrium Prediction from a Segment Contribution Solvation Model", Industrial and Engineering Chemistry Research; 43, 1322, 2004.
- Marsh, K.N., Deev, A., Wu, A.C.T., Tran, E. and Klamt, A., "Room temperature ionic liquids as replacements for conventional solvents—A review" Korean Journal of Chemical Engineering; 19, 357-362, 2002.
- Mustapha, S.I., Okonkwo, P.C. and Waziri, S.M., " Improvement of CO_2 absorption technology using conductor- like screening model for real solvents (COSMO-RS) method", Journal of Environmental Chemistry and Ecotoxicology; 5, 96-105, 2013.
- Niederer, C. and Goss, K.U., "Quantum chemical modeling of Humic acid / Air equilibrium partitioning of organic vapors", Environmental Science and Technology; 41, 3646-3652, 2007.

- Oldland, E. R., Liu, Y. A., Wang, S. and Sandler, S. I., "Sigma-Profile Database for Using COSMO-Based Thermodynamic Methods", Industrial and Engineering Chemistry Research; 45, 4389-4415, 2006.
- Sandler, S. I. and Tai Lin, S., "A Priori Phase Equilibrium Prediction From Segment Contribution Solvation Model", Industrial and Engineering Chemistry Research; 41, 899-913, 2002.
- Sonnenberg, S., Finke, A., Klamt, A., Lohrenz, J., BÜrger, T. and Matthiesen, S., "Selection method for odorants", US 6741954 B2, 2001.
- Szabo, A. and Ostlund,N. S., "Modern Quantum Chemistry: Introduction to advanced Electronic structure theory", Dover Publications, Inc.; 1996.
- Wichmann, K., David, J. am Ende, and Klamt, A., "Drug solubility and reaction thermodynamics", Chemical Engineering in the Pharmaceutical Industry: R&D to Manufacturing, John Wiley & Sons; 457-476, 2010.
- Yamada, H., Yoichi, M., Higashii, T. and Kazama, S., "Density Functional Theory Study on Carbon Dioxide Absorption into Aqueous Solutions of 2-Amino-2-methyl-1-propanol Using a Continuum Solvation Model", The journal of Physical Chemistry; 115, 3079-3086, 2011.

Chapter 4

Thermodynamics of (alkanolamine + water) system

THERMODYNAMICS OF (ALKANOLAMINE + WATER) SYSTEM

Design of gas treating processes requires the knowledge of thermodynamic properties of water-alkanolamine system. Development of a COSMO-RS model for the (alkanolamine-water) systems has been presented here with representation of excess Gibbs free energy, excess enthalpy and activity coefficient, chemical potential for (alkanolamine + H_2O) system.

4.1 THERMODYNAMICS OF (ALKANOLAMINE + WATER) SYSTEMS

To model the thermodynamics of (acid gas + alkanolamine + water) systems, we have to understand the constituent binary systems and they are namely, (alkanolamine + water), (acid gas + water), and (acid gas + alkanolamine) systems. (Alkanolamine + water), (acid gas + water) systems are single weak electrolyte systems and the degree of dissociation of electrolyte in each is negligible except at high dilutions, chemical equilibrium can be ignored. As the acid gas approaches zero in the acid gas - alkanolamine solutions, a binary amine-water system results. The binary parameters associated with acid gas - alkanolamine interactions were found not to affect the representation of VLE in aqueous solutions. Because of chemical reactions these species are never simultaneously present in aqueous solution at significant concentrations. By improving our knowledge of the thermodynamics in the binary alkanolamine-water system, we can extrapolate the binary model to very low acid gas loading. At low acid gas loading, model predictions of acid gas solubility are sensitive to parameters that quantify the interactions in the amine-water system.

4.2 MODEL STRUCTURE

In this thesis the main emphasis is given to the prediction of thermodynamic properties of aqueous AMP, MAE, and EAE solutions through COSMO-RS. Present study also includes the COSMO prediction of thermodynamic properties of aqueous MEA, DEA, and MDEA solutions. The COSMOtherm calculations have been performed the latest version of software that is COSMOtherm C30_1201. The input database for the alkanolamine-water system are derived from the resulted COSMO files through the quantum chemical COSMO calculations

based on the density functional theory (DFT) level over the whole range of amine composition.

4.3 PROCEDURE

Performing COSMO-RS computation to predict VLE and activity coefficient and infinite dilution activity coefficient for any type of molecule requires generating three types of files:

- **.Cosmo file,**
- **.Energy file**
- **.Vap file.**

The .cosmo and .energy files are generated by TURBOMOLE software while the .vap file is generated by COSMOtherm programme package. Once these files are generated the COSMOtherm program can be used to perform thermodynamic calculations. COSMOtherm predicts the thermodynamic properties by using the chemical potential derived from the COSMO-RS theory.

The thermodynamic properties calculated in this work through COSMOtherm includes,

- Excess enthalpy
- Excess Gibbs free energy
- Activity coefficient
- Total pressure
- Activity coefficient at infinite dilution
- Vapor liquid equilibrium of ternary ($\mathbf{CO_2 + EAE + H_2O}$)

The input for the alkanolamine-water system is given from the resulted .cosmo files through the quantum chemical COSMO calculations based on the density functional theory (DFT) level generated by TURBOMOLE software. Because the standard, accuracy, and systematic errors of the electrostatics resulting from the underlying COSMO calculations rely on the quantum chemical method along with the basis set, Figure (4.1) shows main window of COSMOtherm representing different sections. COSMOtherm requires a special parameterization for each and every single method / basis set combination. Each of these

parameterizations was derived from molecular structures quantum chemically optimized at the given method / basis set level. COSMO-RS calculations were done at the different parameterization levels which are as follows:

- BP/TZVP (DFT/COSMO calculation with the BP functional and TZVP basis set using the optimized geometries at the same level of theory) -parameter file: BP_TZVP_C30_1201.ctd.
- BP/SVP/AM1 (DFT/COSMO single-point calculation with the BP functional and SVT basis set upon geometries optimized at semi-empirical MOPAC-AM1/COSMO level) - parameter file: BP_SVP_AM1_C30_1201.ctd.
- B88-VWN/DNP (DFT/COSMO calculation with the B88-VWN functional and numerical DNP basis using the optimized geometries at the same level of theory) - parameter file: DMOL3_PBE_C30_1201.ctd.
- BP/TZVP/FINE (DFT/COSMO calculation with TZVP basis set followed by a single point BP-RI_DFT level calculation) – parameter file: BP_TZVP_FINE_HB2012_C30_1201.

Following are some glossaries used in MM calculations using COSMOtherm:

➔ BP/TZVP and DMOL3-PBE are production level, BP/SVP/AM1 is screening level, BP/TZVP/FINE is high level sets for COSMOtherm parameters.

➔ MOPAC is a computer program in computational chemistry implementing semi-empirical quantum chemistry algorithms.

➔ (Austin Model 1) AM1are semi-empirical quantum chemistry algorithms.

➔ TZVP, SVP, DMOL3 are basis sets.

➔ BP, and PBE (Perdew-Burke-Ernzerhof) are exchange functional correlations available in TURBOMOLE for DFT calculations.

This database levels are listed in the databases panel in general settings menu in the COSMOtherm program (Figure (4.2)). The VLE and thermodynamic properties estimation of alkanolamine-water is done with BP_TZVP_C30_1201.ctd parameterization (parameterization through quantum chemical method which is a full Turbo mole BP-RI-DFT COSMO optimization of the molecular structure using the large TZVP basis set). First step for getting started the COSMOtherm program calculation involves the selection of

alkanolamine and water molecule through two ways from the left section of the COSMOtherm main window:

- From one of the databases, using one of the buttons labeled SVP, TZVP, DMOL3, or TZVPD-FINE.
- From the FILE MANAGER (Figure (4.3)), if the molecule is not available in the database.

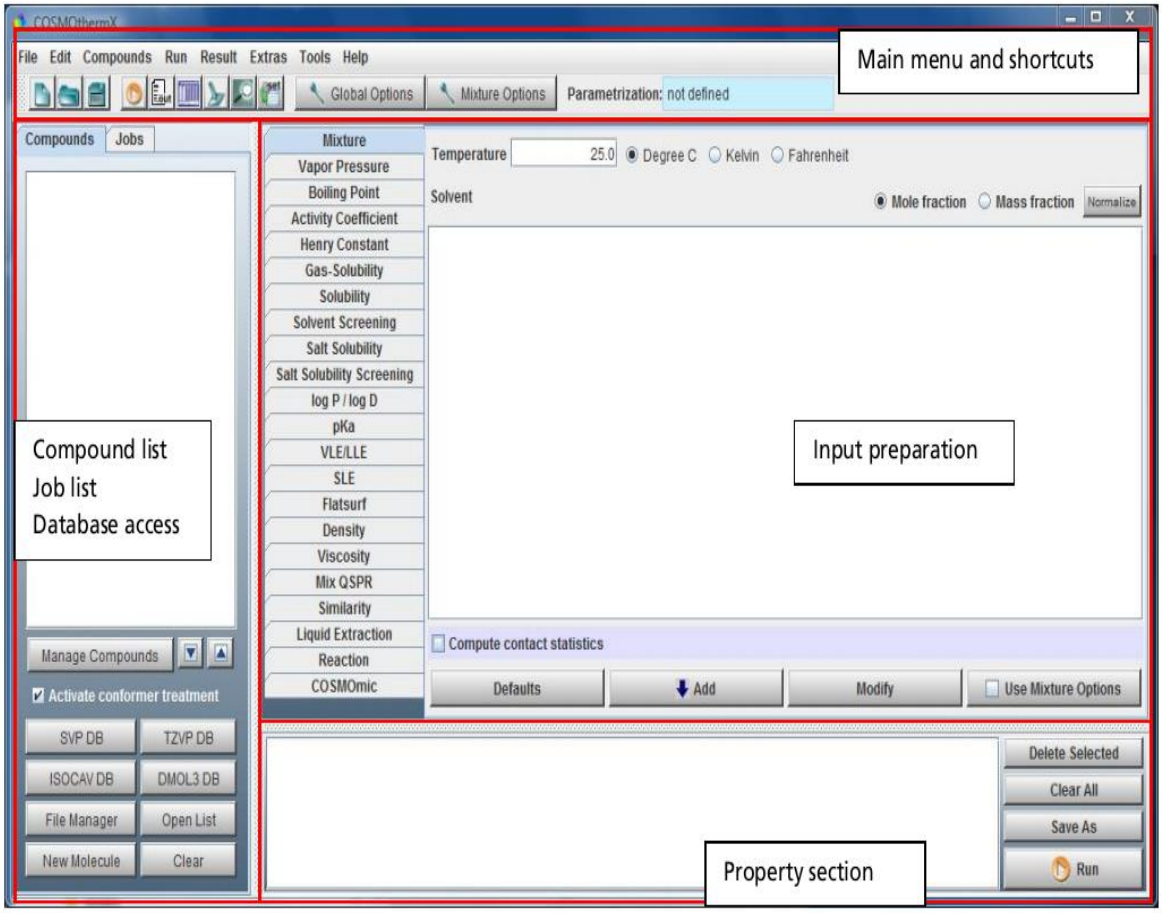

Figure 4.1**:** Main window of COSMOtherm representing different sections

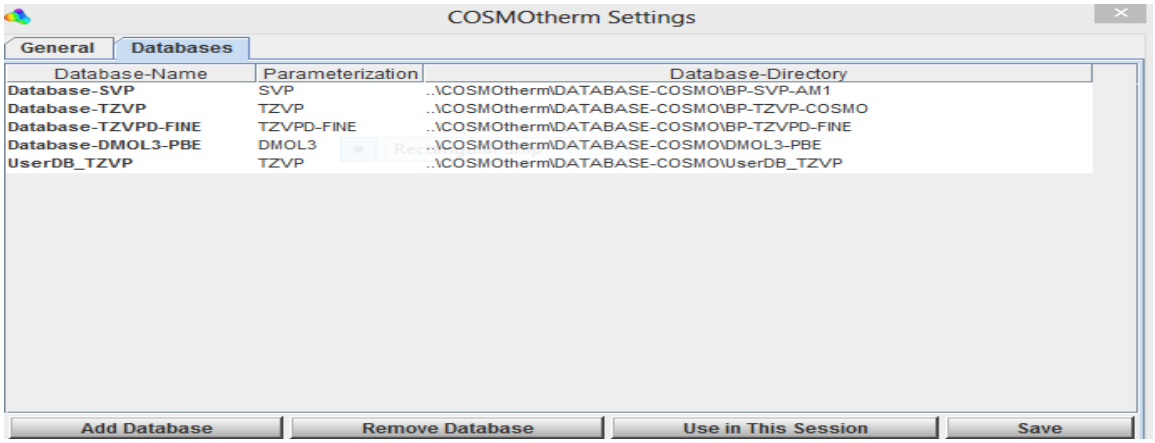

Figure 4.2: Window representing the different parameterizations

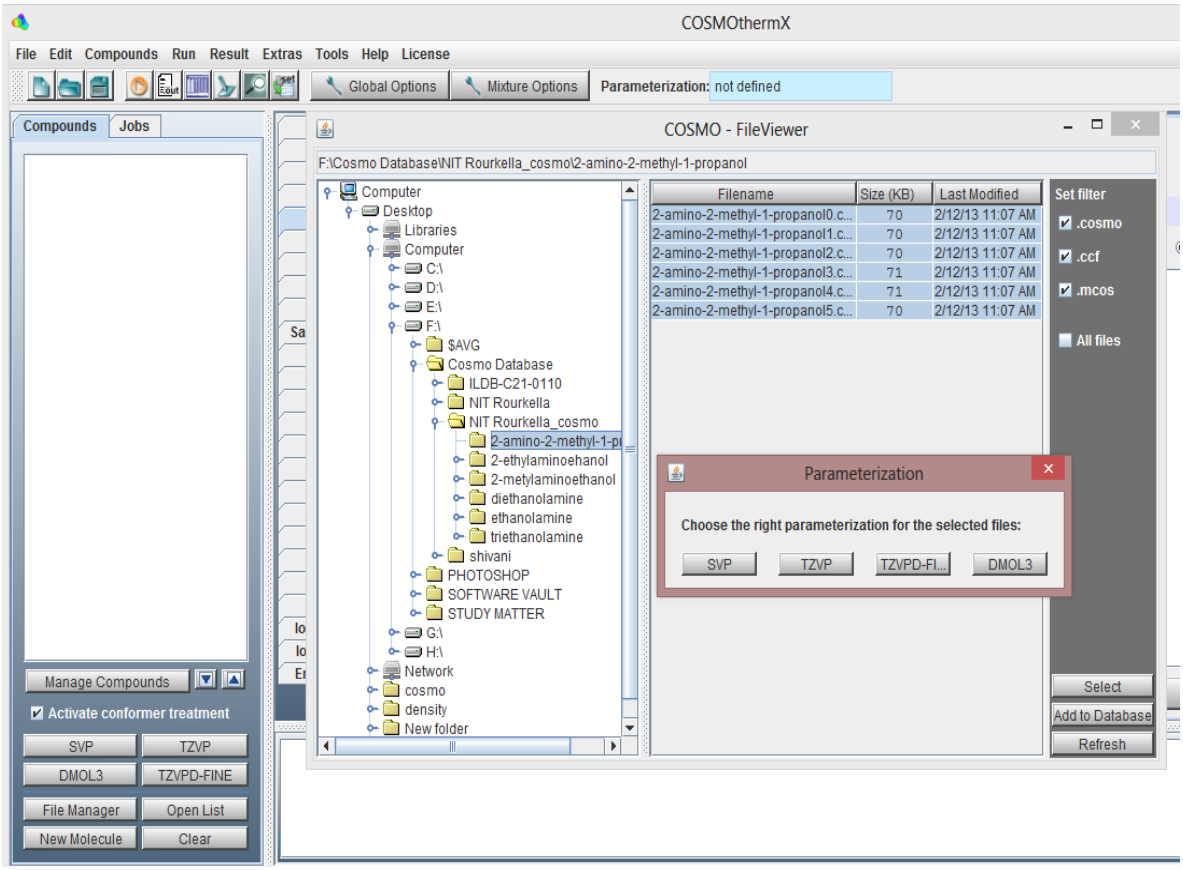

Figure 4.3: File manager window from where we select the .cosmo files for compounds and parameterization as BP-TZVP.

After selecting the alkanolamine and water molecule; we select **.vap** files to the input by right clicking on the compound name and selecting the compound properties and clicking the "USE IN INPUT" button (Figure (4.4)). Other parameters such as unit of gas phase energy

input and additional COSMOtherm output of the calculated properties can be selected from the global option in the main window. The largest section of the COSMOtherm software main window consists of the range of tabulated panels for the properties that can be calculated by the program (Figure (4.1)). Through this panel we select the activity coefficient and fix the mole fraction of pure water for getting the activity coefficient in infinite dilution Figure (4.5) whereas for calculating the other properties such as activity coefficient, excess enthalpy, excess Gibbs free energy, total pressure, chemical potential and activity coefficient model parameters we go through VLE properties Figure (4.6).

We choose the compounds, 2-ethylamino ethanol (EAE) and water from the file manager and the TZVP database repectively for finding out infinite dilution activity coeffiecient of EAE in water. During compound selection by default, the conformers of 2-ethylamino ethanol are also selected and the conformer treatment is also activated. After the selection, we set the the water mole fraction to be 1.0 and temperature to the desired value of 303.1 K, and the activity coefficient is selected from the property panel (Figure (4.5)). For the calculation of VLE properties for 2-ethylamino ethanol and water the conditions are to be set here to "isothermal" calculation, by setting the temperature ranging from 303.1 – 323.1 K and then the selection of VLE property are done from the property panel (Figure (4.6)). The output file resulting from the VLE calculation contains the activity coefficent, excess ethanlpy, excess Gibbs free energy, chemical potential, total pressure and parameters for different activity coefficient model.

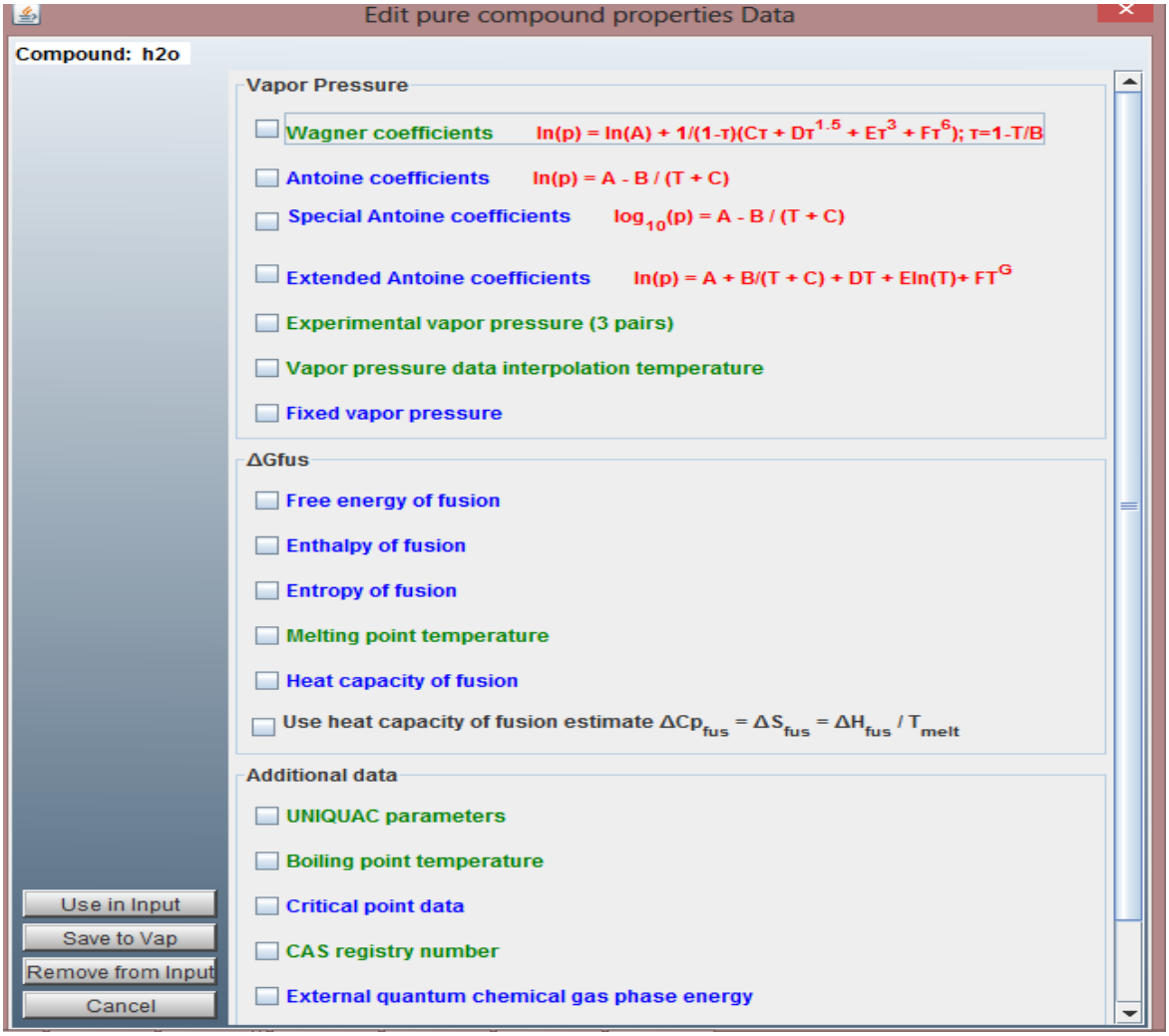

Figure 4.4: Showing the selection of compound properties

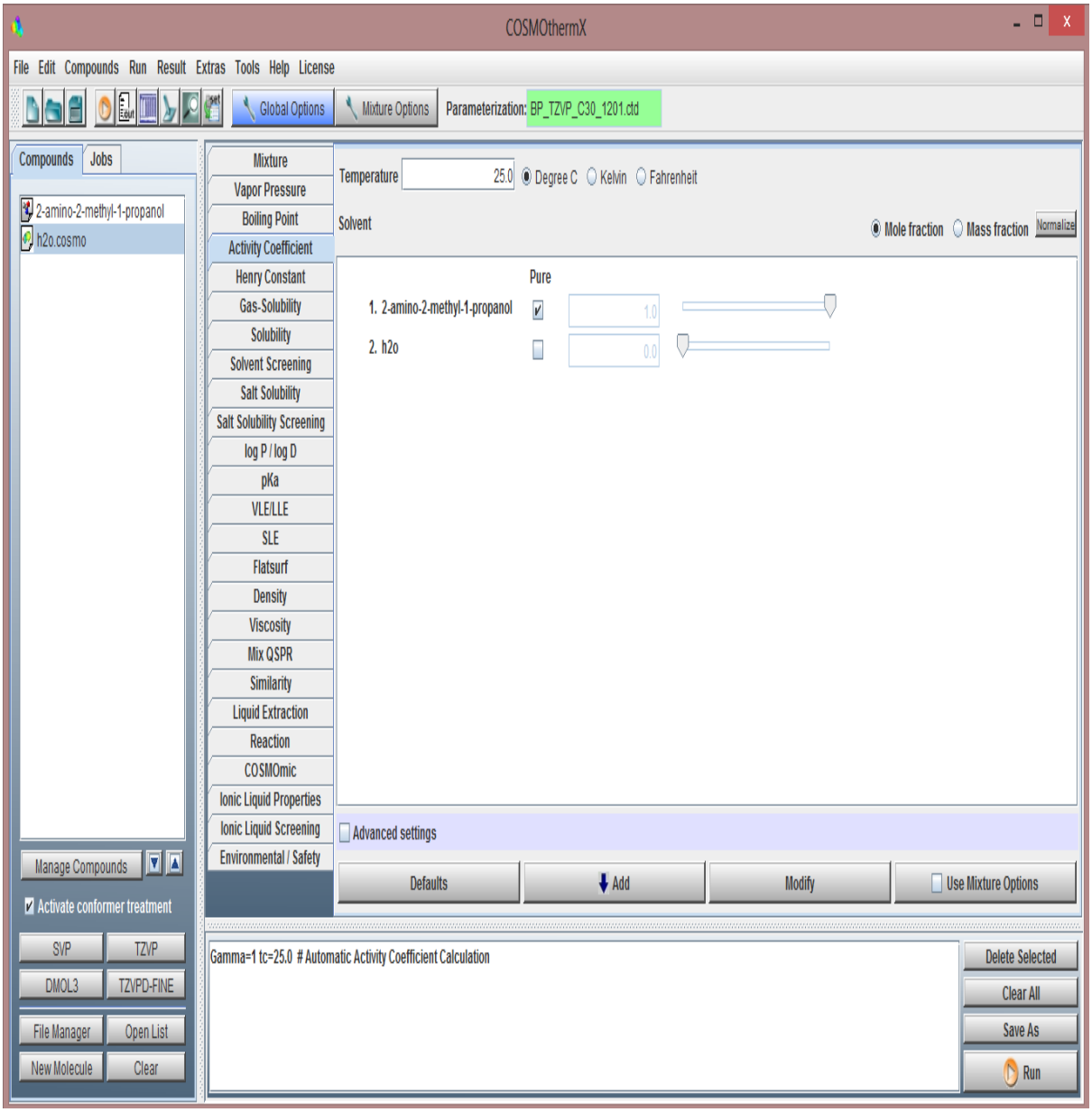

Figure 4.5: window showing the infinite dilution coefficient calcuation

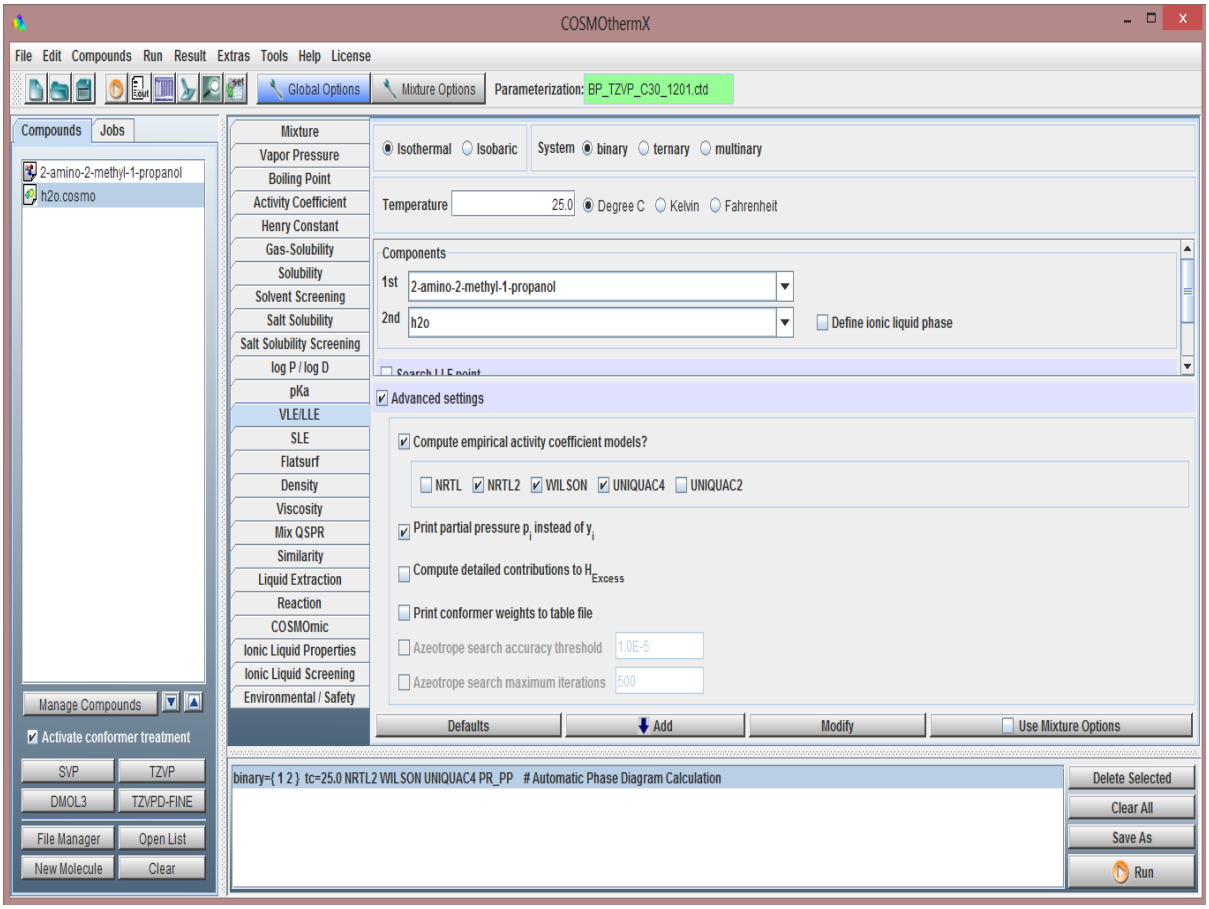

Figure 4.6: Window showing the VLE properties calculation

4.4 CALCULATION

The phase equilibria calculations are done at fixed temperature (isothermal) environment over a whole range of composition of alkanolamine-water mixture. At each composition the program calculated the different properties including the excess properties, chemical potential, activity coefficient and total pressure. The total pressures used in the computation of a phase diagram are obtained from equation (4.1):

$$P^{tot} = \sum_i P_{vap}^{xi} x_i \gamma_s^{xi} \qquad (4.1)$$

Where $\mathbf{P_{vap}^{x_i}}$ are the pure compound vapor pressures for compounds i, $\mathbf{x_i}$ are the mole fractions in the liquid phase and $\boldsymbol{\gamma_s^{x_i}}$ are the activity coefficients of the compounds as predicted by COSMOtherm.

The activity coefficient calculation is done by using the equation (4.2) using the chemical potential prediction

$$\gamma_S^{Xi} = \exp\left\{\frac{\mu_S^{Xi} - \mu_{Xi}^{Xi}}{RT}\right\} \quad (4.2)$$

Where $\mu_S^{Xi}$is the chemical potential in the liquid in phase and μ_{Xi}^{Xi} is the chemical potential of the pure compound X_i.The activity coefficients at infinite dilution is also calculated between the 303-323 K temperature by setting the mole fraction of the alkanolamine zero in the composition of the alkanolamine-water system. Figure (4.7) represents the algorithm flowchart of any property calculation at a specific temperature and any composition.

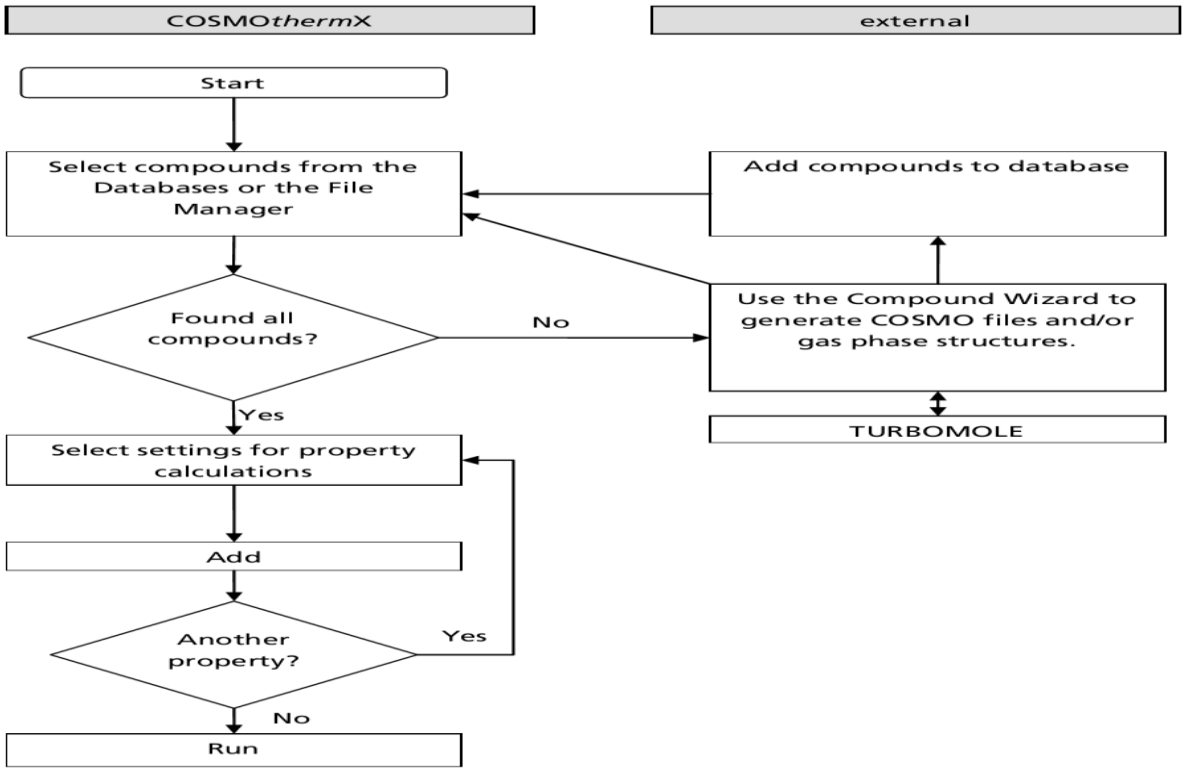

Figure 4.7: Flowchart for property calculation through COSMOtherm (reference COSMO tutorial)

4.5 RESULTS

Thermodynamics of (alkanolamine + water) system have been predicted here. Infinite dilution activity coefficients of MEA, DEA, MDEA, AMP, EAE, MAE in water and their temperature dependence have been found out. The derived values of excess Gibbs energy and

excess enthalpy for aqueous MEA, MDEA, DEA at different temperatures shows the resemblance with the literature predicted data (Kundu, Bandyopadhyay, 2007; Chang, Posey, and Rochelle, 1993). The WILSON, NRTL and UNIQUAC parameter for activity coefficients for alkanolamine- water system are also calculated for the AMP, MAE, and EAE.

COSMO predicted excess enthalpy, excess Gibbs energy, chemical potential, and activity coefficients of (alkanolamine+H_2O) solutions are shown in Figure (4.8-4.31). Excess enthalpy is defined here as the isothermal enthalpy change per mole of solution when two pure liquids mix without a chemical reaction. When defined in this way, the calorimetrically measured heat of mixing is identical to the excess enthalpy of the solution. Excess enthalpy data is useful for modeling because it is directly related to the temperature dependence of excess Gibbs energy. Therefore, in Gibbs energy model for activity coefficient, excess enthalpy measurements will provide more accurate temperature dependence for the model. Unlike others; in $(MEA + H_2O)$ system, excess enthalpy is not a prominent function of temperature. With the addition of methyl group to the amino group of alkanolamines, the value of molar excess Gibbs energy increases (it becomes less negative). Figure (4.17) $(MDEA + H_2O)$ shows positive value (0.4 KJ) for excess Gibbs energy, which is highest among all the alkanolamine + water system considered over here except $(EAE + H_2O)$ system. Very high excess Gibbs energy value (0.7 KJ) of $(EAE + H_2O)$ system is a signature of strong non-ideality, which may be due to the formation of hydrogen bonds between ethanol groups and water. Those figures also reveal that both the excess enthalpy and excess Gibbs energy tends towards less negative or positive values with increasing temperature. The concerned figures show that with the amine mole fraction tends to 1.0, $\ln \gamma_{alkanolaminer}$ tends to zero or it can be stated as activity coefficient of pure alkanolamine tends to 1.0. The COSMO predicted values of excess enthalpy, excess Gibbs energy, chemical potential, total pressure, alkanolamine activity coefficients, NRTL, WILSON, UNIQUAC parameter for activity coefficients for alkanolamine - water system, and infinite dilution activity coefficients of amines in water are also tabulated in the Tables (A.1-A.54) for aqueous MEA, DEA, MDEA, AMP, EAE, MAE systems over the range of temperature studied. COSMO predicted values of all the thermodynamic properties can be considered to be important contribution so far as the acid gas-alkanolamine-water system is concerned.

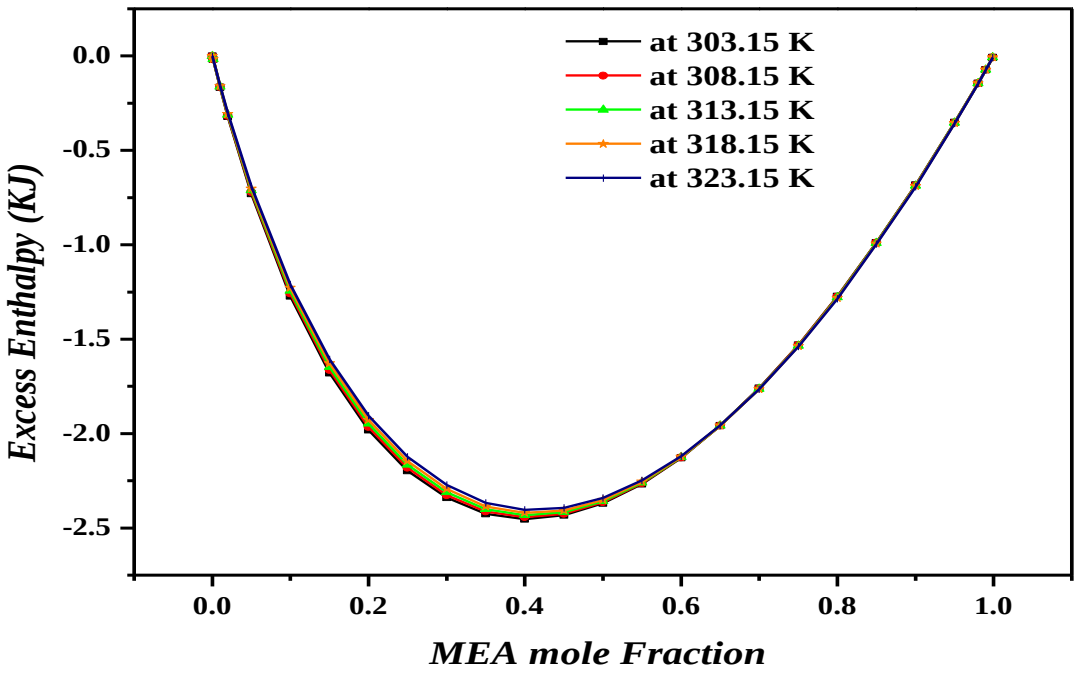

Figure 4.8: COMSO predicted Excess Enthalpy in $(MEA + H_2O)$ system in the temperature range 303.15 – 323.15 K**.**

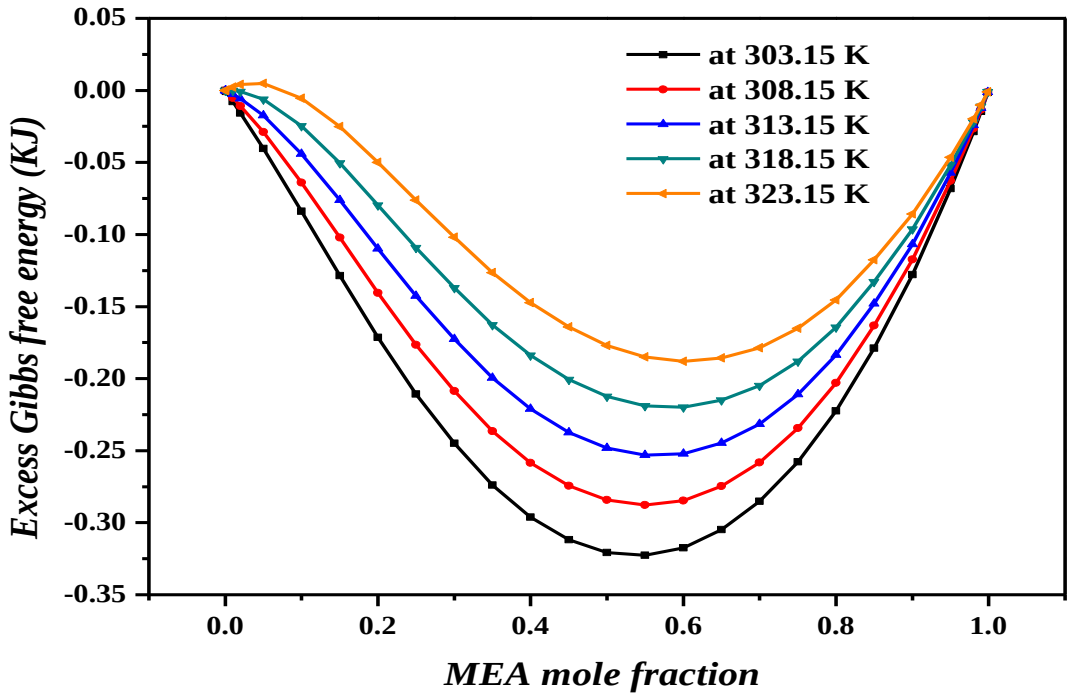

Figure 4.9: COMSO predicted Excess Gibbs free energy in $(MEA + H_2O)$ system in the temperature range 303.15 – 323.15 K**.**

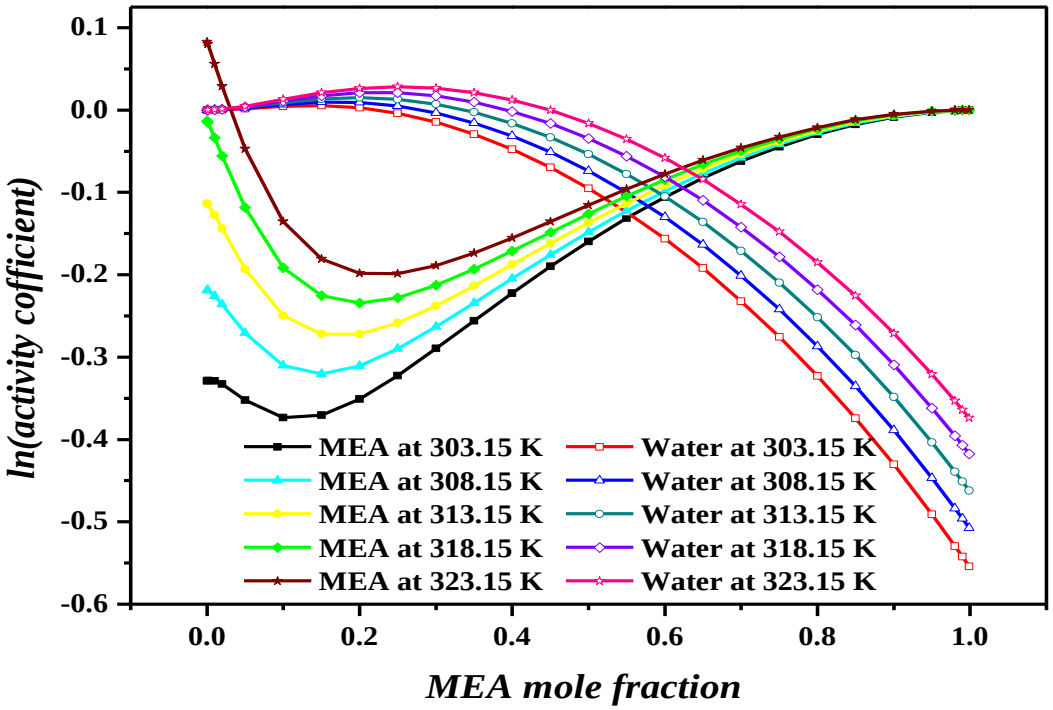

Figure 4.10: COMSO predicted MEA and water ln(activity coefficient)in $(MEA + H_2O)$ system in the temperature range 303.15 – 323.15 K**.**

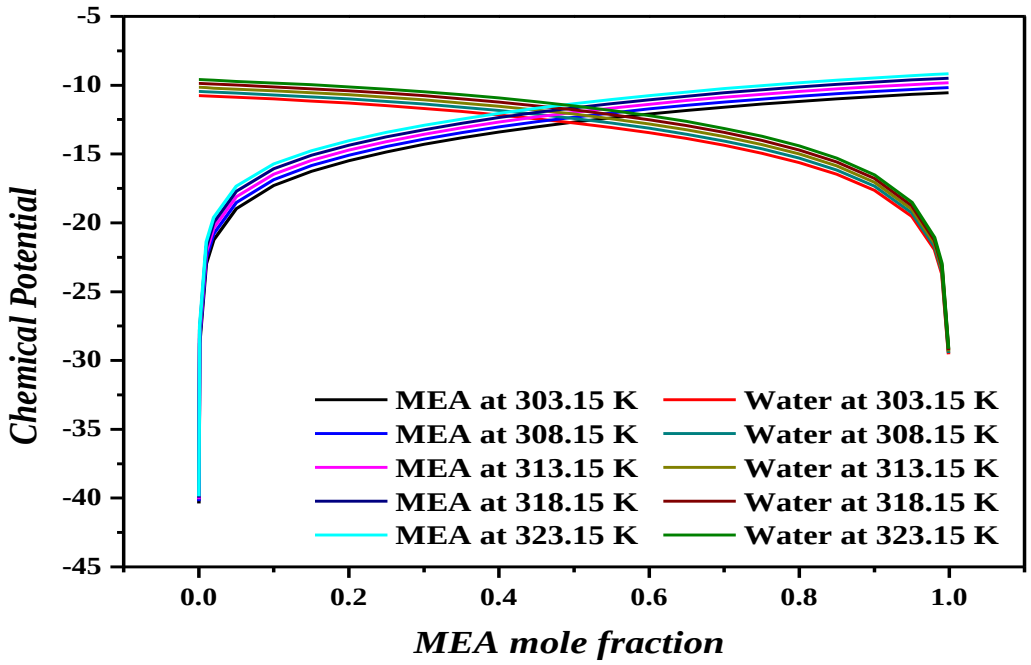

Figure 4.11: COMSO predicted MEA and water Chemical Potential in $(MEA + H_2O)$ system in the temperature range 303.15 – 323.15 K**.**

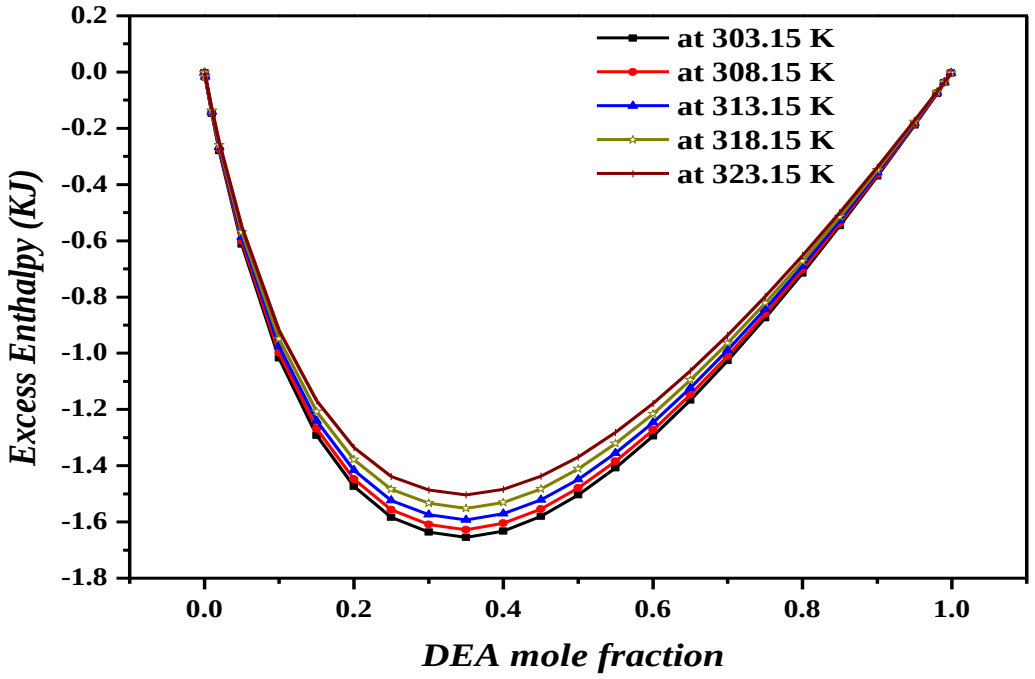

Figure 4.12: COMSO predicted Excess Enthalpy in $(DEA + H_2O)$ system in the temperature range 303.15 – 323.15 K**.**

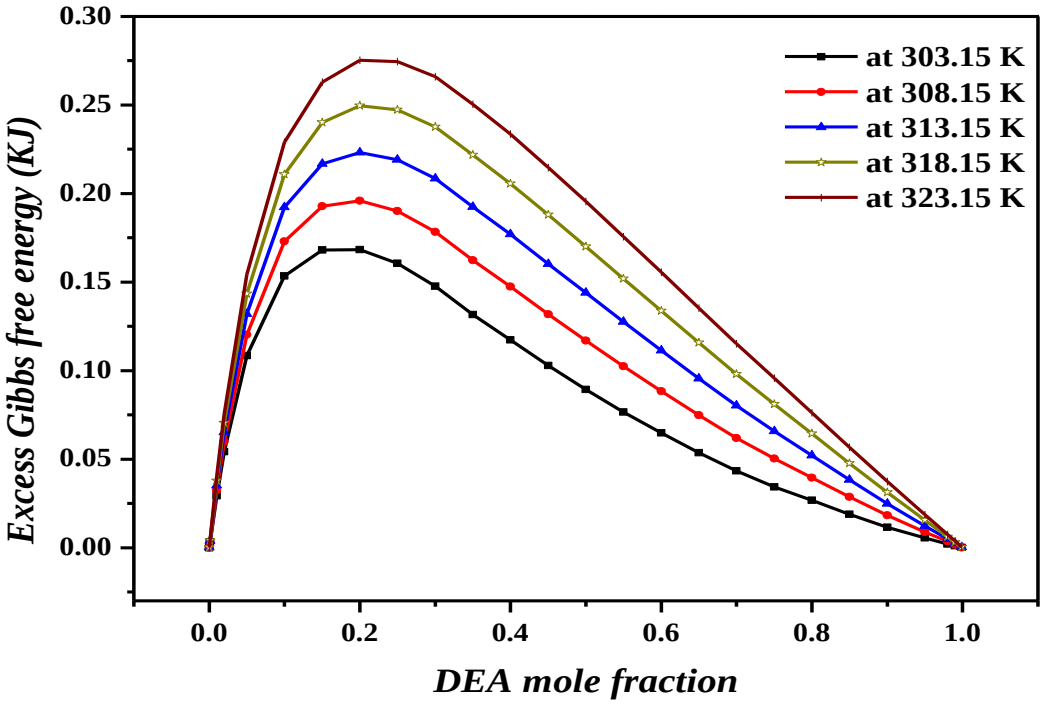

Figure 4.13: COMSO predicted Excess Gibbs free energy in $(DEA + H_2O)$ system in the temperature range 303.15 – 323.15 K**.**

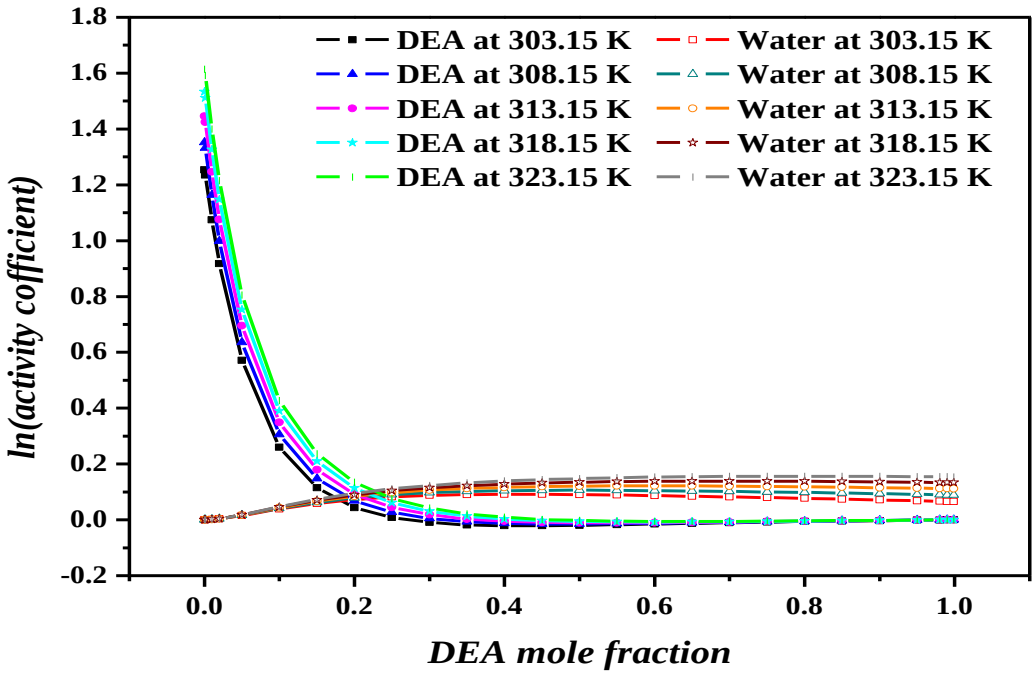

Figure 4.14: COMSO predicted DEA and water ln(activity coefficient) in $(DEA + H_2O)$ system in the temperature range 303.15 – 323.15 K

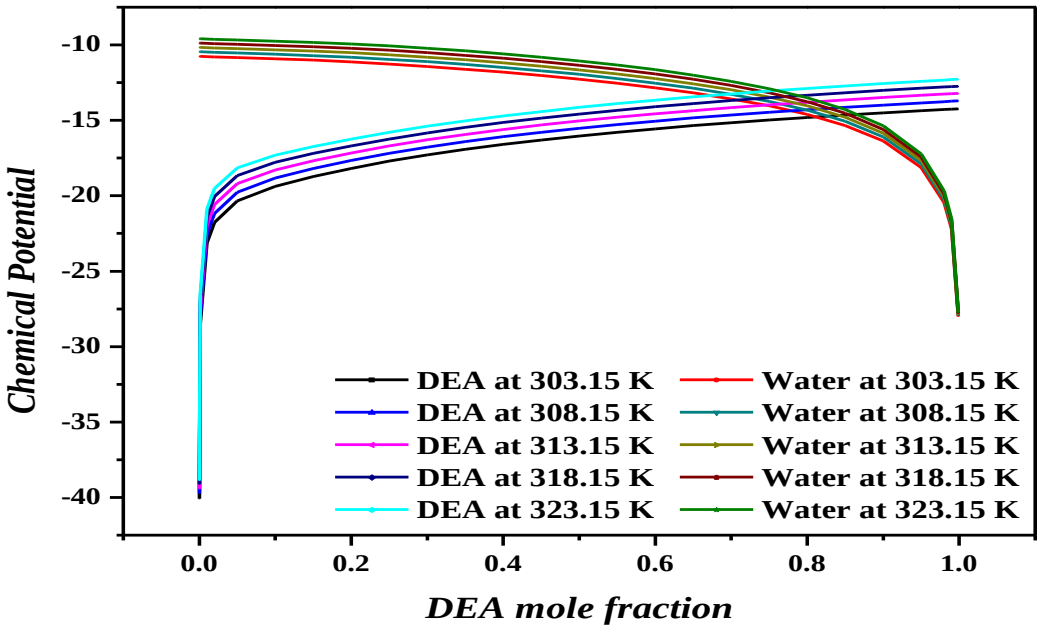

Figure 4.15: COMSO predicted DEA and water Chemical Potential in $(DEA + H_2O)$system in the temperature range 303.15 – 323.15 K**.**

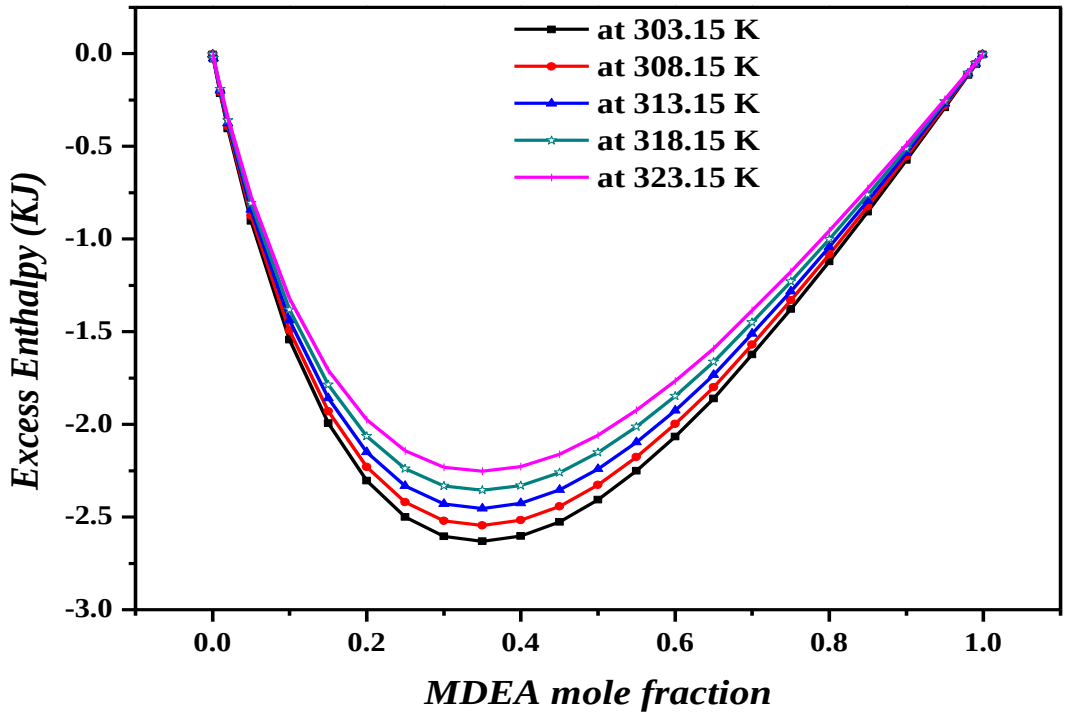

Figure 4.16: COMSO predicted Excess Enthalpy in (MDEA + H_2O) system in the temperature range 303.15 – 323.15 K.

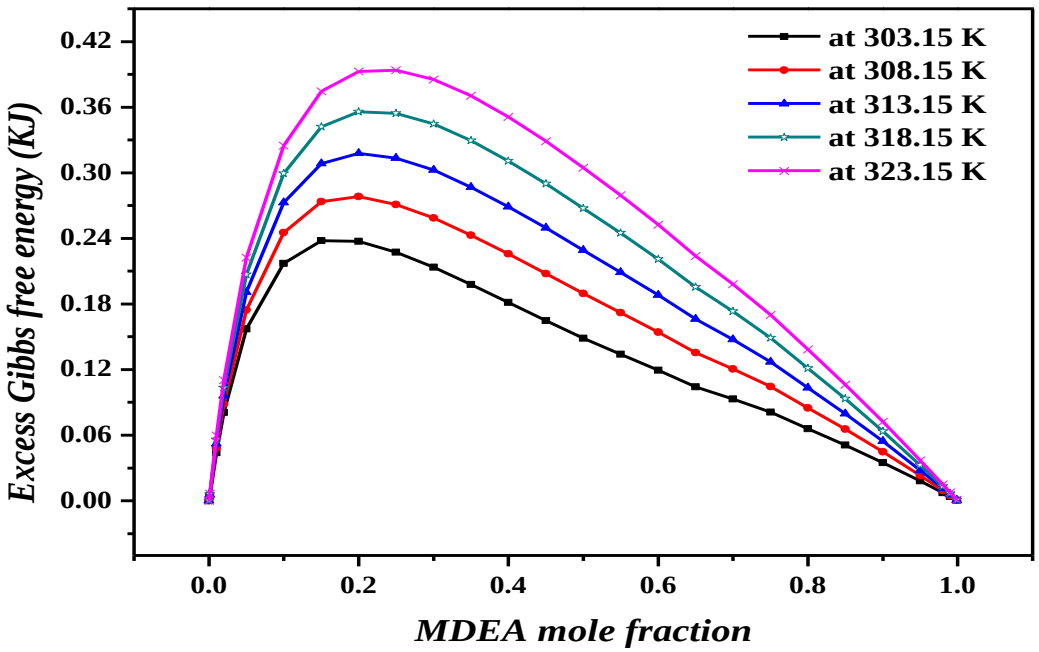

Figure 4.17: COMSO predicted Excess Gibbs free energy in (MDEA + H_2O) system in the temperature range 303.15 – 323.15 K.

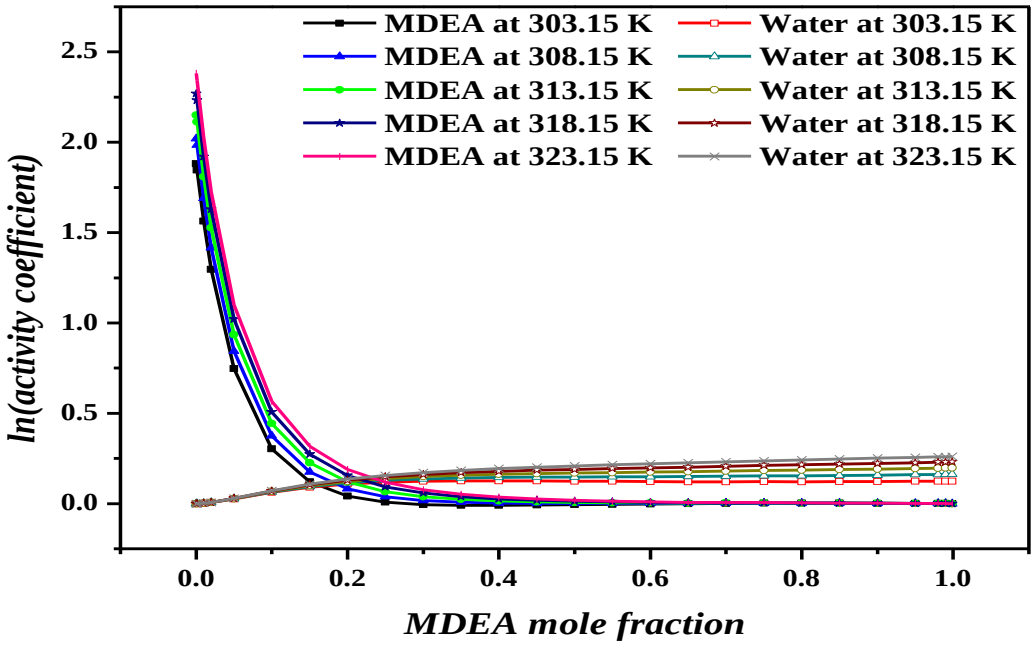

Figure 4.18: COMSO predicted MDEA and water ln(activity coefficient) in (MDEA + H_2O) system in the temperature range 303.15 – 323.15 K.

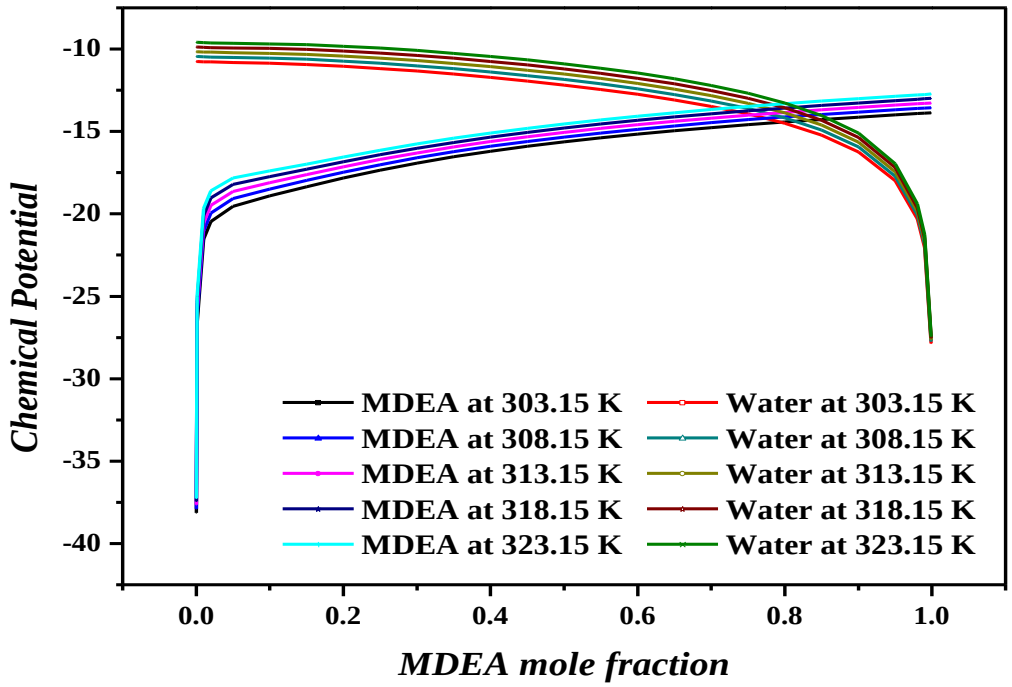

Figure 4.19: COMSO predicted MDEA and water Chemical Potential in (MDEA + H_2O) system in the temperature range 303.15 – 323.15 K.

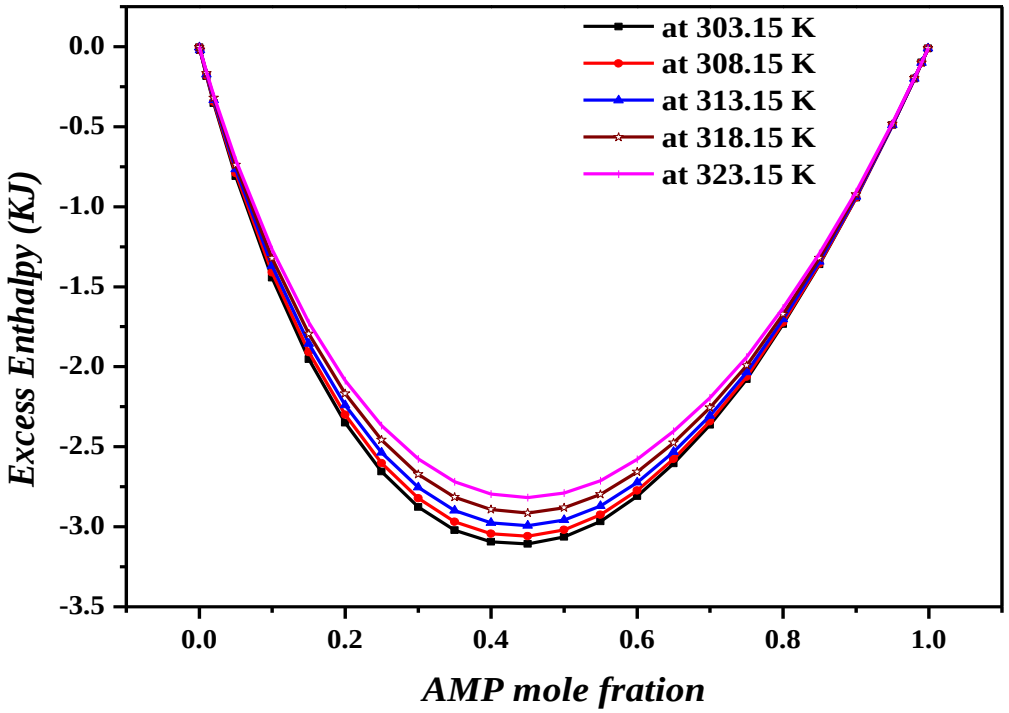

Figure 4.20: COMSO predicted Excess Enthalpy in (AMP + H_2O) system in the temperature range 303.15 – 323.15 K**.**

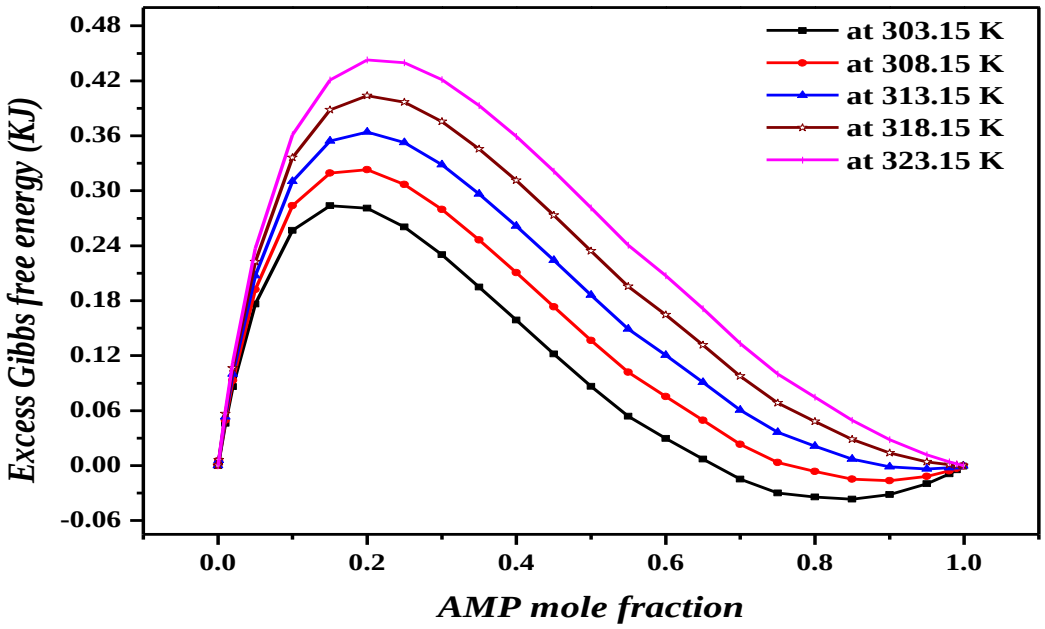

Figure 4.21: COMSO predicted Excess Gibbs free energy in (AMP + H_2O) system in the temperature range 303.15 – 323.15 K.

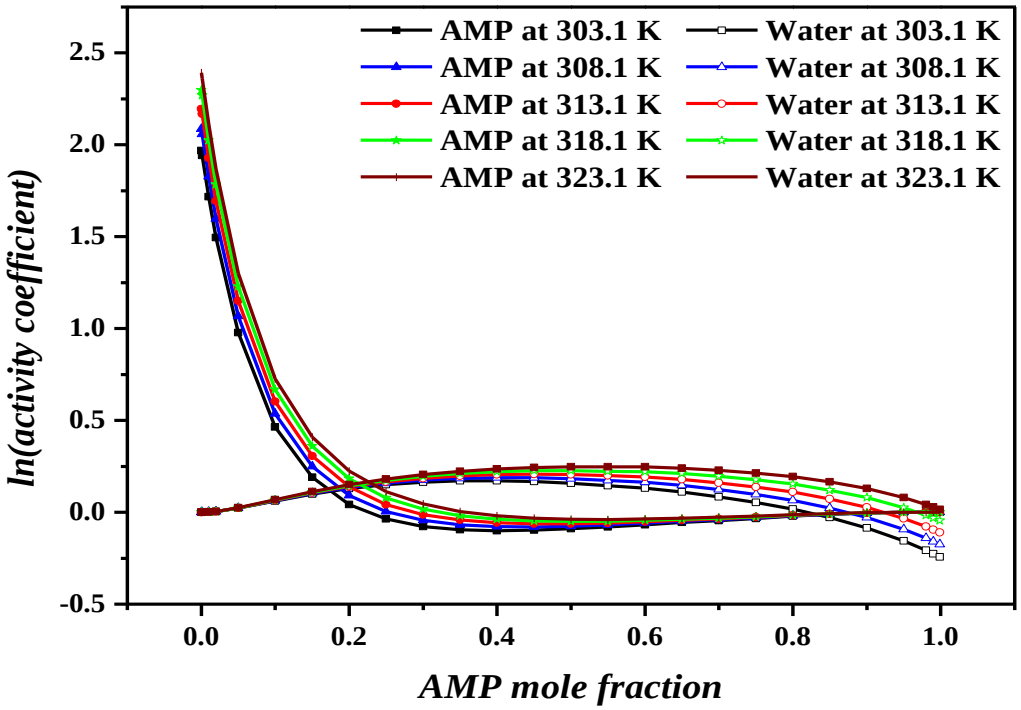

Figure 4.22: COMSO predicted AMP and water ln(activity coefficient) in (AMP + H_2O) system in the temperature range 303.15 – 323.15 K**.**

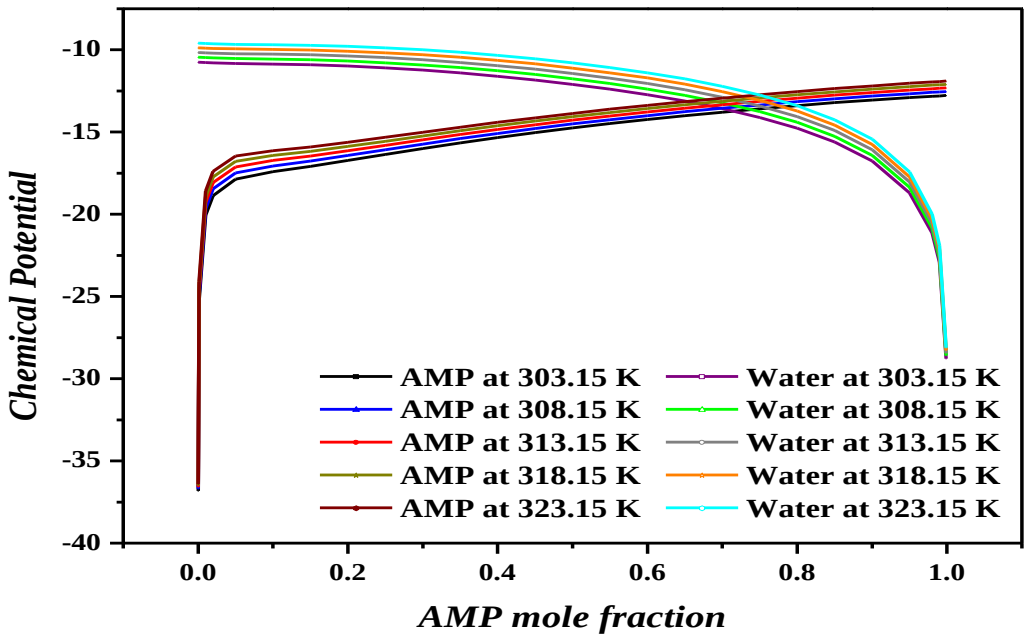

Figure 4.23: COMSO predicted AMP and water Chemical Potential in (AMP + H_2O) system in the temperature range 303.15 – 323.15 K**.**

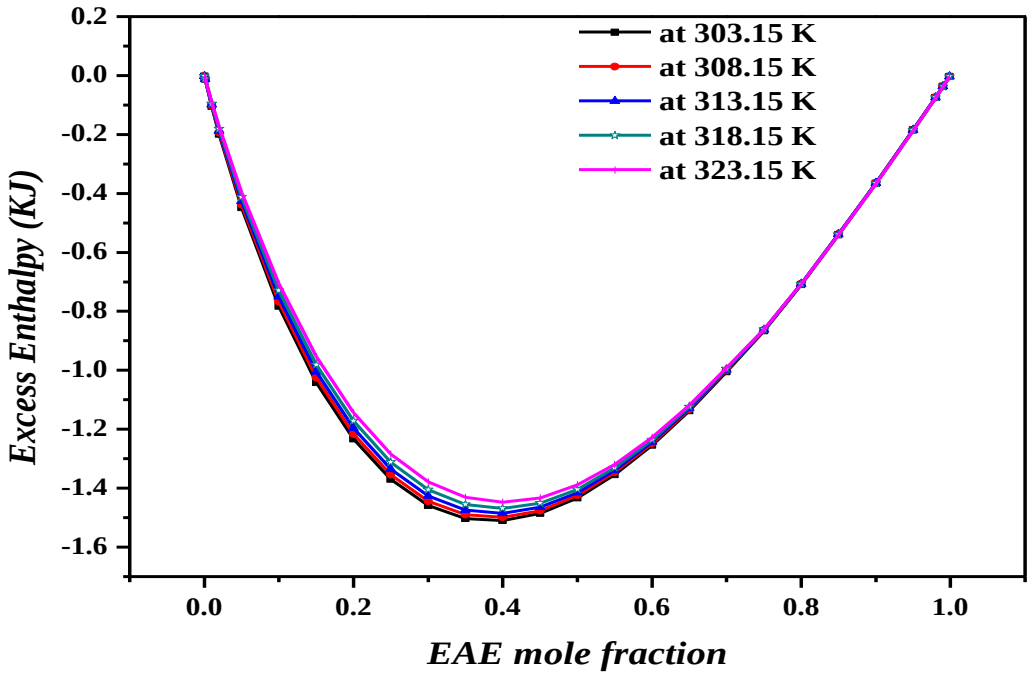

Figure 4.24: COMSO predicted Excess Enthalpy in (EAE + H_2O) system in the temperature range 303.15 – 323.15 K.

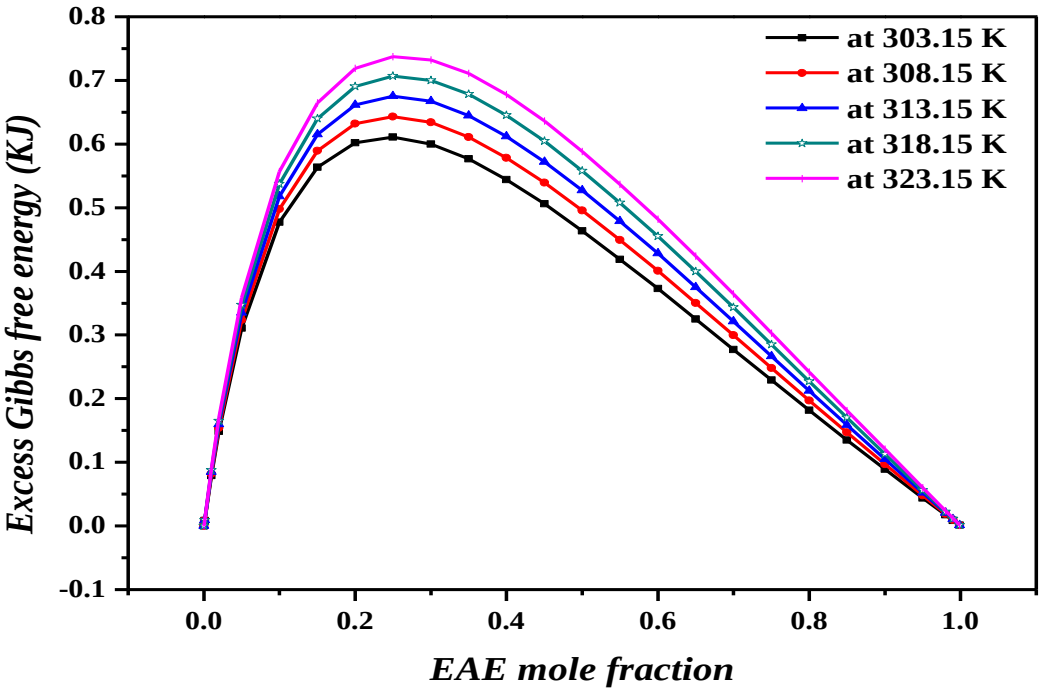

Figure 4.25: COMSO predicted Excess Gibbs free energy in (EAE + H_2O) system in the temperature range 303.15 – 323.15 K**.**

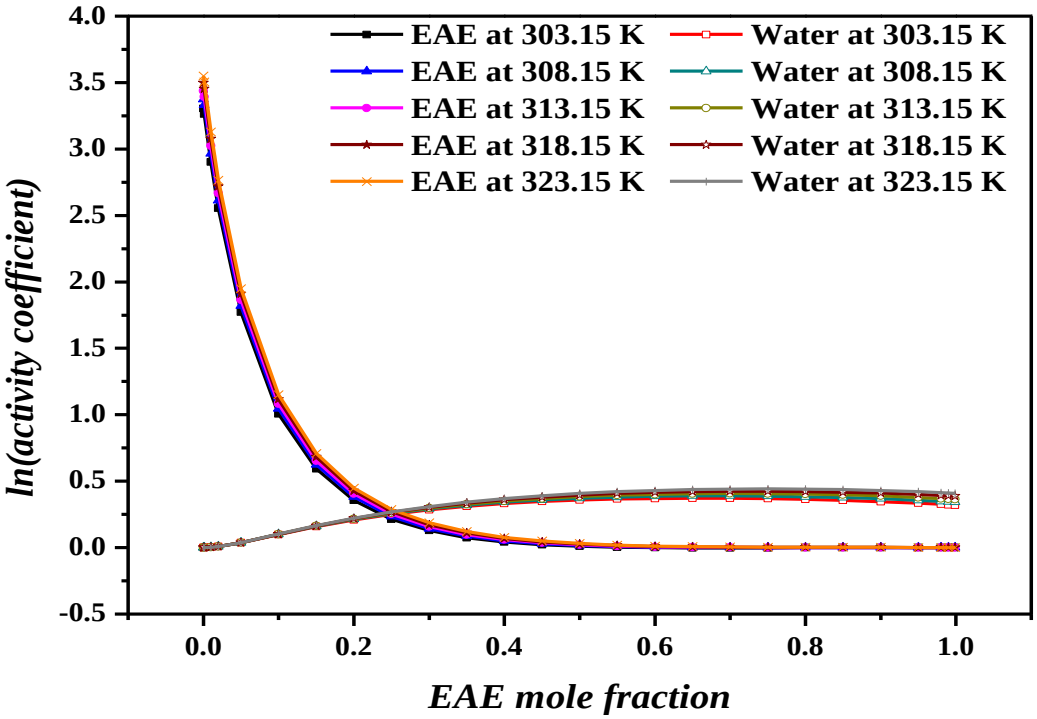

Figure 4.26: COMSO predicted EAE and water ln(activity coefficient) in $(EAE + H_2O)$ system in the temperature range 303.15 – 323.15 K.

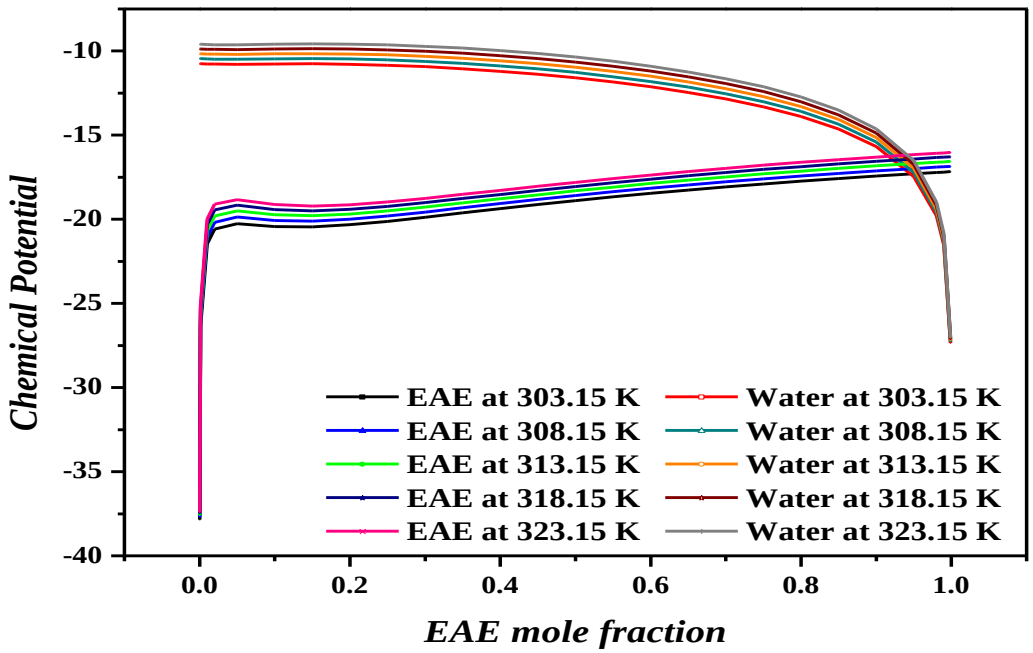

Figure 4.27: COMSO predicted EAE and water Chemical Potential in $(EAE + H_2O)$system in the temperature range 303.15 – 323.15 K.

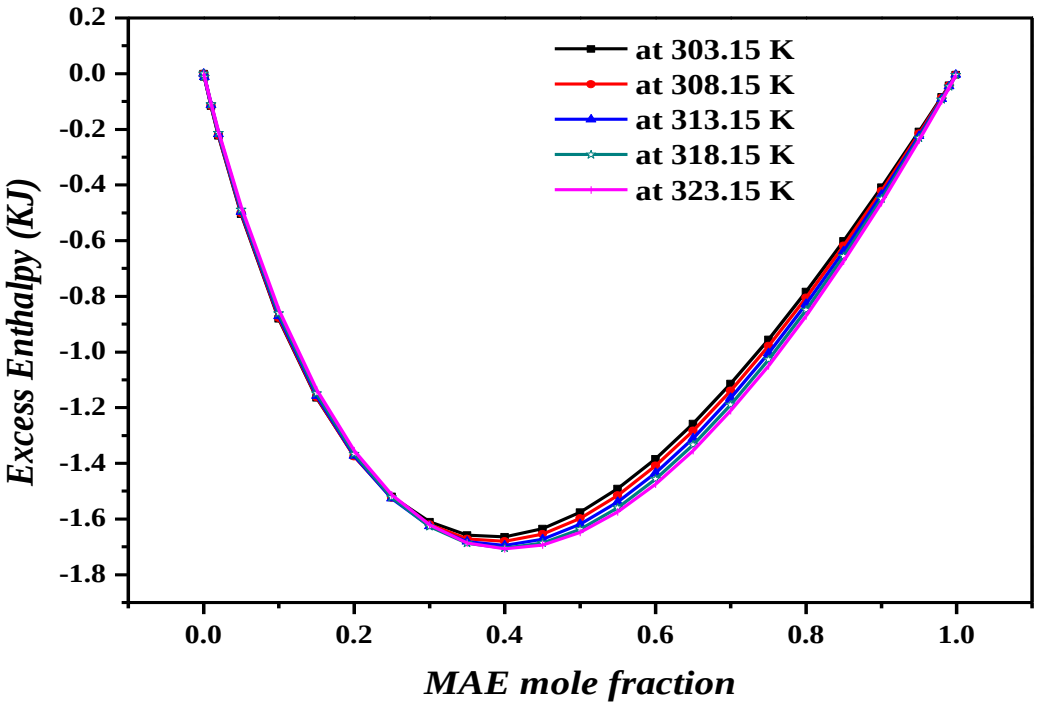

Figure 4.28: COMSO predicted Excess Enthalpy in (MAE + H_2O) system in the temperature range 303.15 – 323.15 K.

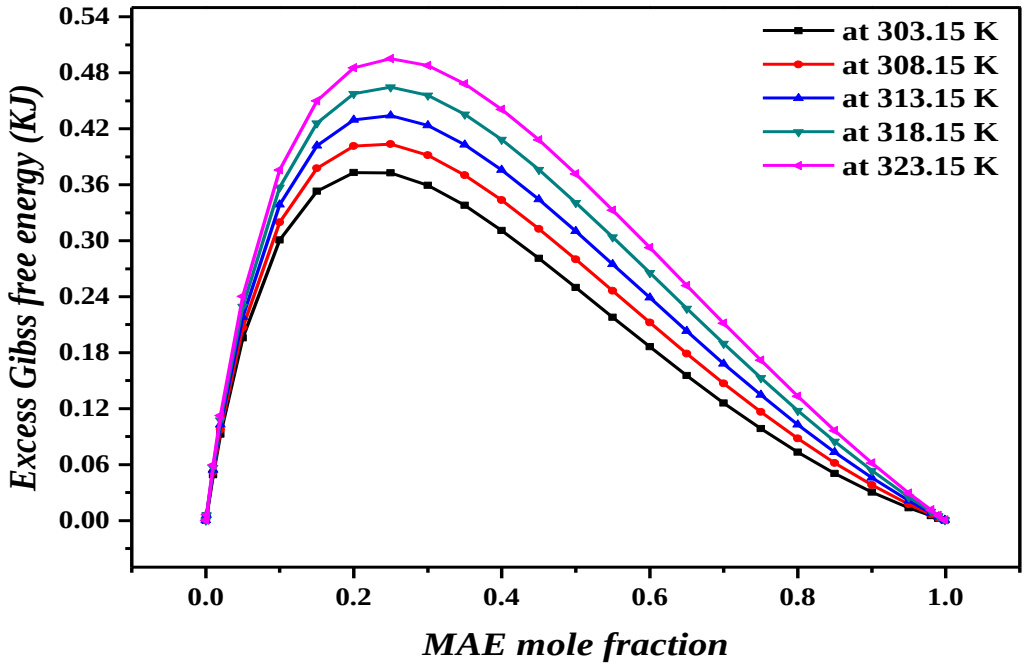

Figure 4.29: COMSO predicted Excess Gibbs free energy in (MAE + H_2O) system in the temperature range 303.15 – 323.15 K**.**

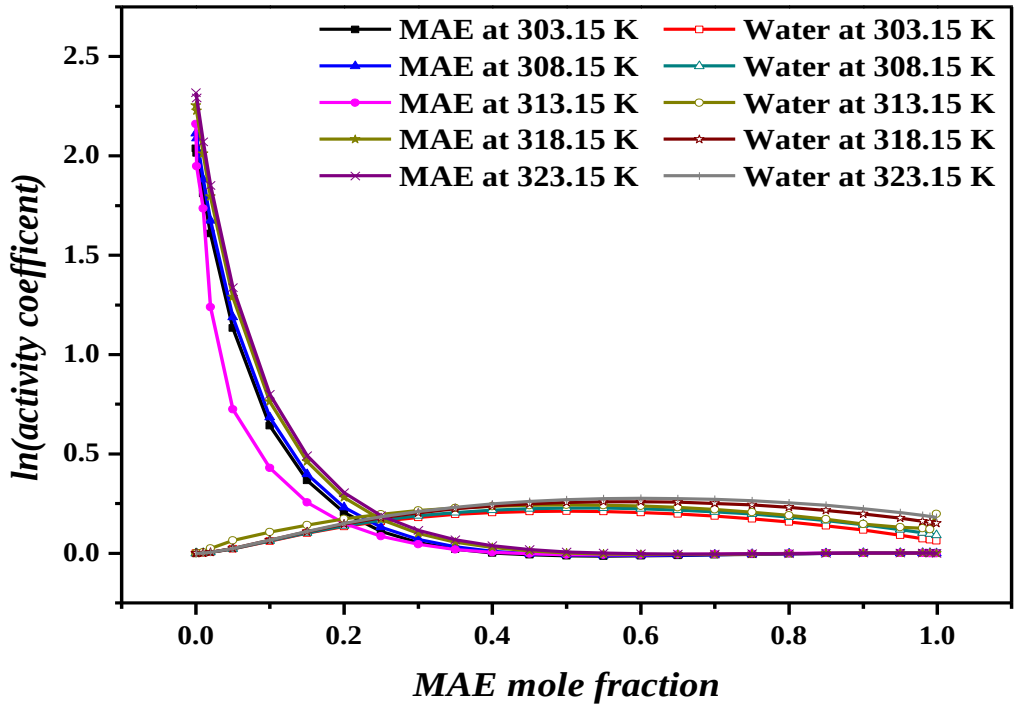

Figure 4.30: COMSO predicted MAE and water ln(activity coefficient) in (MAE + H_2O) system in the temperature range 303.15 – 323.15 K.

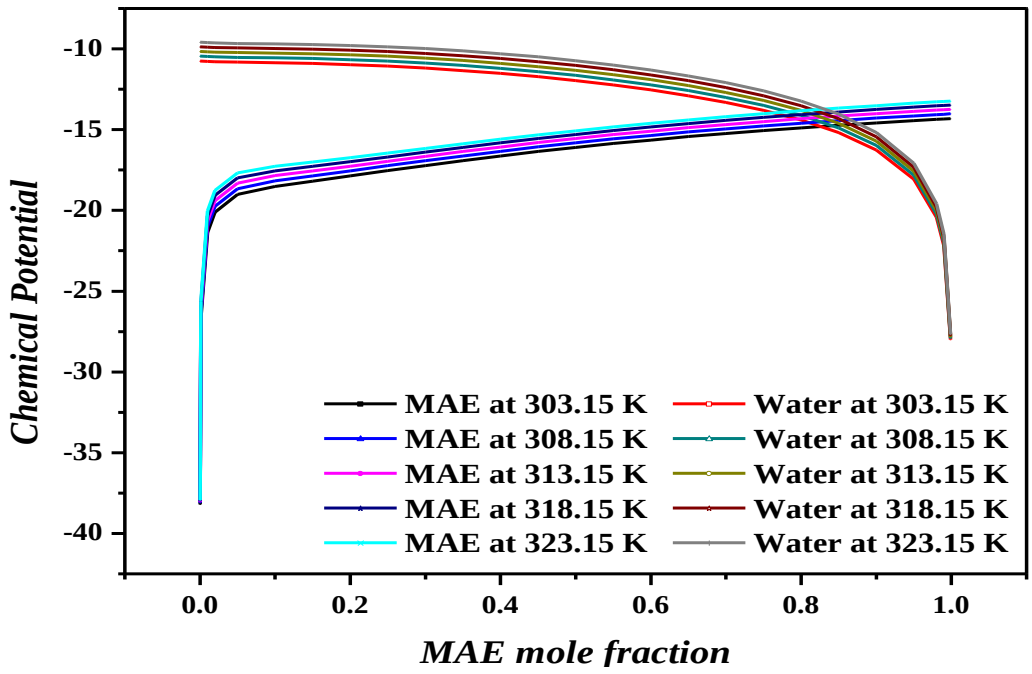

Figure 4.31: COMSO predicted MAE and water Chemical Potential in (MAE + H_2O) system in the temperature range 303.15 – 323.15 K.

REFERENCES

- Chang, H.T., Posey, M., and Rochelle, G.T., "Thermodynamics of alkanolamine-water solutions from freezing point measurements", Industrial and Engineering Chemistry Research; 32, 2324- 2335, 1993.
- Eckert, F. and Klamt, A., COSMOtherm, Version C3.0, Release 12.01; COSMOlogic GmbH & Co. KG, Leverkusen, Germany, 2005.
- Eckert, F., COSMOtherm tutorial, Version C3.0, Release 12.01, COSMOlogic GmbH & Co. KG, Leverkusen, Germany, 2005.
- Eckert, F., COSMOtherm User's Manual, Version C3.0, Release 12.01, COSMOlogic GmbH & Co. KG, Leverkusen, Germany, 2005.
- Eckert, F. and A. Klamt, "Fast Solvent Screening via Quantum Chemistry: COSMO-RS approach", American Institute of Chemical Engineers Journal, 48, 369-385, 2002.
- Kundu, M. and Bandyopadhyay, S.S., "Thermodynamics of alkanolamine and water system", Chemical Engineering Communication; 194, 1138-1159, 2007.

Chapter 5

Vapor- Liquid Equilibria of $(CO_2 + EAE + H_2O)$ system

VAPOR-LIQUID EQUILIBRIA OF $(CO_2 + EAE + H_2O)$ SYSTEM

For the rational design of the gas treating processes, the equilibrium solubility of acid gases over alkanolamines are essential. In this chapter, new experimental equilibrium data are reported for the solubility of CO_2 in EAE over a temperature range of 303.1-323.1K and COSMO-RS predicted VLE for $(CO_2 + EAE + H_2O)$system are also presented, which were tried to validate using our own experimental data.

5.1 EXPERIMENTAL SECTION

5.1.1 Materials

EAE was supplied by E. Merck, Germany, having mole % purity > 97. Double distilled water, degassed by boiling was used for making the alkanolamine solutions. Alkanolamines may be distilled under vacuum in order to remove any possible traces of moisture and other impurities like CO_2before they are used to prepare the solutions. In the present study, the prepared aqueous alkanolamine solutions were kept under vacuum for more than 10-20 minutes before commencement of reaction in the VLE cell, so that the solutions exist under their own vapor pressure only. The mole L^{-1} (strengths) equivalent of requisite mass fraction of single alkanolamine solutions were determined by titration with standard HCl using methyl orange indicator. Following the standard acid-base titration procedure, the normality of aqueous alkanolamine solutions were determined. The uncertainty in determining the composition sneaked in at transfers from pipette and burette. The estimated uncertainty in molarity was ±1 % assuming the precise and perfect determination of endpoints of titrations. Methyl orange indicator used to determine endpoints undergo color change over a narrow range of pH (3.1-4.4) in comparison to other indicators like Bromophenol blue (3.0 – 4.6) and Bromocresol green (3.8 – 5.4). Pure carbon dioxide, obtained from Vadilal Gases Limited, India, had mole % purity of 99.99.

5.1.2 Apparatus

The solubility of CO_2 in aqueous alkanolamine was measured in a stainless steel equilibrium cell. VLE measurements were done at pressures ranging from (1 to 500) kPa and at

temperatures (303.1, 313.1 and 323.1) K. The VLE apparatus consists of two stainless steel cylindrical tanks namely buffer vessel and vapor-liquid equilibrium cell of volumes 1505 ml and 785 ml, respectively, submerged in a water bath. The temperature of the water bath, hence, equilibrium cell and gas buffer is controlled within ±0.2 K of the desired level with the help of a circulator temperature controller (Polyscience, USA model No: 9712) operated on an external mode and the uncertainty in temperature measurement is ±0.1 K. Pre-calibrated platinum sensors (Pt-100, Julabo) with temperature indicator (Julabo TD300) are additionally used for measurement of temperatures in the equilibrium cell and gas buffer and the uncertainty in temperature measurement is ±0.1 K. A vacuum pump (INDVAC, Model-IV-50), capable of creating 2 kPa pressure is attached to the buffer vessel through VLE cell, and is used to evacuate both the vessels before the commencement of the experiment. Pressure transducers in the range of (0 to 1724), and (0 to 689) kPa (PMP450, FUTEK, Germany) are attached to the buffer vessel and the equilibrium cell, respectively. The accuracy and non-repeatability of each of the pressure transducers are ±0.25 % and ±0.1 % of the rated output, respectively. In the event of attainment of pressures equal to the maximum pressure limits measurable by the pressure transducers, the maximum combined uncertainty (k=2) in the pressure measurements can reach up to ± 0.36 % ($\cong \pm 0.4$ %) and ± 0.46 % ($\cong \pm 0.5$ %)of the transducers readings attached to the buffer vessel and the equilibrium cell, respectively. The VLE cell is equipped with a liquid phase stirrer (SPINOT - Magnetic Stirrer, TARSON). There are ball valves (Swagelok, Germany) controlling the transfer of gas from CO_2 cylinder to buffer vessel, and from buffer vessel to VLE cell. Figure (5.1) shows the experimental set up for VLE.

5.1.3 Procedure

For each set of run, the buffer vessel and the VLE cell were allowed to reach in temperature equilibration with water bath undergoing constant water recirculation with the help of the circulator temperature controller. Air was evacuated by vacuum pump from both the vessels at a time by opening the valve connecting both the vessel. After evacuation, the buffer vessel was made isolated from VLE cell by closing the valve between them and was allowed to receive 1.5 to 2.5 times of the desired maximum CO_2 partial pressure (total pressure here) from pure CO_2 gas cylinder. 25 ml of freshly prepared aqueous alkanolamines solution of the desired concentration was sucked into the VLE cell with the help of attached burette, and the

cell was fully sealed. The maximum error in the transferred volume was estimated to be 0.05 ml. A vacuum was initially present in the VLE cell and it was again evacuated for the second time. The VLE cell was kept under this condition over ten to twenty minutes duration so that the liquid existed under its own vapor pressure. This solution vapor pressure (p_v) was noted. The CO_2 gas from the buffer was then allowed to enter to the equilibrium cell and after the transfer, the buffer vessel was temporarily isolated from the VLE cell with the help of the valve.

Amount of CO_2; hence, moles of CO_2 being transferred from the buffer vessel was calculated using the difference in pressure transducer reading attached to it. At the commencement of absorption in VLE cell, the liquid phase stirrer was kept on. The attainment of equilibrium in the VLE cell was ensured when there was no change in total pressure of the VLE cell for at least one hour while the temperature was maintained constant at its desired level. It took about 1 hour to reach equilibrium for each run (one equilibrium point). The pressure transducer attached to the VLE cell was an indication of the total cell pressure (P_t). The equilibrium pressure (P_{CO_2}) was calculated taking the difference of total pressure of cell, P_t and vapor pressure p_v,$\left(\mathrm{P_{CO_2}} = \mathrm{P_t}\text{-}\mathrm{p_v}\right)$. Moles of CO_2absorbed by the aqueous alkanolamine blends in the VLE cell was calculated by the difference in moles of CO_2being transferred from the buffer vessel and moles of CO_2 present in the gas phase of the VLE cell at equilibrium pressure by taking in to account the compressibility factor of the gas. The method of calculation adopted regarding the number of moles of CO_2absorbed in the liquid phase; was that of described by (Park and Sandall, 2001). At that total equilibrium pressure, the CO_2loading has been expressed as moles of CO_2absorbed per moles of alkanolamine. Liquid phase mole fraction of CO_2at equilibrium was also calculated at each equilibrium point. The maximum combined uncertainty (k=2) in CO_2 loading was found to be ±3.0 % of the estimated loading. After the completion of one run, once again the valve between the buffer vessel and the VLE cell was re-opened and gas was transferred from buffer vessel to VLE cell and the whole procedure was repeated for the second run in order to generate solubility data at higher CO_2 pressure than the previous one.

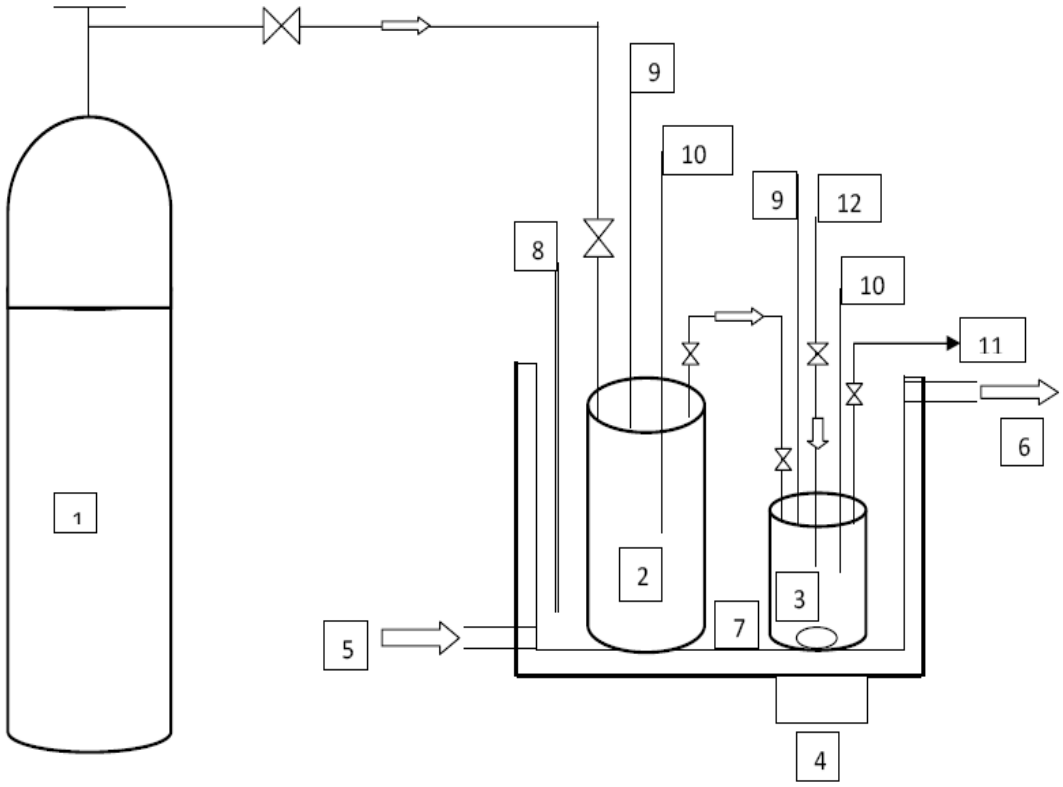

Figure 5.1: Schematic of Experimental Set-up. 1, CO_2 cylinder; 2, Buffer vessel; 3, VLE cell; 4, Magnetic Stirrer; 5, Water from circulator; 6, Water to circulator; 7, Water bath; 8, Pt. 100 temperature sensor; 9, Pressure transducer; 10, Temperature sensor; 11, Vacuum pump; 12, Burette.

5.2 RESULTS

5.2.1 Experimental results

The solubility data of CO_2in aqueous solution of the weight percentages (6, 12, 18, 24 and 30 wt%) are presented at (303.1- 323.1 K) are presented in Table (5.1- 5.2), where the CO_2 loading has been expressed in terms of (number of moles of CO_2/ number of moles of EAE). Form Table (5.1- 5.2) it is evident that at a fixed temperature, an increase in total EAE content leads to a decrease in solution CO_2 loading capacity. Table (5.1- 5.2) also satisfies that at a constant EAE concentration and CO_2 partial pressure, an increase in temperature leads to decrease in solution CO_2 loading. Calculated liquid phase mole fraction of CO_2 is also presented in the Table (5.1- 5.2).

Table 5.1: Solubility of CO_2 in aqueous (6, 12, 18, 24 wt.%) EAE solutions in the temperature range T= 303.1-323.1 K

	T = 303.1 K			**T = 313.1 K**			**T = 323.1 K**		
EAE (wt.%)	**Pco_2 (kPa)**	**α_{CO2}**	**x_{CO2}**	**Pco_2 (kPa)**	**α_{CO2}**	**x_{CO2}**	**Pco_2 (kPa)**	**α_{CO2}**	**x_{CO2}**
6	5	0.884	0.0112	5.9	0.868	0.011	6.5	0.779	0.0099
	64.2	1.155	0.0146	58.5	1.135	0.0143	37.8	0.981	0.0124
	125.8	1.216	0.0153	136.7	1.209	0.0153	139.5	1.024	0.013
	260.3	1.233	0.0156	238.3	1.259	0.0159	246.7	1.054	0.0133
	378.6	1.304	0.0164	371.3	1.305	0.0164	473.1	1.064	0.0134
	524.2	1.355	0.0171	521.5	1.383	0.0174			
12	7.5	0.829	0.022	7.4	0.764	0.0203	6.4	0.691	0.0184
	68.7	1.036	0.0274	72.1	0.985	0.026	49.5	0.917	0.0243
	154.8	1.071	0.0283	166.1	1.043	0.0275	127.6	0.984	0.026
	267.1	1.119	0.0295	244.4	1.072	0.0283	234.1	1.011	0.0267
	381.6	1.125	0.0296	378.3	1.083	0.0286	375.5	1.018	0.0269
	523.3	1.171	0.0308	520.2	1.143	0.0301	516.1	1.067	0.0282
18	0.701	0.479	0.0203	0.803	0.453	0.0192	0.802	0.355	0.0151
	13.41	0.833	0.0348	16.51	0.838	0.035	9.491	0.684	0.0288
	85.78	1.001	0.0416	84.49	1.006	0.0418	55.42	0.882	0.0368
	179.7	1.039	0.0431	157.6	1.044	0.0433	123.9	0.954	0.0397
	285.8	1.075	0.0445	266.1	1.054	0.0437	255.8	1.031	0.0428
	397.7	1.111	0.0459	386.5	1.093	0.0452	377.6	1.066	0.0441
	522.6	1.159	0.0478	508.3	1.122	0.0464	514.7	1.109	0.0458
24	0.8	0.501	0.03	0.5	0.374	0.0226	1.3	0.296	0.0179
	31.7	0.868	0.0508	11.5	0.708	0.0419	8.3	0.588	0.035
	100	0.965	0.0562	62.7	0.875	0.0512	46.8	0.769	0.0453
	207.3	1.006	0.0584	125.6	0.923	0.0539	118.8	0.847	0.0497
	387.7	1.045	0.0606	237.6	0.98	0.057	237.3	0.899	0.0525
	526.5	1.079	0.0624	404.6	1.006	0.0584	370.7	0.954	0.0556
				512.5	1.025	0.0595	519.4	0.995	0.0578

Table 5.2: Solubility of CO_2 in aqueous (30 wt.%) EAE solutions in the temperature range T= 303.1-323.1 K

	T = 303.1 K			T = 313.1 K			T = 323.1 K		
EAE (wt.%)	**Pco_2 (kPa)**	**α_{CO2}**	**x_{CO2}**	**Pco_2 (kPa)**	**α_{CO2}**	**x_{CO2}**	**Pco_2 (kPa)**	**α_{CO2}**	**x_{CO2}**
30	0.3	0.331	0.0267	0.3	0.309	0.0249	0.7	0.339	0.0273
	4.4	0.661	0.0519	8.1	0.676	0.053	8.6	0.616	0.0485
	44.1	0.877	0.0677	49	0.855	0.0661	45.9	0.782	0.0608
	131.2	0.962	0.0737	123.7	0.937	0.072	122.9	0.88	0.0679
	242.8	1	0.0764	234	0.982	0.0752	246.9	0.953	0.0731
	390.6	1.029	0.0785	385.5	1.032	0.0787	367.4	0.989	0.0757
	525.9	1.05	0.0799	523.3	1.058	0.0805	501.5	1.009	0.0771

α_{CO2} = loading of CO_2 = moles of CO_2 / moles of EAE

x_{CO_2} = mole fraction of CO_2 in liquid phase

5.2.2 COSMOtherm results

The same procedure as shown in chapter 4 is adapted here for COSMO calculations. Here the COSMO predicted excess enthalpy, Gibbs free energy and activity coefficient of $(CO_2 + EAE + H_2O)$ system against CO_2 mole fraction are shown in Figures (5.2-5.7) at fixed EAE mole fractions from 0.05-0.1. COSMO simulated results corresponding to 0.05 and 0.1 mole fraction of EAE actually signifies alkanolamine solutions relevant for CO_2 removal (containing less than 0.3 mass fractions of EAE in aqueous solutions). As the temperature increases excess Gibbs energy and enthalpy tends towards values that are more positive. As the CO_2 mole fractions tends to 0.5, excess enthalpy and Gibbs free energy of the ternary solutions tend to their maxima and minima for EAE activity coefficient, which are the signatures of non-ideality of the solution undergoing chemical reaction and vapor-liquid phase equilibrium. In the Figure (5.8) showing equilibrium CO_2 pressure versus liquid phase CO_2 mole fractions, which is generated using our own experimental data on CO_2 solubility in aqueous EAE solutions containing 0.3 mass fractions of EAE. Figures (5.9-5.10), the gas phase mole fraction of CO_2 versus liquid phase CO_2 mole fraction is depicted at fixed EAE

mole fractions. Figure (5.9) shows three distinct segments. In the first segment liquid phase mole fraction increases with increasing gas phase CO_2 mole fractions; a signature of physical equilibrium. In the second segment, liquid phase CO_2 mole fraction increases without increment in gas phase CO_2 mole fractions; rather gas phase CO_2 mole fractions are decreasing, which signifies enhanced role of chemical reaction equilibria over physical equilibria. The last segment again emancipates physical equilibrium. As the alkanolamine mole fraction increases in the ternary solutions (Figure (5.10), where EAE mole fractions is 0.1, this distinct delineation among vapor-liquid phase equilibrium and chemical reaction equilibrium remains but the advantage of chemical reaction equilibria is becoming bleak. The observations from Figure (5.11) shows the gas phase mole fraction of CO_2 versus liquid phase CO_2 mole fractions depicted at fixed EAE mole fraction of 0.08 .Figures (5.9-5.11) affirm the fact, that at lower EAE concentration (say, EAE mole fractions is 0.05), we get maximum CO_2 loading in the liquid phase without a substantial increment in equilibrium CO_2 pressure. This benefit of chemical reaction equilibria is realizable for a solution containing less than 0.1 mole fraction of EAE. Hence, aqueous EAE solutions containing 0.06-0.3 mass fractions of EAE can be considered as potential solvent for effective CO_2 removal. Tables (A.55-A.60) present the values of COSMO predicted excess enthalpy, Gibbs free energy and activity coefficients and VLE data of ($CO_2 + EAE + H_2O$) solutions which further supports the facts already provided in the figure. Tables (A.61-A.62) shows the gas phase mole fraction of CO_2 corresponding to liquid phase CO_2 mole fraction for fixed EAE mole fraction of 0.05 and 0.1.

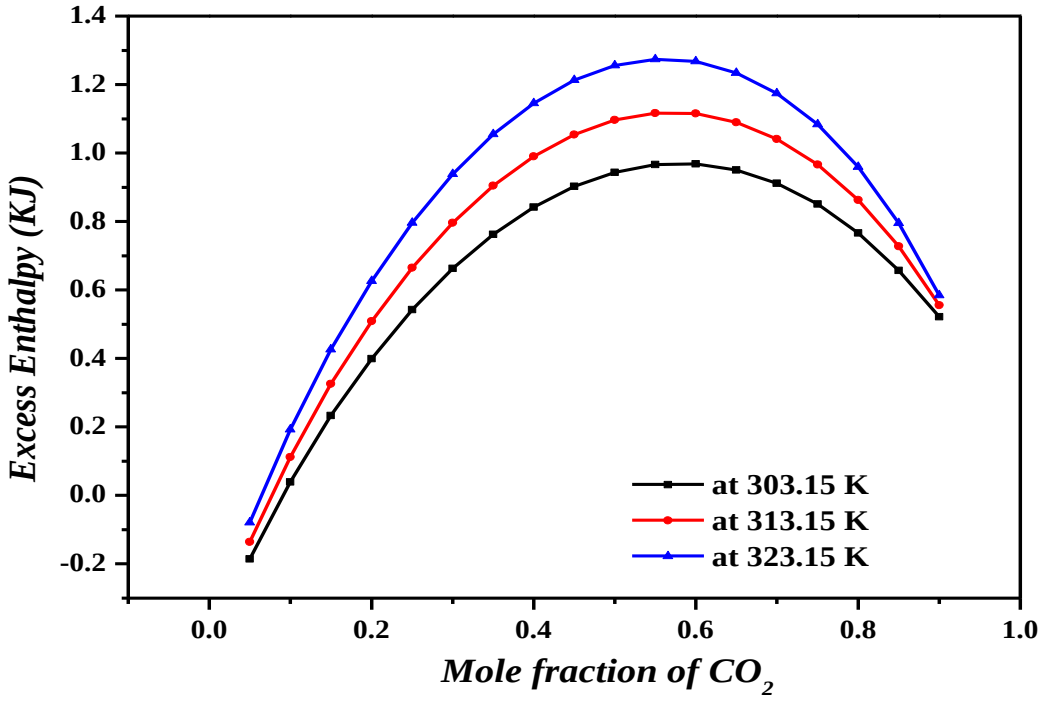

Figure 5.2: COMSO predicted Excess Enthalpy in $(CO_2 + EAE + H_2O)$ system in the temperature range 303.15 – 323.15 K at 0.05 EAE mole fractions.

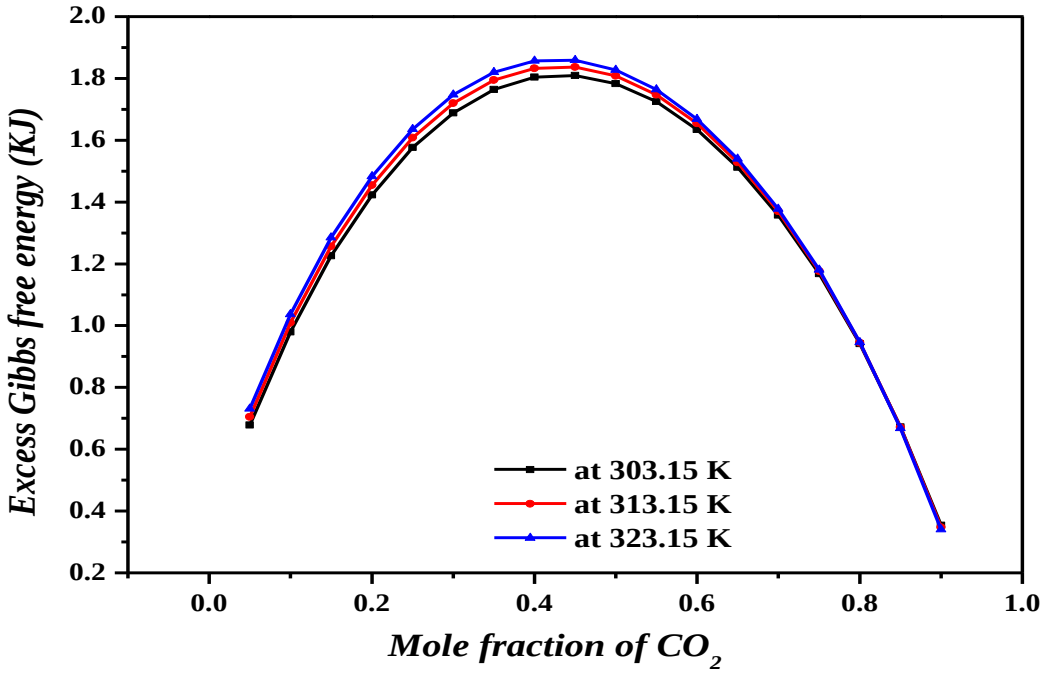

Figure 5.3: COMSO predicted Excess Gibbs free energy in $(CO_2 + EAE + H_2O)$ system in the temperature range 303.15 – 323.15 K at 0.05 EAE mole fractions.

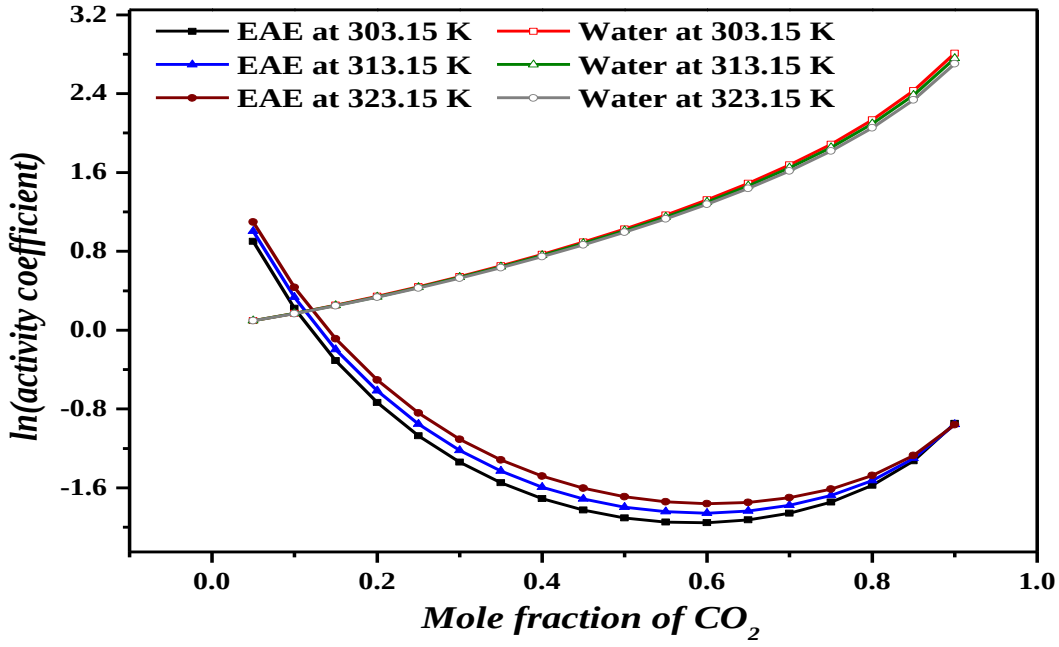

Figure 5.4: COMSO predicted EAE and water ln(activity coefficient) in (CO_2 + EAE + H_2O) system in the temperature range 303.15 – 323.15 K at 0.05 EAE mole fractions.

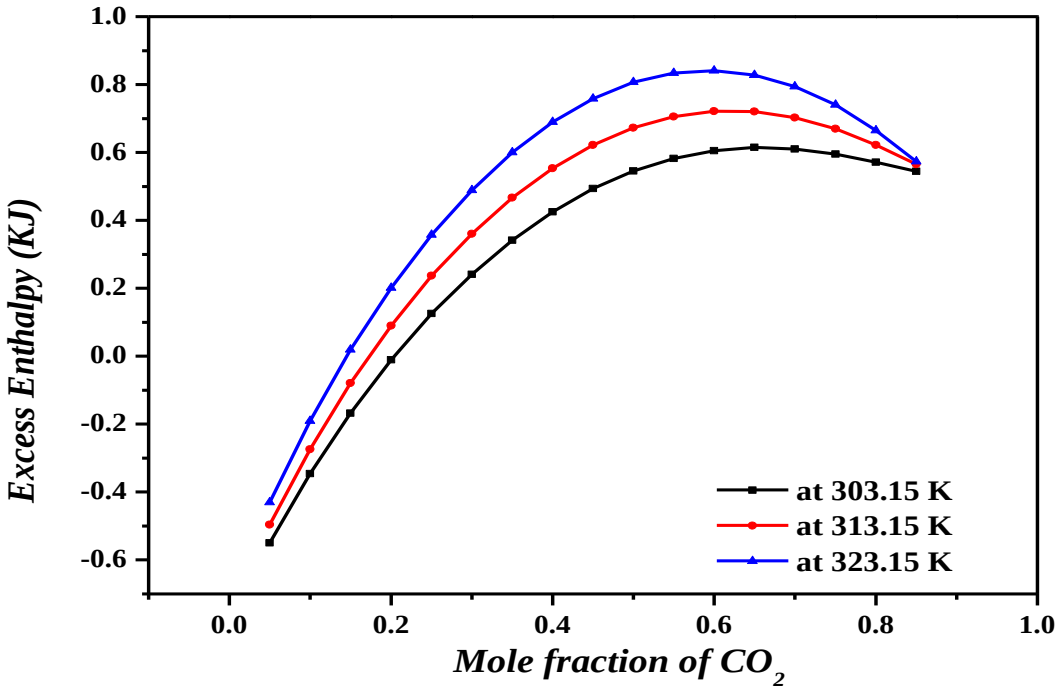

Figure 5.5: COMSO predicted Excess Enthalpy in (CO_2 + EAE + H_2O) system in the temperature range 303.15 – 323.15 K at 0.1 EAE mole fractions.

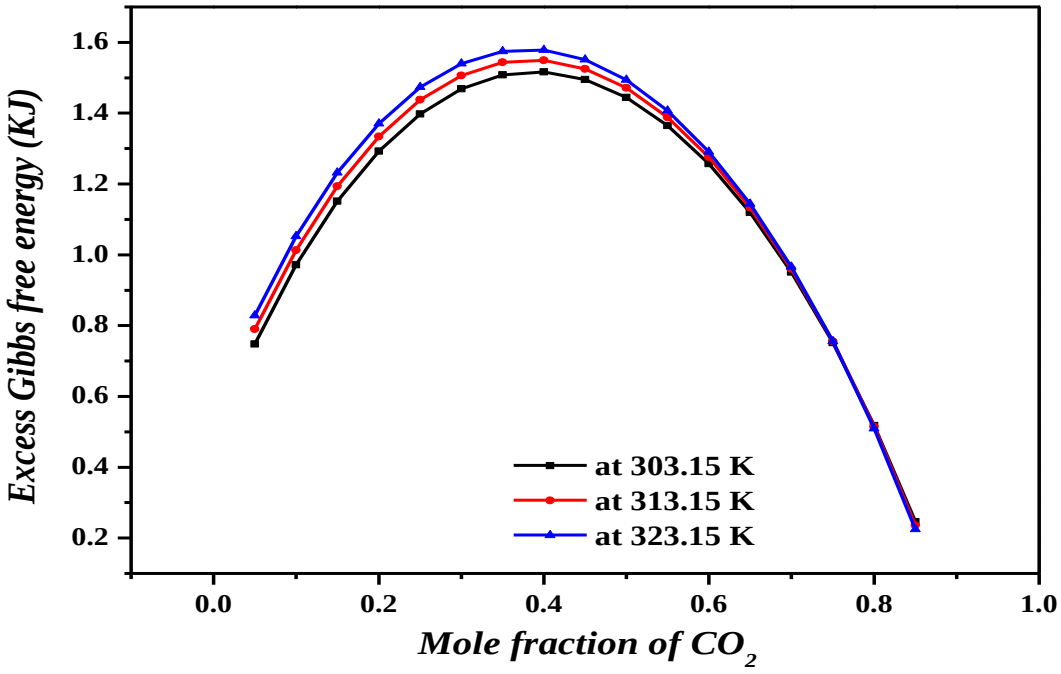

Figure 5.6: COMSO predicted Excess Gibbs free energy in (CO_2 + EAE + H_2O) system in the temperature range 303.15 – 323.15 K at 0.1 EAE mole fractions.

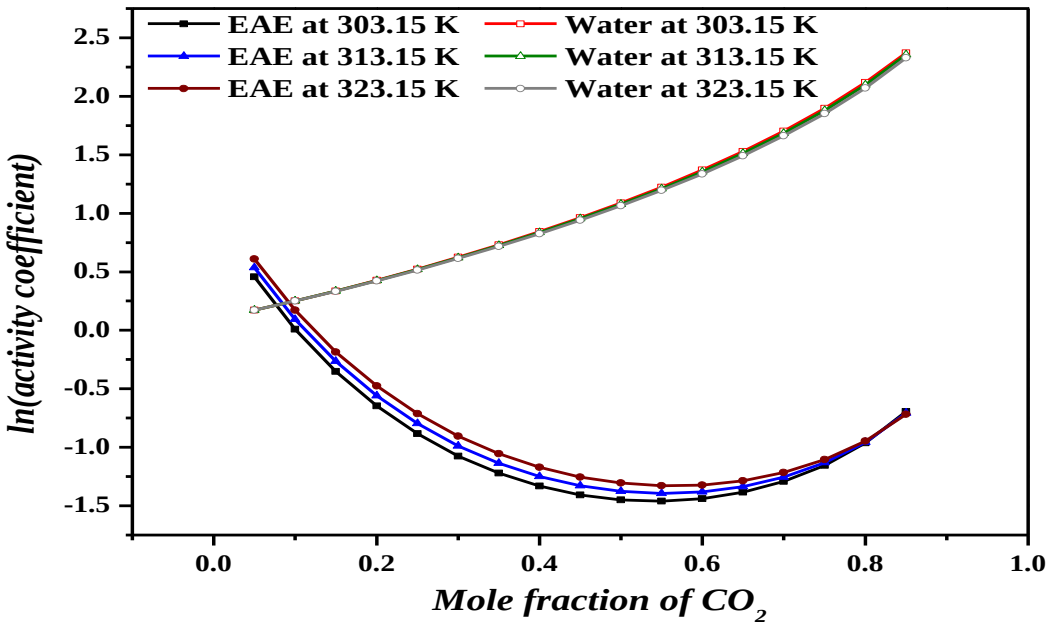

Figure 5.7: COMSO predicted EAE and water ln(activity coefficient) in (CO_2 + EAE + H_2O) system in the temperature range 303.15 – 323.15 K at 0.1 EAE mole fractions.

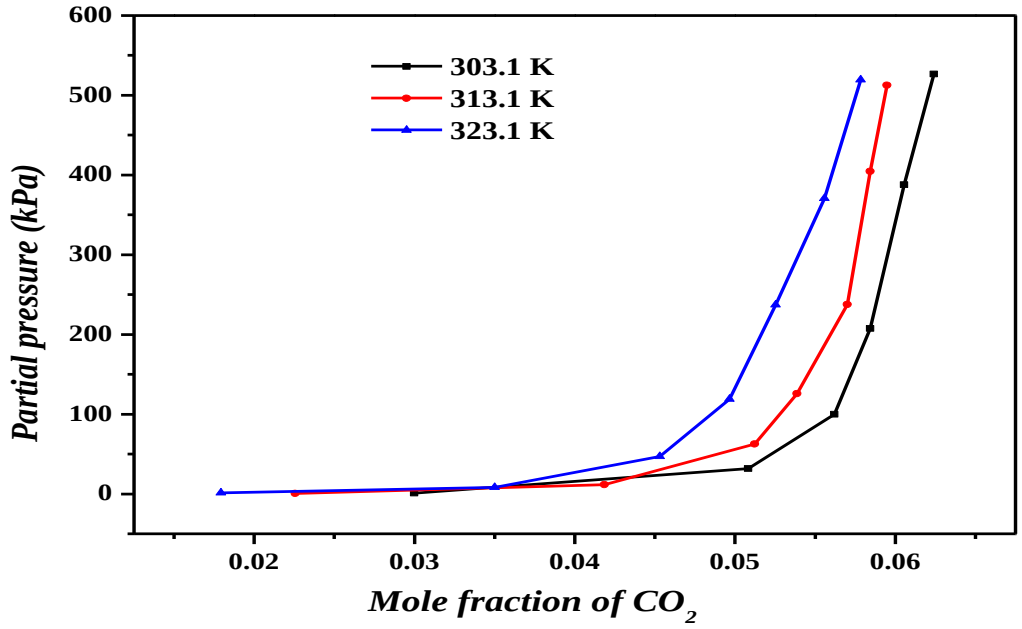

Figure 5.8: Equilibrium CO_2 pressure versus liquid phase mole fraction of CO_2 in the aqueous EAE solutions (0.08 EAE mole fractions) at temperatures 303.1-323.1K

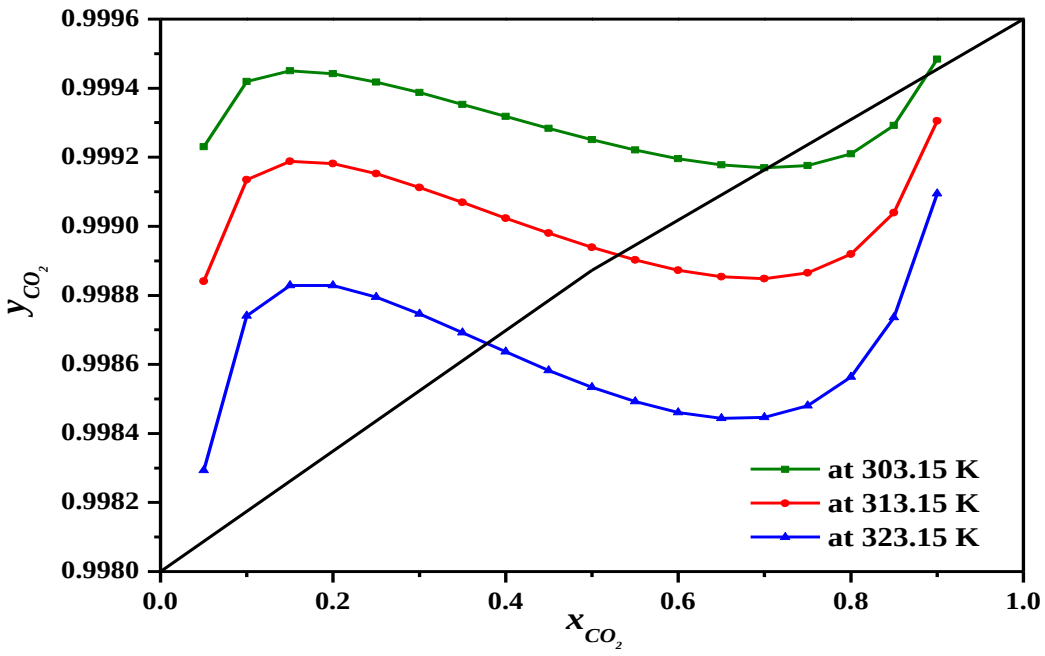

Figure 5.9: COSMO predicted Gas phase versus liquid phase mole fraction of CO_2 (CO_2 + EAE + H_2O) system (0.05 EAE mole fractions) at temperatures 303.15-323.15K.

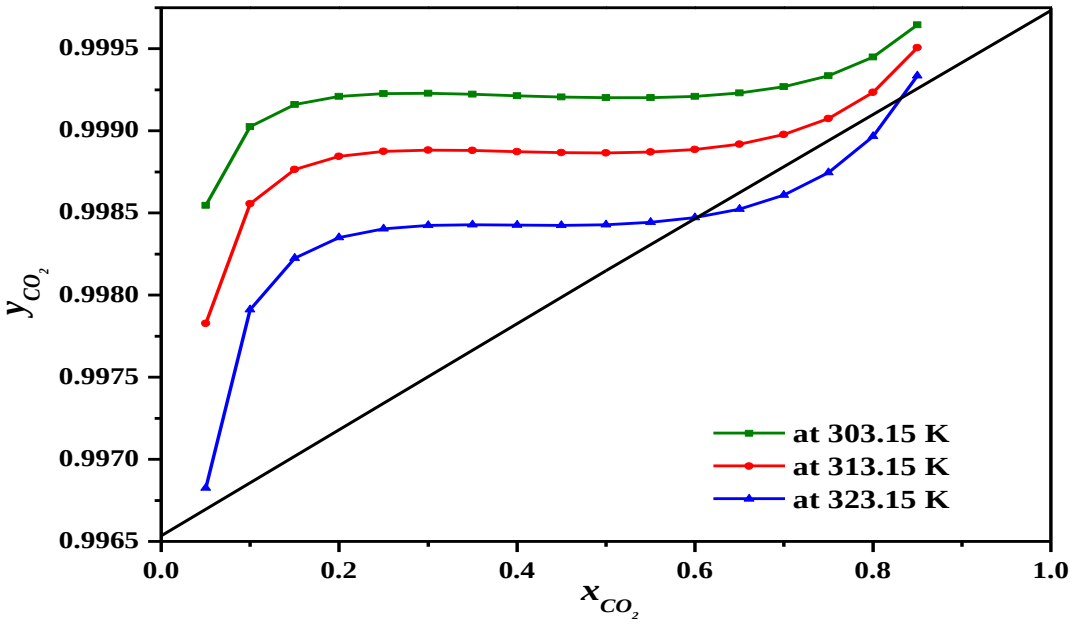

Figure 5.10: COSMO predicted Gas phase versus liquid phase mole fraction of CO_2 ($CO_2 + EAE + H_2O$) system (0.1 EAE mole fractions) at temperatures 303.15-323.15K.

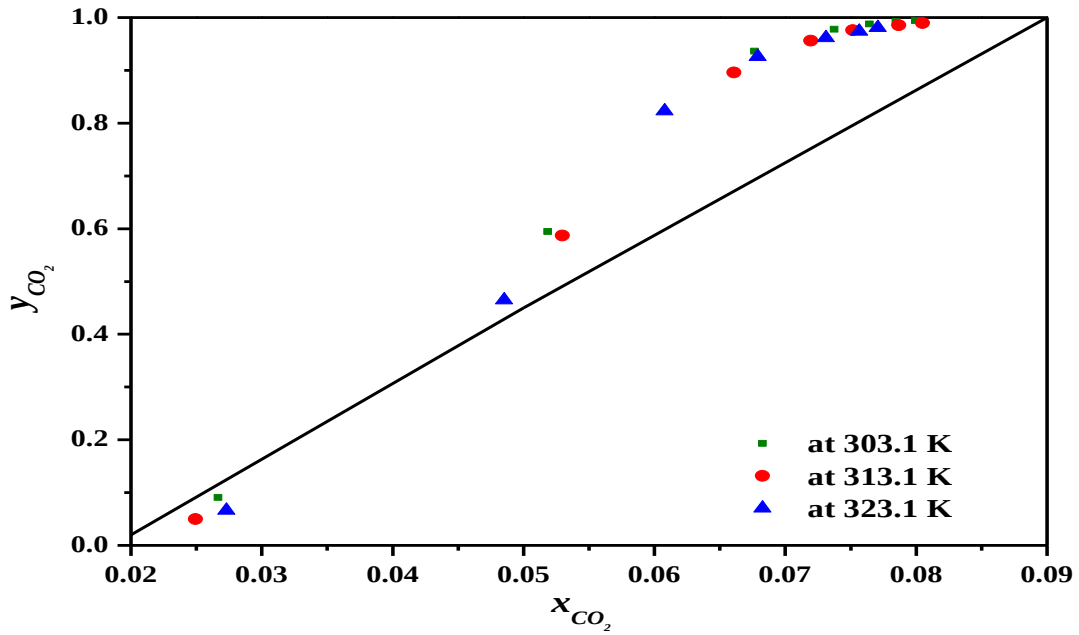

Figure 5.11: Experimentally calculated Gas phase versus liquid phase mole fraction of CO_2 ($CO_2 + EAE + H_2O$) system (0.08 EAE mole fractions $\equiv$ 30 wt%) at temperatures 303.1-323.1K.

REFERENCES

- Park, M. K. and Sandall, O. C., "Solubility of Carbon dioxide and Nitrous oxide in 50 mass % Methyldiethanolamine," Journal of Chemical Engineering and Data; 46, 166-168, 2001.
- Eckert, F. and Klamt, A., COSMOtherm, Version C3.0, Release 12.01; COSMOlogic GmbH & Co. KG, Leverkusen, Germany, 2005.

Chapter 6

Density of Aqueous Blended Alkanolamines

DENSITY OF AQUEOUS BLENDED ALKANOLAMINES

In order to predict the VLE of CO_2 in aqueous solutions of alkanolamines accurately, knowledge of physicochemical properties i.e. density of the aqueous alkanolamine solutions is essential. Liquid density is used in describing the liquid phase equilibrium of CO_2 in aqueous alkanolamine solutions. Keeping in view of the significance of blended solutions, determination of density of aqueous EAE blended AMP and MDEA solutions were taken up. Since the density of the mixed amines is a strong function of relative compositions of amines, it is desirable to measure accurately the densities of blended aqueous alkanolamine solvents for a wide range of relative amine composition and temperature.

6.1 EXPERIMENTAL

6.1.1 Materials

Reagent grade EAE (97% purity), AMP (95% purity) and MDEA (98% purity), were obtained from E. Merck. Distilled water degassed by boiling was used for making the amine solutions. The total amine contents of the solutions were determined by titration with standard HCl using methyl orange indicator.

6.1.2 Apparatus and Procedure

The density of the amine solutions was measured using a 10.3 ml Gay-Lussac pycnometer, manufactured by Borosil Glass Works Limited. For each measurement the pycnometer containing the amine solution was immersed in a constant temperature bath. The bath temperature was controlled within ±0.2 K of the test temperature using a circulator temperature controller (Polyscience, USA model No: 9712) operated on an external mode and the uncertainty in temperature measurement was ±0.1 K. Once the solution reached the desired temperature, it was weighed to within ±0.0002 g with a CPA225D Sartorius analytical balance having accuracy of 0.00001 g.

6.1.3 OBSERVATIONS

Table 6.1 : Standard solution properties

Solution	Mol. wt.	Density	Purity	Molar volume
2-Ethyl amino ethanol	89.14	0.914	97	97.527
2-Amino-2-methyl-1-propanol	89.14	0.932	95	95.644
Methyldiethanolamine	119.16	1.04	98	114.57
Water	18.01	0.997	100	18.064

Table 6.2: Measured density data of aqueous blend of EAE + MDEA (total alkanolamine content = 30 mass %)

Temp(K)	mass % EAE	mass % AMP	Density (kg/m^3)
298	6	24	1.0188
303	6	24	1.01641
308	6	24	1.01327
313	6	24	1.0106
318	6	24	1.00794
323	6	24	1.00484
298	9	21	1.01539
303	9	21	1.01284
308	9	21	1.01105
313	9	21	1.00785
318	9	21	1.00589
323	9	21	1.00224
298	12	18	1.01232
303	12	18	1.00942
308	12	18	1.007
313	12	18	1.00436

318	12	18	0.99943
323	12	18	0.99821
298	15	15	1.00897
303	15	15	1.00671
308	15	15	1.00449
313	15	15	1.00218
318	15	15	0.99921
323	15	15	0.99594
298	18	12	1.00355
303	18	12	1.00255
308	18	12	0.99969
313	18	12	0.99687
318	18	12	0.99464
323	18	12	0.99116
298	21	9	1.00279
303	21	9	1.00065
308	21	9	0.99812
313	21	9	0.99535
318	21	9	0.99255
323	21	9	0.99024
298	24	6	1.00009
303	24	6	0.99725
308	24	6	0.99492
313	24	6	0.99141
318	24	6	0.98888
323	24	6	0.98521
298	30	0	0.9903
303	30	0	0.98927
308	30	0	0.98619
313	30	0	0.98303
318	30	0	0.98026
323	30	0	0.97681

Table 6.3: Measured density data of aqueous blend of EAE + AMP (total alkanolamine content=30 mass %)

Temp(K)	mass % EAE	mass % AMP	Density (kg/m^3)
298	6	24	0.99495
303	6	24	0.99205
308	6	24	0.98915
313	6	24	0.98625
318	6	24	0.98335
323	6	24	0.98059
298	9	21	0.99464
303	9	21	0.9917
308	9	21	0.98876
313	9	21	0.98582
318	9	21	0.98288
323	9	21	0.98008
298	15	15	0.99339
303	15	15	0.99057
308	15	15	0.98775
313	15	15	0.98493
318	15	15	0.98212
323	15	15	0.97944
298	18	12	0.99336
303	18	12	0.99042
308	18	12	0.98748
313	18	12	0.98454
318	18	12	0.9816
323	18	12	0.97881
298	21	9	0.99285
303	21	9	0.98996
308	21	9	0.98707
313	21	9	0.98418
318	21	9	0.98129

323	21	9	0.97855
298	24	6	0.99281
303	24	6	0.98978
308	24	6	0.98676
313	24	6	0.98374
318	24	6	0.98071
323	24	6	0.97784
298	30	0	0.99158
303	30	0	0.98865
308	30	0	0.98572
313	30	0	0.9828
318	30	0	0.97987
323	30	0	0.97709

6.2 MODELLING

The density of liquid mixtures is correlated by the Redlich–Kister type equation for the excess molar volume which is a function of alkanolamine concentration and system temperature. For an alkanolamine + water system, the Redlich–Kister equation has the following expression:

$$V_{jk}^{E} = x_j x_k \sum_i^n A_i \left(x_j - x_k\right)^i \quad (5.1)$$

Where A_i is pair parameters and is assumed to be temperature dependent,

$$A_i = a + b(T/K) + c(T/K)^2 \quad (5.2)$$

The excess volume of liquid mixtures for a ternary system is given by

$$\boldsymbol{V^E = V_{12}^E + V_{13}^E + V_{23}^E} \quad (5.3)$$

The excess volume of the liquid mixtures can be calculated from the measured density of the fluids,

$$V^E = V_m - \sum x_i V_i^0 \quad (5.4)$$

Where V_m is the molar volume of the liquid mixture and V_i^0 is the molar volume of the pure fluids at the system temperature.

The molar volume of the liquid mixtures is calculated by

$$V_m = \frac{\sum x_i M_i}{\rho_m} \quad (5.5)$$

Where M_i is the molar mass of pure component i, ρ_m is the measured liquid density and x_i is the mole fraction of the pure component i.

The temperature dependent parameters in the Redlich-Kister correlation were computed using the non-linear least squares optimization routine (lsqnonlin) in MATLAB 10.0.

6.3 RESULTS

Table (6.1) shows standard solution properties. The measured densities of the solutions of $(EAE + MDEA + H_2O)$ and $(EAE + AMP + H_2O)$ are presented in Tables (6.2-6.3) and Figure (6.1-6.2), keeping the total amine mass fraction at 30%. From Figures (6.1-6.2), it is evident that the mixture density decreases with increasing temperature and with increasing content of EAE in the mixture for both the systems. For the $(EAE + MDEA)$, $(EAE + AMP)$ mixtures, the density data were correlated with an average error of correlation of 0.012238 %, 0.0137427% respectively. To correlate the density of liquid mixtures a Redlich–Kister type equation for the excess molar volume was applied. The determined Redlich- kister binary parameters for $(EAE + MDEA)$, $(EAE + AMP)$ system are listed below in Table (6.4 - 6.5) respectively.

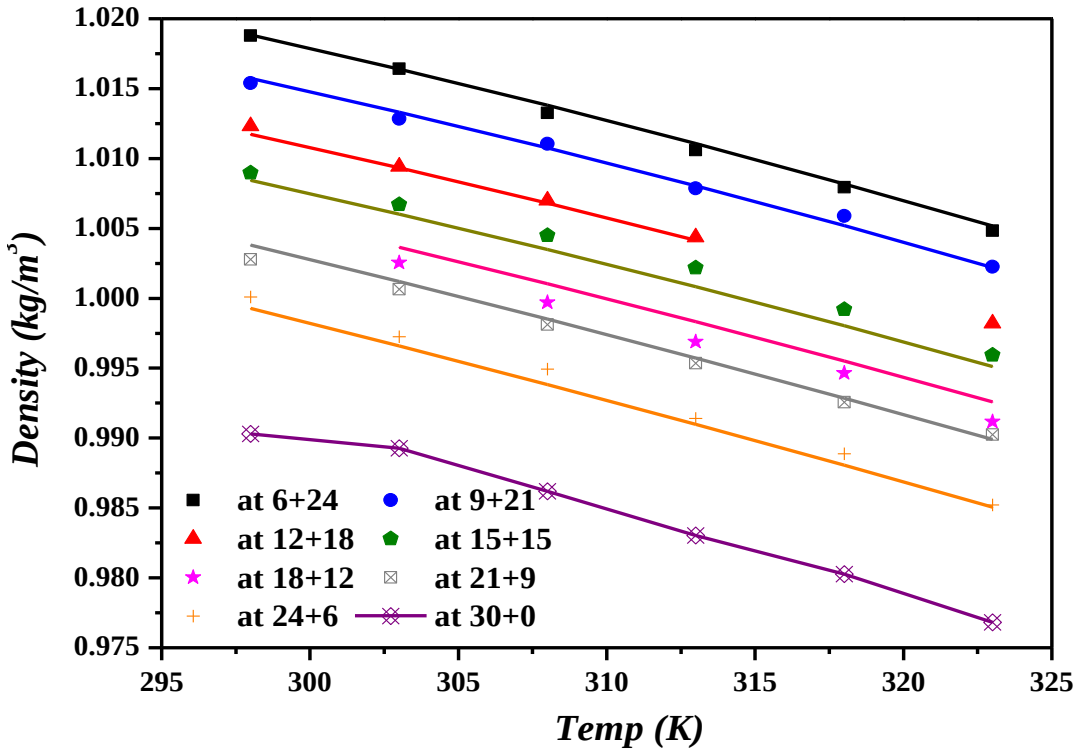

Figure 6.1: Densities of (EAE + MDEA + H_2O) over the temperature range 293.1–323.1K.

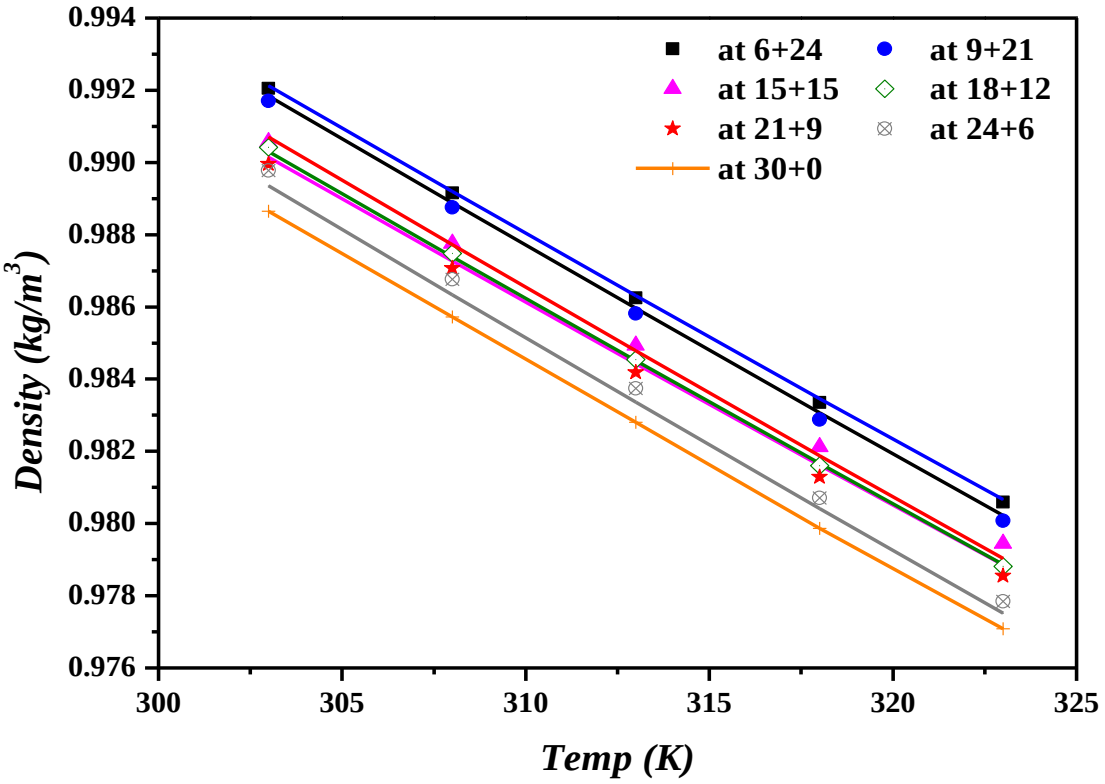

Figure 6.2: Densities of (EAE + MDEA + H_2O) over the temperature range 303.1 – 323.1K.

Table 6.4: Redlich-Kister Binary parameters, A_0, A_1, A_2 for the excess volume for (EAE + MDEA + H_2O)

Estimated Correlation Parameters* 10^5		
A_0	A	0.008644405
	B	-7.94723E-05
	C	1.28889E-07
A_1	A	-0.381075752
	B	0.002588337
	C	-4.31562E-06
A_2	A	-2.56875848
	B	0.005282725
	C	-2.09658E-06

Table 6.5: Redlich-Kister Binary parameters, A_0, A_1, A_2 for the excess volume for (EAE + AMP + H_2O)

Estimated Correlation Parameters*10^6		
A_0	a	-0.00428531
	b	2.55336E-05
	c	-4.07763E-08
A_1	a	-0.000539513
	b	-1.42435E-06
	c	7.67945E-09
A_2	a	-1.036525802
	b	0.005974003
	c	-9.21585E-06

Chapter 7

Conclusion and Future Recommendations

CONCLUSION AND FUTURE RECOMMNEDATIONS

7.1 CONCLUSIONS

Present dissertation concludes the following:

- Absorption with alkanolamine solvents are still the most pertinent technology available for effective CO_2 removal. Newer alkanolamine formulation like $2-$ ethyl $-$ amino ethanol (EAE) in this regard has been found to be an encouraging step.
- Density of EAE blends with AMP and MDEA would prove to be a valuable contribution in gas treating process design data base.
- For the new system like $(CO_2 + EAE + H_2O)$ that have no experimental data, Solvation thermodynamics models based on computational quantum mechanics, such as the Conductor – like Screening Model (COSMO) provide a good alternative to traditional group-contribution and activity coefficient methods for predicting thermodynamic properties.
- VLE of $(CO_2 + EAE + H_2O)$ system was simulated using COSMO. Only over a narrow range, the COSMO predictions are useful because total EAE mass fraction should not go beyond a mass fraction greater than 30 % in the aqueous solutions of EAE. Below that concentration one can take the advantage of chemical reaction equilibria.
- More number of predictions by COSMOtherm in the EAE mole fraction range of 0.05-0.1 in the ternary solution would have been much effective.
- Our data of aqueous EAE solution containing 0.3 mass fraction of EAE revealed the expected CO_2 solubility (in the liquid phase against the specific gas phase CO_2 mole fraction) as predicted by COSMOtherm.

7.2 FURTURE RECOMMENDATIONS

- Prediction of VLE of quaternary systems like $(EAE + AMP + CO_2 + H_2O)$, $(EAE + MDEA + CO_2 + H_2O)$ and $(MAE + AMP + CO_2 + H_2O)$, $(MAE + MDEA + CO_2 + H_2O)$using COSMO would be a major challenge in this regard.
- Simulation and synthesis of ionic liquid solvents suitable for CO_2 absorption.

Appendix

Table A.1: COMSO predicted Excess Enthalpy in $(MEA + H_2O)$ system in the temperature range 303.15 – 323.15 K

MEA Mole Fraction	303.15 K	308.15 K	313.15 K	318.15 K	323.15 K
1E-5	-9.3091E-4	-9.0062E-4	-8.7081E-4	-8.4135E-4	-8.1229E-4
1E-3	-0.0178	-0.01756	-0.0173	-0.01702	-0.0167
0.01	-0.16596	-0.1639	-0.16166	-0.15918	-0.15639
0.02	-0.32044	-0.31656	-0.31233	-0.30763	-0.30235
0.05	-0.72987	-0.72157	-0.7125	-0.70239	-0.69096
0.1	-1.27138	-1.25841	-1.24424	-1.22834	-1.21018
0.15	-1.67864	-1.66343	-1.64682	-1.62805	-1.60636
0.2	-1.98077	-1.96501	-1.94782	-1.92825	-1.90532
0.25	-2.19661	-2.18145	-2.16497	-2.14603	-2.12348
0.3	-2.33989	-2.32609	-2.31118	-2.29386	-2.27283
0.35	-2.4255	-2.4137	-2.40102	-2.38604	-2.36733
0.4	-2.45284	-2.44313	-2.43283	-2.42047	-2.4045
0.45	-2.43207	-2.42449	-2.41665	-2.40703	-2.39404
0.5	-2.36877	-2.36323	-2.35777	-2.35087	-2.3409
0.55	-2.26676	-2.26307	-2.2598	-2.25545	-2.2484
0.6	-2.12933	-2.12723	-2.12586	-2.12378	-2.11942
0.65	-1.95916	-1.95832	-1.9585	-1.95833	-1.95633
0.7	-1.76038	-1.76101	-1.7628	-1.76454	-1.76484
0.75	-1.53112	-1.53239	-1.53496	-1.53777	-1.53959
0.8	-1.27452	-1.27607	-1.27897	-1.28233	-1.28512
0.85	-0.98866	-0.98966	-0.99188	-0.99464	-0.99715
0.9	-0.68412	-0.68518	-0.6872	-0.68973	-0.69222
0.95	-0.35293	-0.35351	-0.35468	-0.35619	-0.35777
0.98	-0.14424	-0.14453	-0.14507	-0.14578	-0.14654
0.99	-0.07251	-0.07265	-0.07293	-0.07329	-0.07368
0.999	-0.00729	-0.00731	-0.00734	-0.00738	-0.00742

Table A.2: COMSO predicted Excess Gibbs free energy in $(MEA + H_2O)$ system in the temperature range 303.15 – 323.15 K

MEA Mole Fraction	303.15 K	308.15 K	313.15 K	318.15 K	323.15 K
1E-5	-1.363E-5	-1.069E-5	-7.81E-6	-4.96E-6	-2.19E-6
1E-3	-8.0031E-4	-5.2855E-4	-2.6097E-4	2.14E-6	2.6035E-4
0.01	-0.00793	-0.00529	-0.0027	-1.5259E-4	0.00235
0.02	-0.01587	-0.01077	-0.00576	-8.285E-4	0.00401
0.05	-0.04041	-0.02883	-0.01742	-0.00618	0.00485
0.1	-0.08395	-0.06387	-0.04407	-0.02456	-0.0054
0.15	-0.12854	-0.10214	-0.0761	-0.05043	-0.02518
0.2	-0.17152	-0.14051	-0.10988	-0.07968	-0.04995
0.25	-0.21075	-0.17646	-0.14259	-0.10915	-0.07622
0.3	-0.24502	-0.20859	-0.17257	-0.137	-0.10194
0.35	-0.27398	-0.23651	-0.19941	-0.16274	-0.12656
0.4	-0.29626	-0.25842	-0.22095	-0.18389	-0.14729
0.45	-0.31195	-0.27447	-0.23733	-0.20057	-0.16425
0.5	-0.32081	-0.28433	-0.24816	-0.21235	-0.17695
0.55	-0.32266	-0.28777	-0.25316	-0.21887	-0.18496
0.6	-0.31738	-0.2846	-0.25207	-0.21984	-0.18795
0.65	-0.30483	-0.27465	-0.2447	-0.21501	-0.18564
0.7	-0.2852	-0.25826	-0.23152	-0.205	-0.17874
0.75	-0.25769	-0.23426	-0.21101	-0.18794	-0.16511
0.8	-0.22243	-0.20293	-0.18357	-0.16437	-0.14537
0.85	-0.17879	-0.16334	-0.14797	-0.1327	-0.11754
0.9	-0.12783	-0.11725	-0.10672	-0.09626	-0.08587
0.95	-0.06818	-0.06271	-0.05727	-0.05186	-0.0465
0.98	-0.02871	-0.02645	-0.02422	-0.022	-0.01979
0.99	-0.01454	-0.01341	-0.01228	-0.01116	-0.01005
0.999	-0.00147	-0.00136	-0.00124	-0.00113	-0.00102

Table A.3: COMSO predicted MEA $\ln(\text{activity coefficient})$ in $(\text{MEA} + H_2O)$ system in the temp range of 303.15 – 323.15 K

MEA Mole fraction	303.15 K	308.15 K	313.15 K	318.15 K	323.15 K
1E-5	-0.32888	-0.21872	-0.1135	-0.01311	0.08253
1E-3	-0.32861	-0.21921	-0.11471	-0.015	0.07999
0.01	-0.32882	-0.22586	-0.12746	-0.03354	0.05598
0.02	-0.33282	-0.23619	-0.14381	-0.05557	0.02857
0.05	-0.35224	-0.27093	-0.19308	-0.11859	-0.04743
0.1	-0.3733	-0.31015	-0.24953	-0.19136	-0.13562
0.15	-0.3704	-0.32026	-0.27201	-0.22559	-0.18097
0.2	-0.35109	-0.31082	-0.27198	-0.23451	-0.19841
0.25	-0.3225	-0.28994	-0.25845	-0.22802	-0.19862
0.3	-0.28968	-0.26322	-0.2376	-0.2128	-0.18879
0.35	-0.25595	-0.23444	-0.21359	-0.19336	-0.17375
0.4	-0.22223	-0.20472	-0.18774	-0.17125	-0.15526
0.45	-0.1899	-0.17567	-0.16186	-0.14847	-0.13547
0.5	-0.15953	-0.14801	-0.13685	-0.12603	-0.11554
0.55	-0.13141	-0.12216	-0.11321	-0.10454	-0.09617
0.6	-0.10575	-0.09838	-0.09128	-0.08444	-0.07784
0.65	-0.08264	-0.07686	-0.07132	-0.06601	-0.06091
0.7	-0.0622	-0.05785	-0.05369	-0.04973	-0.04596
0.75	-0.04449	-0.04127	-0.03821	-0.03533	-0.03262
0.8	-0.02958	-0.0273	-0.02516	-0.02317	-0.02133
0.85	-0.01741	-0.01582	-0.01433	-0.01296	-0.01169
0.9	-0.00854	-0.00764	-0.00681	-0.00605	-0.00538
0.95	-0.00264	-0.00225	-0.0019	-0.00159	-0.00132
0.98	-8.1751E-4	-6.65E-4	-5.2939E-4	-4.1144E-4	-3.1152E-4
0.99	-3.4784E-4	-2.724E-4	-2.0564E-4	-1.4797E-4	-9.963E-5
0.999	-2.971E-5	-2.238E-5	-1.595E-5	-1.048E-5	-5.97E-6

Table A.4: COMSO predicted MEA Chemical Potential in $(MEA + H_2O)$ system in the temperature range 303.15 – 323.15 K

MEA Mole fraction	303.15 K	308.15 K	313.15 K	318.15 K	323.15 K
1E-5	-40.38546	-40.22286	-40.08417	-39.9696	-39.87932
1E-3	-28.7774	-28.42529	-28.09704	-27.79288	-27.51296
0.01	-22.97423	-22.5429	-22.13511	-21.75105	-21.39088
0.02	-21.23722	-20.79348	-20.37294	-19.97581	-19.60217
0.05	-18.97663	-18.53487	-18.11552	-17.71871	-17.34449
0.1	-17.28263	-16.85945	-16.45778	-16.07767	-15.71909
0.15	-16.25334	-15.84652	-15.46062	-15.09565	-14.75152
0.2	-15.47955	-15.08526	-14.71151	-14.35827	-14.02543
0.25	-14.84508	-14.46004	-14.0953	-13.75083	-13.42647
0.3	-14.3028	-13.92447	-13.56631	-13.22828	-12.91018
0.35	-13.82925	-13.45579	-13.10243	-12.7691	-12.45561
0.4	-13.40769	-13.03752	-12.68745	-12.3574	-12.04715
0.45	-13.02933	-12.66132	-12.31343	-11.98556	-11.67752
0.5	-12.68721	-12.32051	-11.97397	-11.64751	-11.34089
0.55	-12.37612	-12.01008	-11.66426	-11.33856	-11.03276
0.6	-12.09211	-11.72623	-11.38063	-11.05521	-10.74974
0.65	-11.83211	-11.46602	-11.12026	-10.79473	-10.4892
0.7	-11.59382	-11.22744	-10.88141	-10.55564	-10.24991
0.75	-11.37528	-11.00819	-10.66147	-10.33505	-10.02869
0.8	-11.17503	-10.80705	-10.45945	-10.13217	-9.82496
0.85	-10.99154	-10.6223	-10.27341	-9.94478	-9.63619
0.9	-10.82511	-10.4549	-10.10499	-9.77531	-9.46564
0.95	-10.67397	-10.30258	-9.95145	-9.62049	-9.30948
0.98	-10.59101	-10.21886	-9.86692	-9.53513	-9.22323
0.99	-10.56424	-10.19184	-9.83965	-9.50758	-9.19538
0.999	-10.54063	-10.16801	-9.81559	-9.48327	-9.17082

Table A.5: COMSO predicted Total Pressure in $(MEA + H_2O)$ system in the temperature range 303.15 – 323.15 K

MEA mole fraction	303.15 K	308.15 K	313.15 K	318.15 K	323.15 K
1E-5	4.25525	5.63884	7.39631	9.60782	12.36606
1E-3	4.25149	5.634	7.39017	9.60016	12.35663
0.01	4.21735	5.59018	7.33475	9.53111	12.27187
0.02	4.1797	5.54209	7.27419	9.45591	12.17982
0.05	4.06879	5.40139	7.09807	9.23834	11.91444
0.1	3.88517	5.16998	6.81004	8.88406	11.48362
0.15	3.69402	4.92926	6.51046	8.51542	11.03477
0.2	3.4917	4.67359	6.19111	8.12083	10.55216
0.25	3.27941	4.404	5.85265	7.70045	10.03522
0.3	3.05994	4.12378	5.4989	7.25861	9.4888
0.35	2.83634	3.83644	5.13385	6.79976	8.91776
0.4	2.61212	3.54707	4.76462	6.33361	8.33505
0.45	2.38974	3.25866	4.3948	5.86442	7.74565
0.5	2.17163	2.97445	4.02864	5.39767	7.15656
0.55	1.95978	2.69716	3.6698	4.93821	6.57405
0.6	1.75594	2.42921	3.32156	4.4904	6.00385
0.65	1.56161	2.17272	2.98683	4.05816	5.45115
0.7	1.37775	1.92895	2.66725	3.64353	4.91843
0.75	1.20628	1.70085	2.36715	3.25278	4.41454
0.8	1.04777	1.48914	2.0875	2.88713	3.94097
0.85	0.90319	1.29545	1.83087	2.55058	3.50375
0.9	0.77256	1.11946	1.59626	2.24086	3.0986
0.95	0.65673	0.96279	1.38655	1.96285	2.73328
0.98	0.59423	0.87794	1.27255	1.8111	2.53302
0.99	0.57465	0.85131	1.2367	1.76328	2.46978
0.999	0.55754	0.82801	1.20529	1.72135	2.41425

Table A.6: COSMO predicted NRTL model parameters for the Activity Coefficients in ($MEA + H_2O$) system

Temp	A	τ_{12}	τ_{21}
303.15 K	0.3	0.51386	-0.84781
308.15 K	0.3	0.86674	-1.01738
313.15 K	0.3	0.81191	-0.94005
318.15 K	0.3	0.68654	-0.81629
323.15 K	0.3	0.57901	-0.69736

- $\tau_{12} = \frac{g_{12} - g_{22}}{RT}$, $\tau_{21} = \frac{g_{21} - g_{11}}{RT}$

Table A.7: COSMO predicted WILSON model parameters for the Activity Coefficients in ($MEA + H_2O$) system

Temp	λ_{12}	λ_{21}
303.15 K	1.91067	0.73945
308.15 K	1.83657	0.73111
313.15 K	2.11574	0.52646
318.15 K	1.76398	0.67693
323.15 K	1.72828	0.65214

- $\lambda_{ij} = \frac{v_j}{v} i \, exp\left(-\frac{\wedge ij - \wedge ii}{RT}\right)$

Table A.8: COSMO predicted UNIQUAC model parameters for the Activity Coefficients in ($MEA + H_2O$) system

Temp	q_1	q_2	r_1	r_2	τ_{12}	τ_{21}
303.15 K	2.34241	1.66126	2.6184	1.09169	1.4298	1.3975
308.15 K	2.58823	1.79704	2.89288	1.18091	1.40339	1.37002
313.15 K	2.72803	1.83583	3.04878	1.2064	1.35861	1.36369
318.15 K	2.79395	1.83193	3.12208	1.20384	1.31061	1.36598
323.15 K	2.92105	1.86914	3.2637	1.2829	1.2816	1.3551

- $\tau_{ij} = e^{-\Delta u_{ij}/RT}$, r and q are structural parameters

Table A.9: COSMO predicted Activity Coefficient of MEA at infinite dilution in water

303.15 K	308.15 K	313.15 K	318.15 K	323.15 K
-0.3906	-0.2765	-0.1673	-0.0629	0.03665

Table A.10: COSMO predicted Excess Enthalpy in $(DEA + H_2O)$ system in the temperature range of 303.15 – 323.15 K

DEA Mole fraction	303.15 K	308.15 K	313.15 K	318.15 K	323.15 K
1E-5	-0.00236	-0.00233	-0.00229	-0.00225	-0.00221
1E-3	-0.01747	-0.01713	-0.01673	-0.01627	-0.01575
0.01	-0.14776	-0.14481	-0.14131	-0.13725	-0.13262
0.02	-0.27953	-0.27401	-0.26743	-0.25976	-0.25102
0.05	-0.61175	-0.60003	-0.58597	-0.56951	-0.55064
0.1	-1.01679	-0.99814	-0.97556	-0.94894	-0.91825
0.15	-1.29175	-1.26879	-1.24082	-1.20769	-1.16933
0.2	-1.47304	-1.44746	-1.41616	-1.37894	-1.33573
0.25	-1.58397	-1.55693	-1.52376	-1.48421	-1.43818
0.3	-1.63675	-1.60874	-1.57446	-1.53363	-1.48613
0.35	-1.65546	-1.6274	-1.59302	-1.55202	-1.50426
0.4	-1.63242	-1.60489	-1.57115	-1.53089	-1.48395
0.45	-1.58045	-1.55403	-1.52164	-1.48292	-1.43774
0.5	-1.50401	-1.47902	-1.44838	-1.41173	-1.36891
0.55	-1.40753	-1.38429	-1.35576	-1.32163	-1.28171
0.6	-1.29419	-1.27293	-1.24684	-1.21559	-1.17902
0.65	-1.16652	-1.14744	-1.12404	-1.09599	-1.06314
0.7	-1.02655	-1.00984	-0.98933	-0.96474	-0.93592
0.75	-0.87453	-0.86037	-0.843	-0.82216	-0.79772
0.8	-0.7148	-0.70352	-0.6896	-0.67281	-0.65303
0.85	-0.54656	-0.53797	-0.52738	-0.51459	-0.49951
0.9	-0.3699	-0.36417	-0.35709	-0.34853	-0.33842
0.95	-0.188	-0.1851	-0.18152	-0.17719	-0.17207
0.98	-0.07589	-0.07472	-0.07328	-0.07154	-0.06947
0.99	-0.03805	-0.03747	-0.03675	-0.03587	-0.03484
0.999	-0.00381	-0.00376	-0.00368	-0.0036	-0.00349

Table A.11: COSMO predicted Excess Gibbs free energy in $(DEA + H_2O)$ system in the temperature range of 303.15 – 323.15 K

DEA Mole fraction	303.15 K	308.15 K	313.15 K	318.15 K	323.15 K
1E-5	2.232E-5	2.576E-5	2.91E-5	3.238E-5	3.553E-5
1E-3	0.00314	0.00344	0.00374	0.00403	0.00431
0.01	0.02931	0.0322	0.03503	0.03779	0.04047
0.02	0.05426	0.05975	0.06513	0.07037	0.07547
0.05	0.10836	0.12031	0.132	0.1434	0.15449
0.1	0.15346	0.17302	0.19216	0.21082	0.22896
0.15	0.16819	0.19274	0.21675	0.24016	0.26291
0.2	0.16822	0.19596	0.22308	0.24951	0.27519
0.25	0.16054	0.19011	0.21902	0.24719	0.27455
0.3	0.14772	0.17842	0.20843	0.23766	0.26603
0.35	0.13158	0.16238	0.1925	0.22183	0.2503
0.4	0.11727	0.14743	0.1769	0.20562	0.23349
0.45	0.10286	0.13189	0.16027	0.18791	0.21474
0.5	0.08942	0.11697	0.14389	0.1701	0.19554
0.55	0.07668	0.10239	0.12752	0.15198	0.17571
0.6	0.06472	0.08831	0.11137	0.13381	0.15558
0.65	0.0536	0.07483	0.09558	0.11577	0.13535
0.7	0.04334	0.062	0.08024	0.09798	0.11518
0.75	0.03429	0.05025	0.06586	0.08103	0.09573
0.8	0.02668	0.03956	0.05215	0.0644	0.07628
0.85	0.01886	0.02871	0.03834	0.0477	0.05678
0.9	0.01153	0.01827	0.02486	0.03126	0.03746
0.95	0.00546	0.00888	0.01224	0.0155	0.01865
0.98	0.00214	0.00352	0.00488	0.00619	0.00747
0.99	0.00107	0.00175	0.00244	0.0031	0.00374
0.999	1.0727E-4	1.6452E-4	2.4519E-4	3.1123E-4	3.752E-4

Table A.12: COMSO predicted DEA ln(activity coefficient) in (DEA + H_2O) system in the temp range of 303.15 – 323.15 K

DEA Mole fraction	303.15 K	308.15 K	313.15 K	318.15 K	323.15 K
1E-5	1.25376	1.35226	1.44522	1.53261	1.61442
1E-3	1.23494	1.33238	1.42434	1.5108	1.59173
0.01	1.07399	1.16289	1.24679	1.32568	1.39952
0.02	0.91749	0.99861	1.07517	1.14716	1.21456
0.05	0.5713	0.63529	0.69569	0.75249	0.80568
0.1	0.26048	0.30612	0.34917	0.38962	0.42748
0.15	0.11428	0.14787	0.17949	0.20916	0.2369
0.2	0.04302	0.06814	0.09173	0.11382	0.13442
0.25	0.0079	0.02684	0.04457	0.06111	0.07651
0.3	-0.00969	0.00479	0.0183	0.03087	0.04252
0.35	-0.01854	-0.00743	0.0029	0.01247	0.02131
0.4	-0.02112	-0.01267	-0.00484	0.00237	0.00901
0.45	-0.0211	-0.01464	-0.00869	-0.00324	0.00175
0.5	-0.01967	-0.01473	-0.01022	-0.00611	-0.00237
0.55	-0.01761	-0.01384	-0.01043	-0.00734	-0.00455
0.6	-0.0153	-0.01244	-0.00987	-0.00757	-0.00551
0.65	-0.01296	-0.0108	-0.00888	-0.00718	-0.00568
0.7	-0.0107	-0.00909	-0.00767	-0.00644	-0.00535
0.75	-0.00838	-0.00718	-0.00613	-0.00523	-0.00445
0.8	-0.00604	-0.00526	-0.00458	-0.00401	-0.00353
0.85	-0.00429	-0.00377	-0.00332	-0.00295	-0.00265
0.9	-0.00281	-0.00248	-0.00219	-0.00195	-0.00176
0.95	-0.00131	-0.00116	-0.00102	-9.1982E-4	-8.3622E-4
0.98	-4.9255E-4	-4.3687E-4	-3.8268E-4	-3.433E-4	-3.1228E-4
0.99	-2.386E-4	-2.137E-4	-1.846E-4	-1.6536E-4	-1.5027E-4
0.999	-2.301E-5	-2.496E-5	-1.763E-5	-1.576E-5	-1.43E-5

Table A.13: COMSO predicted DEA Chemical Potential in $(DEA + H_2O)$ system in the temperature range of 303.15 – 323.15 K

DEA Mole fraction	303.15 K	308.15 K	313.15 K	318.15 K	323.15 K
1E-5	-40.09183	-39.74206	-39.42161	-39.13074	-38.86964
1E-3	-28.53187	-27.99415	-27.48567	-27.0067	-26.55742
0.01	-23.13385	-22.52898	-21.95281	-21.40552	-20.88725
0.02	-21.78123	-21.17398	-20.59493	-20.04419	-19.52184
0.05	-20.34427	-19.75722	-19.19726	-18.6644	-18.15856
0.1	-19.3806	-18.82467	-18.29478	-17.79074	-17.31234
0.15	-18.72714	-18.1913	-17.68086	-17.19554	-16.73499
0.2	-18.18163	-17.6585	-17.16033	-16.68677	-16.2374
0.25	-17.70772	-17.19261	-16.70215	-16.23592	-15.79344
0.3	-17.29253	-16.78197	-16.29582	-15.83363	-15.39489
0.35	-16.9263	-16.41833	-15.93458	-15.47455	-15.03771
0.4	-16.59623	-16.08963	-15.60707	-15.14803	-14.71198
0.45	-16.29929	-15.79291	-15.31042	-14.85132	-14.41504
0.5	-16.03013	-15.52321	-15.04007	-14.5802	-14.14302
0.55	-15.78469	-15.27674	-14.79245	-14.33134	-13.8928
0.6	-15.55956	-15.05021	-14.56446	-14.10177	-13.66159
0.65	-15.35191	-14.84095	-14.35349	-13.88903	-13.44699
0.7	-15.15942	-14.64669	-14.15739	-13.69102	-13.247
0.75	-14.97968	-14.46502	-13.97374	-13.50532	-13.05921
0.8	-14.81112	-14.29474	-13.80166	-13.33138	-12.88333
0.85	-14.6539	-14.1356	-13.64053	-13.16821	-12.71807
0.9	-14.50611	-13.98585	-13.48876	-13.01438	-12.56213
0.95	-14.36606	-13.84395	-13.34497	-12.86862	-12.41437
0.98	-14.28563	-13.76244	-13.26234	-12.78486	-12.32943
0.99	-14.2594	-13.73586	-13.2354	-12.75753	-12.30171
0.999	-14.23604	-13.71219	-13.2114	-12.7332	-12.27703

Table A.14: COSMO predicted Total Pressure in $(DEA + H_2O)$ system in the temperature range of 303.15 – 323.15 K

DEA Mole fraction	303.15 K	308.15 K	313.15 K	318.15 K	323.15 K
1E-5	4.25524	5.63883	7.39629	9.60779	12.36602
1E-3	4.25109	5.63334	7.3891	9.59848	12.35406
0.01	4.21661	5.58797	7.33	9.52223	12.25659
0.02	4.18388	5.54531	7.27493	9.45181	12.16732
0.05	4.10464	5.44377	7.14607	9.2897	11.96509
0.1	3.98126	5.28817	6.95181	9.04948	11.67059
0.15	3.83474	5.10255	6.71908	8.76046	11.31486
0.2	3.66141	4.88087	6.43844	8.40856	10.87748
0.25	3.46591	4.62863	6.1163	8.00104	10.36651
0.3	3.25313	4.35261	5.76185	7.55019	9.79814
0.35	3.02827	4.05854	5.38123	7.06231	9.17847
0.4	2.79925	3.75735	4.98921	6.55707	8.53331
0.45	2.56577	3.44884	4.58583	6.03484	7.86353
0.5	2.33083	3.1372	4.17679	5.50333	7.17942
0.55	2.09486	2.82306	3.76303	4.96384	6.48277
0.6	1.85872	2.50768	3.34634	4.41891	5.77705
0.65	1.62296	2.19193	2.92801	3.8704	5.0649
0.7	1.38796	1.87641	2.50899	3.3197	4.34832
0.75	1.15395	1.56154	2.08996	2.76787	3.62889
0.8	0.92143	1.24797	1.67174	2.21598	2.90793
0.85	0.68978	0.93514	1.25396	1.66392	2.18585
0.9	0.45934	0.62349	0.83715	1.11239	1.46348
0.95	0.23041	0.31344	0.42191	0.5622	0.74195
0.98	0.09367	0.12807	0.17342	0.23266	0.30941
0.99	0.04819	0.06639	0.0907	0.12292	0.16532
0.999	0.0073	0.01093	0.01631	0.0242	0.03567

Table A.15: COMSO predicted NRTL model parameters for the Activity Coefficients in $(DEA + H_2O)$ system

Temp	A	τ_{12}	τ_{21}
303.15 K	0.3	-1.30385	3.07753
308.15 K	0.3	-1.27871	3.11805
313.15 K	0.3	-1.25871	3.17111
318.15 K	0.3	-1.24339	3.23458
323.15 K	0.3	-1.22135	3.26839

Table A.16: COMSO predicted WILSON model parameters for the Activity Coefficients in $(DEA + H_2O)$ system

Temp	λ_{12}	λ_{21}
303.15 K	0.28761	1.45855
308.15 K	0.12669	1.88118
313.15 K	0.25179	1.35323
318.15 K	0.24936	1.34367
323.15 K	0.08189	1.95625

Table A.17: COSMO predicted UNIQUAC model parameters for the Activity Coefficients in $(DEA + H_2O)$ system

Temp	q_1	q_2	r_1	r_2	τ_{12}	τ_{21}
303.15 K	3.43318	1.19627	4.24469	0.78612	1.22047	0.88225
308.15 K	3.91699	1.01244	4.84376	0.66532	0.45397	1.42139
313.15 K	3.48679	0.92683	4.31253	0.60906	0.60847	1.04604
318.15 K	3.95154	0.92375	4.88814	0.60704	0.46113	1.1539
323.15 K	3.97235	0.93352	4.91464	0.61346	0.46128	1.15114

Table A.18: COSMO predicted Activity Coefficient of DEA at infinite dilution in water

303.15 K	308.15 K	313.15 K	318.15 K	323.15 K
1.27555	1.37451	1.46806	1.55614	1.63894

Table A.19: COSMO predicted Excess Enthalpy in ($MDEA + H_2O$) system in the temperature range of 303.15 – 323.15 K

MDEA Mole fraction	303.15 K	308.15 K	313.15 K	318.15 K	323.15 K
1E-5	-0.00572	-0.00556	-0.0054	-0.00523	-0.00506
1E-3	-0.02712	-0.02623	-0.0253	-0.02431	-0.02327
0.01	-0.21314	-0.20603	-0.19841	-0.19031	-0.18173
0.02	-0.40439	-0.39093	-0.37653	-0.36119	-0.34493
0.05	-0.90304	-0.87333	-0.84151	-0.80762	-0.77171
0.1	-1.54324	-1.49295	-1.43913	-1.38186	-1.32124
0.15	-1.99388	-1.92903	-1.85971	-1.78601	-1.70808
0.2	-2.30431	-2.22929	-2.14918	-2.06411	-1.97426
0.25	-2.50074	-2.41913	-2.33206	-2.23969	-2.14221
0.3	-2.60532	-2.52007	-2.42919	-2.33284	-2.23123
0.35	-2.63178	-2.54539	-2.45335	-2.35582	-2.25302
0.4	-2.60339	-2.51779	-2.42662	-2.33004	-2.22827
0.45	-2.52571	-2.44242	-2.35373	-2.2598	-2.16086
0.5	-2.40629	-2.32675	-2.24207	-2.15238	-2.05792
0.55	-2.25054	-2.17603	-2.09668	-2.01263	-1.92409
0.6	-2.06649	-1.99797	-1.92496	-1.84762	-1.76613
0.65	-1.86114	-1.79929	-1.73337	-1.66352	-1.58991
0.7	-1.6233	-1.56921	-1.51153	-1.45039	-1.38593
0.75	-1.37711	-1.33123	-1.28224	-1.23027	-1.17543
0.8	-1.1205	-1.08311	-1.04317	-1.00076	-0.956
0.85	-0.85227	-0.82377	-0.7933	-0.76093	-0.72675
0.9	-0.57434	-0.55512	-0.53455	-0.51267	-0.48956
0.95	-0.28941	-0.27974	-0.26937	-0.25833	-0.24666
0.98	-0.11581	-0.11194	-0.10779	-0.10336	-0.09868
0.99	-0.05786	-0.05593	-0.05385	-0.05164	-0.04929
0.999	-0.00578	-0.00558	-0.00537	-0.00515	-0.00492

Table A.20: COSMO predicted Excess Gibbs free energy in (MDEA + H_2O) system in the temperature range of 303.15 – 323.15 K

MDEA Mole fraction	303.15 K	308.15 K	313.15 K	318.15 K	323.15 K
1E-5	4.404E-5	4.836E-5	5.255E-5	5.664E-5	6.059E-5
1E-3	0.00477	0.00519	0.00561	0.00601	0.0064
0.01	0.04404	0.0481	0.05205	0.05587	0.05958
0.02	0.08071	0.08845	0.09597	0.10325	0.1103
0.05	0.15727	0.17426	0.19077	0.20678	0.22225
0.1	0.21702	0.24525	0.27267	0.29924	0.32491
0.15	0.23791	0.27364	0.30834	0.34193	0.37437
0.2	0.23744	0.27813	0.31762	0.35584	0.39275
0.25	0.22744	0.27106	0.31338	0.35435	0.39388
0.3	0.21373	0.25874	0.30242	0.34468	0.38546
0.35	0.1977	0.24296	0.28688	0.32937	0.37036
0.4	0.18133	0.22582	0.26899	0.31074	0.35103
0.45	0.16475	0.20781	0.24958	0.28999	0.32896
0.5	0.14871	0.18958	0.22922	0.26758	0.30457
0.55	0.13392	0.17204	0.20902	0.2448	0.2793
0.6	0.11939	0.15433	0.18823	0.22101	0.25263
0.65	0.10418	0.1356	0.16607	0.19556	0.22398
0.7	0.09319	0.12071	0.14739	0.1732	0.19807
0.75	0.08101	0.10436	0.12699	0.14887	0.16995
0.8	0.06587	0.08489	0.10332	0.12113	0.1383
0.85	0.05101	0.06554	0.07962	0.09323	0.10633
0.9	0.03498	0.0448	0.05431	0.0635	0.07235
0.95	0.01817	0.02313	0.02793	0.03257	0.03703
0.98	0.00748	0.00948	0.01141	0.01328	0.01507
0.99	0.00379	0.00479	0.00576	0.00669	0.00759
0.999	3.8485E-4	4.8495E-4	5.8184E-4	6.7541E-4	7.6535E-4

Table A.21: COSMO predicted MDEA $\ln(\text{activity coefficient})$ in $(\text{MDEA} + H_2O)$ system in the temperature range of 303.15 – 323.15 K

MDEA Mole fraction	303.15 K	308.15 K	313.15 K	318.15 K	323.15 K
1E-5	1.88037	2.01916	2.14889	2.26974	2.38188
1E-3	1.8464	1.9839	2.11243	2.23216	2.34327
0.01	1.56264	1.6899	1.80891	1.91985	2.02285
0.02	1.29713	1.41522	1.52572	1.62876	1.72448
0.05	0.74713	0.84438	0.93546	1.02048	1.09956
0.1	0.30286	0.37528	0.44315	0.50654	0.56556
0.15	0.11988	0.17411	0.22493	0.27241	0.31663
0.2	0.04117	0.08181	0.11991	0.15552	0.18868
0.25	0.0073	0.03774	0.06628	0.09297	0.11784
0.3	-0.00543	0.01729	0.03861	0.05855	0.07714
0.35	-0.009	0.0079	0.02378	0.03865	0.05252
0.4	-0.00922	0.00329	0.01506	0.0261	0.0364
0.45	-0.00796	0.00127	0.00998	0.01815	0.0258
0.5	-0.00614	5.6485E-4	0.0069	0.01287	0.01846
0.55	-0.00409	6.9532E-4	0.00523	0.00951	0.01352
0.6	-0.00239	9.3819E-4	0.00411	0.00711	0.00993
0.65	-0.00148	7.8038E-4	0.00294	0.00501	0.00695
0.7	9.5478E-4	0.00237	0.00373	0.00504	0.00627
0.75	0.00241	0.00321	0.00399	0.00474	0.00546
0.8	0.00236	0.00277	0.00318	0.00359	0.00398
0.85	0.00235	0.00252	0.00271	0.00289	0.00308
0.9	0.00184	0.00187	0.00191	0.00196	0.00201
0.95	0.00111	0.00108	0.00106	0.00105	0.00103
0.98	5.0437E-4	4.8406E-4	4.6711E-4	4.5309E-4	4.4145E-4
0.99	2.6785E-4	2.56E-4	2.4588E-4	2.373E-4	2.2997E-4
0.999	2.857E-5	2.724E-5	2.608E-5	2.51E-5	2.421E-5

Table A.22: COSMO predicted MDEA Chemical Potential in $(MDEA + H_2O)$ system in the temperature range of 303.15 – 323.15 K

MDEA Mole fraction	303.15 K	308.15 K	313.15 K	318.15 K	323.15 K
1E-5	-38.14519	-37.8837	-37.64923	-37.44224	-37.26311
1E-3	-26.62342	-26.17521	-25.75389	-25.35991	-24.99364
0.01	-21.53495	-21.02904	-20.54899	-20.09519	-19.66797
0.02	-20.45708	-19.95688	-19.48162	-19.03166	-18.60728
0.05	-19.53385	-19.0718	-18.63273	-18.21688	-17.82442
0.1	-18.90655	-18.49777	-18.10983	-17.74283	-17.39683
0.15	-18.34577	-17.97437	-17.62231	-17.28962	-16.97626
0.2	-17.81904	-17.47376	-17.14671	-16.83784	-16.54707
0.25	-17.34198	-17.01497	-16.70535	-16.41303	-16.13788
0.3	-16.91453	-16.60025	-16.30271	-16.0218	-15.75735
0.35	-16.53499	-16.22935	-15.93995	-15.66668	-15.40934
0.4	-16.19897	-15.89904	-15.61499	-15.34667	-15.09389
0.45	-15.89893	-15.60245	-15.32156	-15.05611	-14.80591
0.5	-15.62879	-15.33431	-15.05524	-14.79138	-14.54253
0.55	-15.38337	-15.08979	-14.81145	-14.54817	-14.29973
0.6	-15.15978	-14.86623	-14.58782	-14.32434	-14.07559
0.65	-14.95574	-14.66156	-14.38244	-14.11817	-13.86853
0.7	-14.76281	-14.46762	-14.18744	-13.92206	-13.67124
0.75	-14.58525	-14.28871	-14.00714	-13.74034	-13.48807
0.8	-14.4227	-14.12447	-13.8412	-13.57267	-13.31865
0.85	-14.26992	-13.96978	-13.68459	-13.41414	-13.15817
0.9	-14.12713	-13.82501	-13.53784	-13.26541	-13.00747
0.95	-13.9927	-13.68851	-13.39929	-13.12481	-12.86482
0.98	-13.91586	-13.61038	-13.31988	-13.04414	-12.78288
0.99	-13.89087	-13.58495	-13.29402	-13.01785	-12.75617
0.999	-13.86866	-13.56235	-13.27103	-12.99447	-12.73241

Table A.23: COSMO predicted Total Pressure in $(MDEA + H_2O)$ system in the temperature range of 303.15 – 323.15 K

MDEA Mole fraction	303.15 K	308.15 K	313.15 K	318.15 K	323.15 K
1E-5	4.25525	5.63884	7.39631	9.60783	12.36606
1E-3	4.25148	5.63395	7.39004	9.59993	12.35628
0.01	4.22251	5.5964	7.34205	9.53945	12.28115
0.02	4.19907	5.56631	7.30389	9.49164	12.2219
0.05	4.15471	5.51149	7.23691	9.41064	12.12492
0.1	4.08021	5.42287	7.13308	9.2908	11.98864
0.15	3.96397	5.28123	6.96265	9.08812	11.75029
0.2	3.79877	5.07534	6.70878	8.77826	11.37558
0.25	3.60083	4.82481	6.39494	8.38883	10.89662
0.3	3.38208	4.54476	6.04002	7.94327	10.34216
0.35	3.14971	4.24448	5.65589	7.45652	9.73084
0.4	2.91201	3.93457	5.25597	6.94539	9.08347
0.45	2.67085	3.61792	4.84453	6.41603	8.40869
0.5	2.42876	3.29777	4.42567	5.87353	7.71271
0.55	2.18756	2.97688	4.00339	5.32353	7.00335
0.6	1.94692	2.65503	3.57768	4.76638	6.28143
0.65	1.70662	2.33209	3.14861	4.20243	5.54778
0.7	1.46884	2.01116	2.72044	3.63743	4.80999
0.75	1.23113	1.68911	2.28924	3.06654	4.0622
0.8	0.99283	1.36516	1.85413	2.4888	3.30338
0.85	0.75491	1.04075	1.41717	1.90705	2.53742
0.9	0.51691	0.71532	0.97769	1.32053	1.76345
0.95	0.27868	0.38879	0.53571	0.72942	0.98188
0.98	0.13554	0.19223	0.26921	0.37245	0.50924
0.99	0.08778	0.12659	0.18015	0.25308	0.35108
0.999	0.04478	0.06747	0.09991	0.14547	0.20847

Table A.24: CSOMO predicted NRTL model parameters for the Activity Coefficients in $(\mathrm{MDEA} + \mathrm{H_2O})$ system

Temp	A	τ_{12}	τ_{21}
303.15 K	0.3	-1.32142	3.72388
308.15 K	0.3	-1.27171	3.7425
313.15 K	0.3	-1.23465	3.80453
318.15 K	0.3	-1.1965	3.85466
323.15 K	0.3	-1.16784	3.92548

Table A.25: COSMO predicted WILSON model parameters for the Activity Coefficients in $(\mathrm{MDEA} + \mathrm{H_2O})$ system

Temp	λ_{12}	λ_{21}
303.15 K	0.11826	1.56059
308.15 K	0.15989	1.28401
313.15 K	0.19834	1.09633
318.15 K	0.07709	1.48283
323.15 K	0.15093	1.02845

Table A.26: COSMO predicted UNIQUAC model parameters for the Activity Coefficients in $(\mathrm{MDEA} + \mathrm{H_2O})$ system

Temp	q_1	q_2	r_1	r_2	τ_{12}	τ_{21}
303.15 K	3.539	1.11077	4.72974	0.72993	1.20857	0.87555
308.15 K	4.25766	0.95434	5.69604	0.62714	0.35366	1.51617
313.15 K	4.31293	0.87679	5.77078	0.97618	0.35796	1.23699
318.15 K	4.29049	0.8689	5.74148	0.57099	0.35669	1.18234
323.15 K	4.26803	0.89288	5.7121	0.58675	0.36252	1.212

Table A.27: COSMO predicted Activity Coefficient of MDEA at infinite dilution in water

303.15 K	**308.15 K**	**313.15 K**	**318.15 K**	**323.15 K**
3.28789	3.4031	3.51007	3.60879	3.69923

Table A.28: COSMO predicted Excess Enthalpy in (AMP + H_2O) system in the temperature range of 303.15 – 323.15 K

AMP Mole fraction	303.15 K	308.15 K	313.15 K	318.15 K	323.15 K
1E-5	-0.00388	-0.00377	-0.00365	-0.00354	-0.00343
1E-3	-0.02236	-0.02175	-0.02106	-0.02029	-0.01945
0.01	-0.18453	-0.17961	-0.17391	-0.16744	-0.16024
0.02	-0.35401	-0.34472	-0.33389	-0.32156	-0.3078
0.05	-0.81087	-0.79047	-0.76646	-0.73892	-0.70803
0.1	-1.44444	-1.41034	-1.36968	-1.32261	-1.26946
0.15	-1.95205	-1.90856	-1.85607	-1.79478	-1.72515
0.2	-2.34986	-2.30022	-2.23958	-2.16819	-2.08659
0.25	-2.65577	-2.60259	-2.5368	-2.45867	-2.36882
0.3	-2.87718	-2.82261	-2.75415	-2.67209	-2.57712
0.35	-3.02251	-2.96831	-2.89927	-2.81569	-2.71828
0.4	-3.09485	-3.04266	-2.97498	-2.89209	-2.79474
0.45	-3.10812	-3.05902	-2.99404	-2.91346	-2.81803
0.5	-3.06384	-3.0188	-2.95778	-2.88102	-2.78926
0.55	-2.96628	-2.9261	-2.87008	-2.79844	-2.71189
0.6	-2.80808	-2.77346	-2.7235	-2.65837	-2.57873
0.65	-2.6046	-2.57609	-2.53298	-2.47538	-2.4039
0.7	-2.36356	-2.34125	-2.30533	-2.25585	-2.19335
0.75	-2.07786	-2.06175	-2.03336	-1.99267	-1.94011
0.8	-1.73357	-1.72385	-1.70363	-1.67279	-1.63162
0.85	-1.36069	-1.35632	-1.34351	-1.32208	-1.29216
0.9	-0.94283	-0.94259	-0.93642	-0.92406	-0.90553
0.95	-0.48852	-0.49013	-0.48866	-0.4839	-0.47578
0.98	-0.1991	-0.20022	-0.20011	-0.19866	-0.1958
0.99	-0.09998	-0.10063	-0.10067	-0.10003	-0.09868
0.999	-0.01015	-0.01022	-0.01023	-0.01017	-0.01003

Table A.29: COSMO predicted Excess Gibbs free energy in ($AMP + H_2O$) system in the temperature range of 303.15 – 323.15 K

AMP Mole fraction	303.15 K	308.15 K	313.15 K	318.15 K	323.15 K
1E-5	3.936E-5	4.348E-5	4.747E-5	5.138E-5	5.515E-5
1E-3	0.00488	0.00525	0.00562	0.00598	0.00633
0.01	0.04599	0.04962	0.05316	0.05661	0.05995
0.02	0.08601	0.09299	0.0998	0.10643	0.11286
0.05	0.17631	0.19203	0.20738	0.22232	0.23679
0.1	0.25666	0.28377	0.31026	0.33603	0.361
0.15	0.2838	0.31943	0.35426	0.38816	0.42102
0.2	0.28094	0.32292	0.36396	0.40393	0.44267
0.25	0.26043	0.30696	0.35248	0.39682	0.43982
0.3	0.23016	0.27974	0.32827	0.37556	0.42144
0.35	0.19489	0.24622	0.2965	0.34552	0.39309
0.4	0.15877	0.21071	0.2616	0.31125	0.35946
0.45	0.12185	0.17341	0.22396	0.27331	0.32125
0.5	0.08649	0.13677	0.18611	0.2343	0.28114
0.55	0.05373	0.10191	0.14924	0.19551	0.2405
0.6	0.02961	0.07541	0.12043	0.16447	0.20731
0.65	0.00709	0.04936	0.09094	0.13164	0.17127
0.7	-0.01485	0.02321	0.0607	0.09743	0.13323
0.75	-0.02984	0.00343	0.03625	0.06844	0.09983
0.8	-0.03442	-0.00643	0.02119	0.04829	0.07473
0.85	-0.03663	-0.01462	0.00713	0.0285	0.04937
0.9	-0.03169	-0.01635	-0.00116	0.01378	0.02838
0.95	-0.01982	-0.0118	-0.00383	0.00402	0.01171
0.98	-0.00891	-0.0056	-0.00231	9.3093E-4	0.00411
0.99	-0.0046	-0.00293	-0.00127	3.7308E-4	0.00198
0.999	-5.1825E-4	-3.5215E-4	-1.8685E-4	-2.345E-5	1.3698E-4

Table A.30: COSMO predicted AMP ln(activity coefficient) in (AMP + H_2O) system in the temperature range of 303.15 – 323.15 K

AMP Mole fraction	303.15 K	308.15 K	313.15 K	318.15 K	323.15 K
1E-5	1.96863	2.08553	2.19512	2.29733	2.39214
1E-3	1.94252	2.05855	2.16731	2.26877	2.36289
0.01	1.71784	1.82683	1.92905	2.02446	2.11301
0.02	1.49516	1.59782	1.69418	1.78416	1.86773
0.05	0.9779	1.06655	1.14992	1.22791	1.30049
0.1	0.46326	0.53558	0.60374	0.66767	0.72733
0.15	0.1902	0.24991	0.3063	0.35929	0.40884
0.2	0.04292	0.09221	0.13882	0.1827	0.22379
0.25	-0.03665	0.00397	0.04243	0.0787	0.1127
0.3	-0.0774	-0.04407	-0.01246	0.01738	0.0454
0.35	-0.09562	-0.06842	-0.04257	-0.01814	0.00483
0.4	-0.10006	-0.07803	-0.05707	-0.03723	-0.01856
0.45	-0.09723	-0.07952	-0.06264	-0.04664	-0.03155
0.5	-0.08994	-0.07586	-0.0624	-0.04963	-0.03757
0.55	-0.08019	-0.06915	-0.05858	-0.04853	-0.03902
0.6	-0.06812	-0.05952	-0.05127	-0.0434	-0.03594
0.65	-0.05555	-0.04912	-0.04293	-0.03702	-0.03139
0.7	-0.04474	-0.04009	-0.0356	-0.03129	-0.02718
0.75	-0.0335	-0.03031	-0.02722	-0.02424	-0.02139
0.8	-0.02139	-0.01936	-0.0174	-0.01551	-0.0137
0.85	-0.01196	-0.01081	-0.00971	-0.00865	-0.00763
0.9	-0.00445	-0.00395	-0.00347	-0.00302	-0.0026
0.95	-4.848E-5	8.775E-5	2.042E-4	3.0315E-4	3.8689E-4
0.98	6.2232E-4	6.5638E-4	6.7877E-4	6.9071E-4	6.936E-4
0.99	4.3815E-4	4.5244E-4	4.6011E-4	4.618E-4	4.583E-4
0.999	3.786E-5	3.833E-5	3.818E-5	3.746E-5	3.626E-5

Table A.31: COSMO predicted AMP Chemical Potential in $(AMP + H_2O)$ system in the temperature range of 303.15 – 323.15 K

AMP Mole Fraction	303.15 K	308.15 K	313.15 K	318.15 K	323.15 K
1E-5	-36.83005	-36.68711	-36.56839	-36.47407	-36.40425
1E-3	-25.28845	-24.9574	-24.65049	-24.36788	-24.10968
0.01	-20.05108	-19.65168	-19.2757	-18.92326	-18.59444
0.02	-18.86525	-18.46249	-18.08251	-17.72538	-17.39112
0.05	-17.8595	-17.47604	-17.11388	-16.77299	-16.45329
0.1	-17.40956	-17.06055	-16.73122	-16.42141	-16.13091
0.15	-17.07584	-16.75361	-16.44996	-16.1646	-15.89723
0.2	-16.72194	-16.4206	-16.13699	-15.87075	-15.62148
0.25	-16.36006	-16.07496	-15.80696	-15.55559	-15.32041
0.3	-16.00324	-15.73092	-15.47518	-15.2355	-15.01137
0.35	-15.66063	-15.39834	-15.15222	-14.9217	-14.7062
0.4	-15.33524	-15.08086	-14.84231	-14.61898	-14.41026
0.45	-15.03124	-14.7829	-14.55014	-14.33229	-14.12871
0.5	-14.74731	-14.50357	-14.27521	-14.06151	-13.86181
0.55	-14.4825	-14.24219	-14.0171	-13.80648	-13.60962
0.6	-14.23275	-13.99459	-13.77152	-13.56276	-13.36756
0.65	-13.99933	-13.76287	-13.5414	-13.33413	-13.14029
0.7	-13.78528	-13.54985	-13.32935	-13.12294	-12.92985
0.75	-13.58306	-13.34805	-13.12791	-12.92181	-12.72893
0.8	-13.38987	-13.15464	-12.9343	-12.72799	-12.53487
0.85	-13.21329	-12.97741	-12.75643	-12.54946	-12.35567
0.9	-13.05029	-12.81337	-12.59136	-12.38338	-12.18857
0.95	-12.90293	-12.66451	-12.44103	-12.23157	-12.03529
0.98	-12.82287	-12.5834	-12.35884	-12.14831	-11.95093
0.99	-12.79775	-12.55791	-12.33298	-12.12206	-11.92428
0.999	-12.77595	-12.53578	-12.31051	-12.09924	-11.9011

Table A.32: COSMO predicted Total Pressure in $(AMP + H_2O)$ system in the temperature range of 303.15 – 323.15 K

AMP Mole fraction	303.15 K	308.15 K	313.15 K	318.15 K	323.15 K
1E-5	4.25527	5.63888	7.39637	9.60792	12.3662
1E-3	4.25444	5.63866	7.39736	9.61099	12.37261
0.01	4.24471	5.63188	7.39717	9.62285	12.40429
0.02	4.23208	5.61931	7.38644	9.61672	12.40675
0.05	4.19854	5.5812	7.34468	9.57295	12.36354
0.1	4.15159	5.52672	7.28252	9.50319	12.28644
0.15	4.08229	5.44462	7.18666	9.39277	12.16088
0.2	3.97414	5.3129	7.02818	9.20423	11.93887
0.25	3.8265	5.12954	6.80297	8.93044	11.60912
0.3	3.64487	4.90092	6.51828	8.57939	11.18014
0.35	3.43648	4.63584	6.18462	8.16349	10.66636
0.4	3.20952	4.3446	5.81479	7.69843	10.08681
0.45	2.96798	4.03203	5.41459	7.19107	9.44949
0.5	2.71815	3.70632	4.99445	6.65453	8.77071
0.55	2.46434	3.37304	4.56153	6.09789	8.06181
0.6	2.21724	3.04725	4.13664	5.54941	7.36059
0.65	1.96712	2.71438	3.69854	4.97882	6.62482
0.7	1.71889	2.38166	3.25761	4.40077	5.87473
0.75	1.47882	2.0577	2.82545	3.83058	5.13031
0.8	1.25126	1.74852	2.41024	3.27917	4.40579
0.85	1.0333	1.44987	2.00589	2.73799	3.68953
0.9	0.83152	1.17093	1.62493	2.2238	3.00339
0.95	0.64945	0.91674	1.27436	1.74604	2.35988
0.98	0.55175	0.77917	1.08293	1.48282	2.00217
0.99	0.52136	0.73617	1.02282	1.39975	1.88872
0.999	0.49497	0.69877	0.9704	1.32716	1.78932

Table A.33: COSMO predicted NRTL model parameters for the Activity Coefficients in $(AMP + H_2O)$ system

Temp	A	τ_{12}	τ_{21}
303.15 K	0.3	-1.2794	4.12394
308.15 K	0.3	-1.37074	4.11347
313.15 K	0.3	-1.31629	4.10685
318.15 K	0.3	-1.2636	4.09878
323.15 K	0.3	-1.21334	4.09127

Table A.34: COSMO predicted WILSON model parameters for the Activity Coefficients in $(AMP + H_2O)$ system

Temp	λ_{12}	λ_{21}
303.15 K	0.09608	1.57421
308.15 K	0.22733	1.09003
313.15 K	0.19557	1.07961
318.15 K	0.16471	1.0794
323.15 K	0.14307	1.04684

Table A.35: COSMO predicted UNIQUAC model parameters for the Activity Coefficients in $(AMP + H_2O)$ system

Temp	q_1	q_2	r_1	r_2	τ_{12}	τ_{21}
303.15 K	4.15611	1.78288	5.35466	1.17161	1.00793	1.59159
308.15 K	4.38032	1.90117	5.64316	1.24934	1.1091	1.48476
313.15 K	4.4602	1.9196	5.74571	1.26145	1.13101	1.431
318.15 K	4.49039	1.9064	5.78428	1.25277	1.13356	1.38824
323.15 K	4.39574	1.82144	5.66206	1.19694	1.07759	1.37813

Table A.36: COSMO predicted Activity Coefficient of AMP at infinite dilution in water

303.15 K	**308.15 K**	**313.15 K**	**318.15 K**	**323.15 K**
1.9163	2.03892	2.15406	2.26161	2.36152

Table A.37: COSMO predicted Excess Enthalpy in (EAE + H_2O) system in the temperature range of 303.15 – 323.15 K

EAE Mole fraction	303.15 K	308.15 K	313.15 K	318.15 K	323.15 K
1E-5	-0.00211	-0.00208	-0.00205	-0.00202	-0.00199
1E-3	-0.01273	-0.0124	-0.01204	-0.01163	-0.01117
0.01	-0.10481	-0.102	-0.09882	-0.09523	-0.09119
0.02	-0.19881	-0.19366	-0.18781	-0.18117	-0.17368
0.05	-0.44818	-0.43781	-0.42593	-0.41232	-0.39681
0.1	-0.78278	-0.76771	-0.7502	-0.72984	-0.70627
0.15	-1.04148	-1.02469	-1.00492	-0.98159	-0.95415
0.2	-1.2332	-1.21634	-1.1963	-1.17232	-1.14368
0.25	-1.37027	-1.35432	-1.33522	-1.31206	-1.28397
0.3	-1.45885	-1.44424	-1.42671	-1.40523	-1.37881
0.35	-1.50302	-1.48997	-1.4744	-1.45518	-1.43123
0.4	-1.50994	-1.49851	-1.48506	-1.46841	-1.44738
0.45	-1.4859	-1.47603	-1.46471	-1.45071	-1.43281
0.5	-1.43267	-1.4243	-1.41507	-1.40374	-1.38907
0.55	-1.35379	-1.34678	-1.33949	-1.33072	-1.31924
0.6	-1.25429	-1.24842	-1.24278	-1.23624	-1.2276
0.65	-1.13759	-1.1328	-1.12871	-1.12428	-1.11836
0.7	-1.00469	-1.00083	-0.99806	-0.99543	-0.9919
0.75	-0.86613	-0.86358	-0.8623	-0.8615	-0.86024
0.8	-0.70905	-0.70719	-0.70674	-0.70703	-0.70728
0.85	-0.53998	-0.5385	-0.53838	-0.53912	-0.54012
0.9	-0.3658	-0.36484	-0.36502	-0.36599	-0.36734
0.95	-0.18506	-0.18458	-0.18478	-0.18551	-0.18655
0.98	-0.07448	-0.07428	-0.07439	-0.07474	-0.07526
0.99	-0.03729	-0.03719	-0.03725	-0.03744	-0.03771
0.999	-0.00374	-0.00373	-0.00373	-0.00375	-0.00378

Table A.38: COSMO predicted Excess Gibbs free energy in ($EAE + H_2O$) system in the temperature range of 303.15 – 323.15 K

EAE Mole fraction	**303.15 K**	**308.15 K**	**313.15 K**	**318.15 K**	**323.15 K**
1E-5	7.527E-5	7.87E-5	8.205E-5	8.533E-5	8.852E-5
1E-3	0.00835	0.00866	0.00896	0.00925	0.00954
0.01	0.07894	0.08186	0.08473	0.08754	0.09029
0.02	0.14835	0.15392	0.15938	0.16474	0.16998
0.05	0.31101	0.32324	0.33525	0.34703	0.35856
0.1	0.4772	0.4976	0.51766	0.53736	0.55664
0.15	0.56329	0.58934	0.61498	0.64017	0.66486
0.2	0.60216	0.63213	0.66164	0.69066	0.71911
0.25	0.61074	0.6432	0.67518	0.70664	0.73752
0.3	0.60005	0.63388	0.66723	0.70003	0.73224
0.35	0.57656	0.61095	0.64484	0.6782	0.71095
0.4	0.54426	0.57846	0.61217	0.64533	0.67791
0.45	0.50589	0.53923	0.57208	0.60439	0.63613
0.5	0.46358	0.49554	0.52702	0.55798	0.5884
0.55	0.41884	0.44901	0.47871	0.50792	0.5366
0.6	0.37272	0.40063	0.42811	0.45515	0.48172
0.65	0.32507	0.35037	0.37527	0.39975	0.42381
0.7	0.27708	0.29948	0.32152	0.34318	0.36445
0.75	0.22905	0.24803	0.26668	0.28501	0.30299
0.8	0.18151	0.19705	0.2123	0.22728	0.24197
0.85	0.13496	0.14691	0.15864	0.17016	0.18148
0.9	0.08891	0.09702	0.10498	0.11278	0.12045
0.95	0.04384	0.04797	0.05202	0.05598	0.05987
0.98	0.01741	0.01907	0.0207	0.02229	0.02385
0.99	0.00869	0.00952	0.01034	0.01114	0.01192
0.999	8.6732E-4	9.508E-4	0.00103	0.00111	0.00119

Table A.39: COSMO predicted EAE ln(activity coefficient) in (EAE + H_2O) system in the temperature range of 303.15 – 323.15 K

EAE Mole fraction	303.15 K	308.15 K	313.15 K	318.15 K	323.15K
1E-5	3.30563	3.37342	3.43687	3.49597	3.55071
1E-3	3.26308	3.33019	3.39302	3.45157	3.5058
0.01	2.90277	2.96469	3.02279	3.07704	3.12743
0.02	2.55536	2.61292	2.66703	2.71769	2.76486
0.05	1.77117	1.81974	1.86566	1.90894	1.94952
0.1	1.00745	1.04591	1.08254	1.11732	1.15023
0.15	0.5939	0.62468	0.65412	0.68222	0.70897
0.2	0.3566	0.38118	0.40475	0.42732	0.44889
0.25	0.21475	0.23431	0.25308	0.27108	0.28833
0.3	0.12818	0.14361	0.15841	0.17261	0.18622
0.35	0.07497	0.08709	0.0987	0.10982	0.12048
0.4	0.04213	0.0516	0.06063	0.06927	0.07753
0.45	0.0219	0.02924	0.0362	0.04283	0.04914
0.5	0.00994	0.0156	0.02093	0.02596	0.03073
0.55	0.00333	0.0077	0.01178	0.01558	0.01916
0.6	-9.823E-5	0.00324	0.00632	0.00915	0.01178
0.65	-0.00158	9.5785E-4	0.00325	0.00533	0.00722
0.7	-0.00178	1.5319E-4	0.00186	0.00338	0.00472
0.75	-0.00142	-3.928E-5	0.00115	0.00217	0.00303
0.8	-6.4357E-4	3.5327E-4	0.00118	0.00186	0.0024
0.85	2.7899E-4	9.8458E-4	0.00156	0.00202	0.00236
0.9	7.6968E-4	0.00122	0.00157	0.00184	0.00202
0.95	7.3487E-4	9.591E-4	0.00113	0.00126	0.00133
0.98	4.064E-4	4.9397E-4	5.6024E-4	6.0577E-4	6.3156E-4
0.99	2.2401E-4	2.6811E-4	3.0136E-4	3.2402E-4	3.3656E-4
0.999	2.44E-5	2.88E-5	3.21E-5	3.432E-5	3.551E-5

Table A.40: COSMO predicted EAE Chemical Potential in ($EAE + H_2O$) system in the temperature range of 303.15 – 323.15 K

EAE Mole fraction	303.15 K	308.15 K	313.15 K	318.15 K	323.15 K
1E-5	-37.85256	-37.70613	-37.58434	-37.48748	-37.41579
1E-3	-26.35242	-26.01805	-25.70822	-25.42322	-25.16329
0.01	-21.45689	-21.05507	-20.67703	-20.32305	-19.9933
0.02	-20.58544	-20.18045	-19.7986	-19.4401	-19.10512
0.05	-20.25248	-19.86502	-19.49937	-19.15563	-18.83387
0.1	-20.43037	-20.07173	-19.73364	-19.41611	-19.11907
0.15	-20.45075	-20.11212	-19.7934	-19.49449	-19.21523
0.2	-20.32376	-19.99892	-19.69365	-19.40777	-19.14107
0.25	-20.11885	-19.8035	-19.50756	-19.2308	-18.97293
0.3	-19.87752	-19.56877	-19.27935	-19.00901	-18.7574
0.35	-19.62309	-19.31862	-19.03346	-18.76733	-18.51986
0.4	-19.3693	-19.06743	-18.7849	-18.52138	-18.2765
0.45	-19.1234	-18.82294	-18.54184	-18.27976	-18.03631
0.5	-18.88801	-18.58796	-18.30729	-18.04567	-17.80269
0.55	-18.66443	-18.364	-18.08296	-17.821	-17.57771
0.6	-18.45375	-18.15249	-17.87063	-17.60785	-17.36374
0.65	-18.25574	-17.95327	-17.6702	-17.40622	-17.16093
0.7	-18.06945	-17.76546	-17.48087	-17.21536	-16.96855
0.75	-17.89465	-17.58919	-17.30309	-17.03606	-16.78772
0.8	-17.73002	-17.42283	-17.13497	-16.86614	-16.61599
0.85	-17.57489	-17.26589	-16.97614	-16.70537	-16.45322
0.9	-17.42959	-17.11885	-16.82729	-16.55465	-16.30056
0.95	-17.2934	-16.98098	-16.68766	-16.41317	-16.15714
0.98	-17.21586	-16.90252	-16.6082	-16.33265	-16.07549
0.99	-17.19073	-16.87709	-16.58244	-16.30654	-16.04901
0.999	-17.16842	-16.85451	-16.55958	-16.28336	-16.0255

Table A.41: COSMO predicted Total Pressure ($EAE + H_2O$) system in the temperature range of 303.15 – 323.15 K

EAE Mole fraction	303.15 K	308.15 K	313.15 K	318.15 K	323.15 K
1E-5	4.25535	5.639	7.39656	9.6082	12.36661
1E-3	4.26171	5.65007	7.41486	9.63726	12.4112
0.01	4.29546	5.71022	7.51575	9.79887	12.66061
0.02	4.30639	5.73175	7.55383	9.86178	12.75952
0.05	4.31115	5.74153	7.5709	9.88904	12.8006
0.1	4.33552	5.77478	7.61461	9.94448	12.86848
0.15	4.34535	5.79256	7.64322	9.98733	12.92944
0.2	4.31191	5.75582	7.60418	9.94746	12.89074
0.25	4.2281	5.65339	7.48062	9.80019	12.71716
0.3	4.09814	5.49008	7.27769	9.55066	12.41323
0.35	3.92802	5.27327	7.00438	9.2096	11.99162
0.4	3.7248	5.0116	6.67107	8.78932	11.46665
0.45	3.4954	4.71383	6.2887	8.30327	10.85467
0.5	3.24541	4.38728	5.86673	7.76355	10.17096
0.55	2.97989	4.03857	5.41373	7.18109	9.42927
0.6	2.70395	3.67441	4.93841	6.56711	8.64401
0.65	2.41904	3.2968	4.44339	5.9249	7.81899
0.7	2.12895	2.91093	3.93571	5.26389	6.96682
0.75	1.8365	2.5203	3.41965	4.58916	6.09336
0.8	1.54311	2.12775	2.90013	3.90873	5.21095
0.85	1.25103	1.73609	2.38069	3.22694	4.32487
0.9	0.96189	1.34758	1.86429	2.54758	3.43979
0.95	0.67767	0.96513	1.3552	1.87677	2.56433
0.98	0.51031	0.73976	1.05493	1.4807	2.04683
0.99	0.45514	0.66544	0.95589	1.35002	1.876
0.999	0.40577	0.59894	0.86725	1.23304	1.72306

Table A.42: COSMO predicted NRTL model parameters for the Activity Coefficients in $(EAE + H_2O)$ system

Temp	A	τ_{12}	τ_{21}
303.15 K	0.3	-0.97912	4.56439
308.15 K	0.3	-0.95219	4.59131
313.15 K	0.3	-0.92352	4.6041
318.15 K	0.3	-0.89703	4.62171
323.15 K	0.3	-0.87191	4.6395

Table A.43: COSMO predicted WILSON model parameters for the Activity Coefficients in $(EAE + H_2O)$ system

Temp	λ_{12}	λ_{21}
303.15 K	0.01402	1.95206
308.15 K	0.03241	1.11856
313.15 K	0.03038	1.10955
318.15 K	0.02837	1.09918
323.15 K	0.02739	1.08788

Table A.44: COSMO predicted UNIQUAC model parameters for the Activity Coefficients in $(EAE + H_2O)$ system

Temp	q_1	q_2	r_1	r_2	τ_{12}	τ_{21}
303.15 K	5.29206	1.43181	6.40967	0.94091	0.89129	0.91058
308.15 K	5.31132	1.44919	6.43491	0.95232	0.088632	0.91729
313.15 K	5.33515	1.48158	6.46571	0.97361	0.90992	0.90859
318.15 K	5.25906	1.44399	6.37537	0.9489	0.86853	0.90806
323.15 K	5.2619	1.42968	6.38067	0.9395	0.81794	0.93597

Table A.45: COSMO predicted activity coefficient of EAE at infinite dilution in water

303.1 5K	308.15 K	313.15 K	318.15 K	323.15 K
3.3259	3.39504	3.45989	3.52068	3.57686

Table A.46: COSMO predicted Excess Enthalpy in (MAE + H_2O) system in the temperature range of 303.15 – 323.15 K

MAE Mole fraction	303.15 K	308.15 K	313.15 K	318.15 K	323.15 K
1E-5	-8.8369E-4	-8.5126E-4	-8.1892E-4	-7.8652E-4	-7.5418E-4
1E-3	-0.01278	-0.01261	-0.01239	-0.01214	-0.01183
0.01	-0.11651	-0.11519	-0.1135	-0.11137	-0.10875
0.02	-0.22365	-0.22133	-0.2183	-0.21444	-0.20961
0.05	-0.5058	-0.50182	-0.49627	-0.48883	-0.47919
0.1	-0.88175	-0.87792	-0.8715	-0.86183	-0.84831
0.15	-1.16473	-1.16309	-1.15825	-1.14925	-1.13518
0.2	-1.37314	-1.37478	-1.37297	-1.36641	-1.35394
0.25	-1.51858	-1.52403	-1.52602	-1.52298	-1.51349
0.3	-1.61013	-1.61952	-1.62565	-1.62673	-1.62108
0.35	-1.65801	-1.67126	-1.68159	-1.68699	-1.6856
0.4	-1.66355	-1.68032	-1.69464	-1.70436	-1.70742
0.45	-1.6345	-1.65435	-1.67232	-1.68611	-1.69353
0.5	-1.57553	-1.59793	-1.61902	-1.63646	-1.64794
0.55	-1.49066	-1.51496	-1.53854	-1.55904	-1.5741
0.6	-1.38331	-1.40878	-1.43411	-1.45693	-1.47492
0.65	-1.25785	-1.28362	-1.30974	-1.33395	-1.35398
0.7	-1.11389	-1.13915	-1.16518	-1.18988	-1.21108
0.75	-0.95516	-0.97894	-1.00383	-1.02789	-1.04915
0.8	-0.78361	-0.8049	-0.82746	-0.84965	-0.86973
0.85	-0.60097	-0.61867	-0.63767	-0.65662	-0.67412
0.9	-0.40876	-0.42174	-0.43583	-0.45008	-0.46347
0.95	-0.20848	-0.21558	-0.22336	-0.23132	-0.23892
0.98	-0.08437	-0.08736	-0.09066	-0.09405	-0.09732
0.99	-0.04236	-0.04388	-0.04556	-0.04729	-0.04897
0.999	-0.00425	-0.00441	-0.00458	-0.00475	-0.00493

Table A.47: COSMO predicted Excess Gibbs free energy in (MAE + H_2O) system in the temperature range of 303.15 – 323.15 K

MAE Mole fraction	303.15 K	308.15 K	313.15 K	318.15 K	323.15 K
1E-5	4.645E-5	4.942E-5	5.234E-5	5.525E-5	5.809E-5
1E-3	0.00516	0.00543	0.00571	0.00597	0.00624
0.01	0.04901	0.05165	0.05427	0.05685	0.0594
0.02	0.09255	0.09761	0.10263	0.10759	0.11248
0.05	0.1958	0.20707	0.21824	0.2293	0.24022
0.1	0.30076	0.31971	0.33855	0.35726	0.37576
0.15	0.35315	0.37755	0.40186	0.42603	0.44999
0.2	0.3732	0.40138	0.42951	0.45751	0.48531
0.25	0.37287	0.40353	0.43417	0.46473	0.49512
0.3	0.35951	0.39159	0.4237	0.45577	0.48772
0.35	0.33787	0.37039	0.40299	0.43561	0.46818
0.4	0.31107	0.34339	0.37585	0.40838	0.44091
0.45	0.28119	0.31271	0.34441	0.37623	0.40809
0.5	0.24974	0.27994	0.31034	0.34092	0.37158
0.55	0.2178	0.24622	0.27488	0.30374	0.33274
0.6	0.18616	0.21242	0.23893	0.26568	0.2926
0.65	0.15521	0.17897	0.203	0.22728	0.25178
0.7	0.12595	0.14692	0.16816	0.18966	0.21139
0.75	0.09851	0.11643	0.13462	0.15307	0.17174
0.8	0.07324	0.0879	0.1028	0.11795	0.13331
0.85	0.05046	0.06167	0.07308	0.0847	0.09652
0.9	0.03047	0.03806	0.04581	0.05371	0.06177
0.95	0.01343	0.01727	0.0212	0.02521	0.02931
0.98	0.00495	0.00649	0.00807	0.00968	0.01134
0.99	0.0024	0.00317	0.00396	0.00477	0.0056
0.999	2.3398E-4	3.1107E-4	3.9E-4	4.7088E-4	5.5344E-4

Table A.48: COSMO predicted MAE ln(activity coefficient) in (MAE + H_2O) system in the temperature range of 303.15 – 323.15 K

MAE Mole fraction	303.15 K	308.15 K	313.15 K	318.15 K	323.15 K
1E-5	2.03707	2.11246	2.15967	2.25284	2.31767
1E-3	2.01362	2.08835	1.94707	2.22753	2.29183
0.01	1.81133	1.88072	1.73614	2.01031	2.07035
0.02	1.60974	1.67429	1.23933	1.79521	1.8514
0.05	1.13361	1.18747	0.72353	1.28914	1.33678
0.1	0.6414	0.6831	0.42992	0.76264	0.80035
0.15	0.36532	0.39802	0.25582	0.46098	0.49112
0.2	0.20503	0.23067	0.14987	0.28045	0.3045
0.25	0.11016	0.13016	0.08453	0.16929	0.18838
0.3	0.05372	0.06919	0.04411	0.09973	0.11476
0.35	0.02045	0.03229	0.01943	0.05589	0.06761
0.4	0.00147	0.01044	0.00482	0.02845	0.0375
0.45	-0.00862	-0.00193	-0.00328	0.01164	0.01852
0.5	-0.01316	-0.00826	-0.00716	0.00179	0.00694
0.55	-0.01425	-0.01074	-0.00831	-0.00347	3.0888E-4
0.6	-0.01327	-0.01083	-0.00789	-0.00571	-0.00302
0.65	-0.01123	-0.00959	-0.00635	-0.00612	-0.00427
0.7	-0.00848	-0.00744	-0.00436	-0.00521	-0.00401
0.75	-0.00561	-0.00499	-0.00232	-0.00369	-0.00297
0.8	-0.00296	-0.00265	-5.735E-4	-0.00198	-0.00161
0.85	-8.3289E-4	-7.0076E-4	5.8046E-4	-4.4461E-4	-3.0889E-4
0.9	5.3421E-4	5.6303E-4	8.0695E-4	5.904E-4	5.9631E-4
0.95	8.42E-4	8.2958E-4	4.749E-4	7.7574E-4	7.3753E-4
0.98	5.0317E-4	4.9164E-4	2.6413E-4	4.5352E-4	4.279E-4
0.99	2.8092E-4	2.7393E-4	2.89E-5	2.5181E-4	2.37E-4
0.999	3.087E-5	3.003E-5	2.608E-5	2.75E-5	2.577E-5

Table A.49: COSMO predicted MAE Chemical Potential in $(MAE + H_2O)$ system in the temperature range of 303.15 – 323.15 K

MAE Mole fraction	303.15 K	308.15 K	313.15 K	318.15 K	323.15 K
1E-5	-38.2053	-38.10395	-38.02533	-37.96963	-37.93698
1E-3	-26.657	-26.36689	-26.09944	-25.85484	-25.63322
0.01	-21.36317	-20.99943	-20.65784	-20.33857	-20.04169
0.02	-20.12421	-19.75241	-19.40232	-19.07403	-18.76762
0.05	-19.01478	-18.65208	-18.31012	-17.98891	-17.68842
0.1	-18.50829	-18.16841	-17.84837	-17.54807	-17.26735
0.15	-18.1822	-17.85998	-17.55715	-17.27349	-17.00877
0.2	-17.86109	-17.55168	-17.26143	-16.99006	-16.73725
0.25	-17.53777	-17.23748	-16.95628	-16.69382	-16.4497
0.3	-17.22049	-16.92655	-16.6517	-16.39555	-16.15764
0.35	-16.91583	-16.62614	-16.3556	-16.10376	-15.87015
0.4	-16.62709	-16.34003	-16.07218	-15.82311	-15.59228
0.45	-16.35564	-16.06994	-15.80356	-15.55602	-15.3268
0.5	-16.10152	-15.81621	-15.55032	-15.30338	-15.07483
0.55	-15.86405	-15.57838	-15.31225	-15.06517	-14.83658
0.6	-15.64225	-15.35566	-15.08871	-14.84093	-14.61173
0.65	-15.43538	-15.14743	-14.87922	-14.63028	-14.40004
0.7	-15.24164	-14.95203	-14.68226	-14.43185	-14.20024
0.75	-15.0605	-14.76901	-14.49743	-14.24531	-14.01207
0.8	-14.89117	-14.59764	-14.32409	-14.07007	-13.83501
0.85	-14.733	-14.43733	-14.16169	-13.90565	-13.66863
0.9	-14.58548	-14.28765	-14.00987	-13.75171	-13.51262
0.95	-14.44843	-14.14844	-13.86851	-13.6082	-13.36697
0.98	-14.37092	-14.06965	-13.78842	-13.52681	-13.28427
0.99	-14.34589	-14.0442	-13.76254	-13.50049	-13.25751
0.999	-14.32371	-14.02163	-13.73959	-13.47715	-13.23376

Table A.50: COSMO predicted Total Pressure in $(MAE + H_2O)$ system in the temperature range of 303.15 – 323.15 K

MAE Mole fraction	303.15 K	308.15 K	313.15 K	318.15 K	323.15 K
1E-5	4.25533	5.63897	7.3965	9.60811	12.36647
1E-3	4.25964	5.64657	7.40914	9.6282	12.39723
0.01	4.28751	5.69682	7.49365	9.76329	12.60477
0.02	4.30246	5.72577	7.54415	9.84571	12.7329
0.05	4.30835	5.74594	7.58693	9.92237	12.85829
0.1	4.28643	5.72575	7.57117	9.91459	12.86294
0.15	4.243	5.67704	7.51788	9.85781	12.80411
0.2	4.16899	5.58924	7.41529	9.73964	12.66978
0.25	4.06245	5.45913	7.2584	9.5526	12.44911
0.3	3.92633	5.28991	7.05041	9.29963	12.14432
0.35	3.7657	5.08734	6.79776	8.98767	11.76265
0.4	3.58562	4.85835	6.50966	8.62873	11.3194
0.45	3.39088	4.60872	6.19299	8.23088	10.82397
0.5	3.18565	4.34382	5.85461	7.80276	10.28706
0.55	2.97344	4.06827	5.50049	7.35198	9.71826
0.6	2.75718	3.78599	5.13577	6.88519	9.12605
0.65	2.53923	3.50013	4.76465	6.40788	8.51752
0.7	2.32203	3.21408	4.39169	5.92612	7.90059
0.75	2.10728	2.93022	4.02014	5.44425	7.28095
0.8	1.89676	2.65098	3.65337	4.9668	6.66463
0.85	1.6921	2.37872	3.2946	4.49818	6.0575
0.9	1.49494	2.11574	2.94706	4.04276	5.46541
0.95	1.30681	1.86423	2.6138	3.60476	4.89405
0.98	1.19901	1.7199	2.42222	3.35242	4.56407
0.99	1.16399	1.67298	2.35988	3.27025	4.45648
0.999	1.13287	1.63129	2.30448	3.19717	4.36075

Table A.51: COSMO predicted NRTL model parameters for the Activity Coefficients in $(MAE + H_2O)$ system

Temp	A	τ_{12}	τ_{21}
303.15 K	0.3	-1.2266	3.75088
308.15 K	0.3	-1.19698	3.7676
313.15 K	0.3	-1.1792	3.78371
318.15 K	0.3	-1.3981	3.80121
323.15 K	0.3	-1.11038	3.80891

Table A.52: COSMO predicted WILSON model parameters for the Activity Coefficients in $(MAE + H_2O)$ system

Temp	λ_{12}	λ_{21}
303.15 K	0.22026	1.05118
308.15 K	0.0313	2.32767
313.15 K	0.07961	1.45416
318.15 K	0.15297	1.03381
323.15 K	0.1552	0.99812

Table A.53: COSMO predicted UNIQUAC model parameters for the Activity Coefficients in $(MAE + H_2O)$ system

Temp	q_1	q_2	r_1	r_2	τ_{12}	τ_{21}
303.15 K	5.39484	2.05442	6.34185	1.35005	1.04531	1.24098
308.15 K	5.32084	2.02005	6.25656	1.32756	1.00362	1.263036
313.15 K	5.34557	2.00627	6.28733	1.31841	1.0095	1.23177
318.15 K	5.29686	1.875	6.23169	1.23214	1.02513	1.13809
323.15 K	5.34015	1.97407	6.28424	1.29725	1.00921	1.18964

Table A.54: COSMO predicted Activity Coefficient of MAE at infinite dilution in water

303.15 K	**308.15 K**	**313.15 K**	**318.15 K**	**323.15 K**
1.27555	2.03993	2.11784	2.19223	2.26301

Table A.55: COSMO predicted Excess Enthalpy in ($CO_2 + EAE + H_2O$) system in the temperature range 303.15 – 323.15 K at 0.05 EAE mole fractions.

Liquid Mole Fraction of CO_2	**303.15 k**	**313.15 k**	**323.15 k**
0.9	0.52204	0.55572	0.58436
0.85	0.657	0.7272	0.79551
0.8	0.76664	0.86272	0.95916
0.75	0.85133	0.96649	1.08375
0.7	0.91171	1.04108	1.17397
0.65	0.94995	1.08964	1.23401
0.6	0.96858	1.11529	1.2676
0.55	0.96591	1.11674	1.27397
0.5	0.94382	1.09612	1.25543
0.45	0.90261	1.05385	1.21259
0.4	0.84228	0.99003	1.14563
0.35	0.76256	0.90441	1.05434
0.3	0.6629	0.79639	0.93809
0.25	0.54238	0.66498	0.79581
0.2	0.39965	0.50869	0.62587
0.15	0.23278	0.32537	0.42593
0.1	0.039	0.11196	0.19261
0.05	-0.1858	-0.13609	-0.07906

Table A.56: COSMO predicted Excess Gibbs free energy in ($CO_2 + EAE + H_2O$) system in the temperature range 303.15 – 323.15 K at 0.05 EAE mole fractions.

Liquid Mole Fraction of CO_2	**303.15 k**	**313.15 k**	**323.15k**
0.9	0.35423	0.3477	0.34001
0.85	0.67227	0.67113	0.66761
0.8	0.94102	0.94475	0.94522
0.75	1.16806	1.17617	1.18039

0.7	1.35751	1.36966	1.37745
0.65	1.51243	1.52827	1.53941
0.6	1.63489	1.65407	1.6683
0.55	1.72491	1.7471	1.76419
0.5	1.78324	1.80807	1.82775
0.45	1.80968	1.83676	1.85873
0.4	1.80357	1.8325	1.85643
0.35	1.76379	1.79413	1.81967
0.3	1.6887	1.72	1.74675
0.25	1.57612	1.60785	1.6354
0.2	1.42315	1.45476	1.48262
0.15	1.226	1.25687	1.28453
0.1	0.97973	1.00918	1.03605
0.05	0.67776	0.70502	0.73046

Table A.57: COSMO predicted EAE $\ln(\text{activity coefficient})$ in $(CO_2 + EAE + H_2O)$ system in the temperature range 303.15 – 323.15 K at 0.05 EAE mole fractions.

Liquid Mole Fraction of CO_2	**303.15k**	**313.15k**	**323.15k**
0.9	-0.94657	2.80779	-0.95667
0.85	-1.32521	2.428	-1.30084
0.8	-1.57433	2.13179	-1.52609
0.75	-1.74374	1.88703	-1.67811
0.7	-1.85714	1.67586	-1.77815
0.65	-1.92531	1.48927	-1.8359
0.6	-1.95334	1.32156	-1.85584
0.55	-1.94649	1.16791	-1.84242
0.5	-1.90433	1.02597	-1.79507
0.45	-1.82587	0.89374	-1.71262
0.4	-1.70855	0.76982	-1.59238
0.35	-1.54813	0.65323	-1.43006

0.3	-1.33844	0.54333	-1.21948
0.25	-1.07087	0.43982	-0.95208
0.2	-0.73353	0.34271	-0.61607
0.15	-0.30993	0.25243	-0.19515
0.1	0.2232	0.16994	0.33367
0.05	0.89975	0.097	1.00377

Table A.58: COSMO predicted Excess Enthalpy in (CO_2 + EAE + H_2O) system in the temperature range 303.15 – 323.15 K at 0.1 EAE mole fractions.

Liquid Mole Fraction of CO_2	**303.15 k**	**313.15 k**	**323.15 k**
0.85	0.5442	0.56498	0.573
0.8	0.57121	0.62179	0.66505
0.75	0.59534	0.66941	0.73992
0.7	0.61043	0.70268	0.79423
0.65	0.61467	0.7207	0.8283
0.6	0.60535	0.72154	0.84115
0.55	0.58222	0.70539	0.83353
0.5	0.54573	0.67301	0.80653
0.45	0.49328	0.6221	0.75826
0.4	0.42547	0.55336	0.68952
0.35	0.34174	0.46634	0.59997
0.3	0.24142	0.36039	0.48902
0.25	0.12557	0.23657	0.35771
0.2	-0.01087	0.08976	0.20095
0.15	-0.16743	-0.07964	0.01901
0.1	-0.34613	-0.27382	-0.19042
0.05	-0.54984	-0.49584	-0.4306

Table A.59: COSMO predicted Excess Gibbs free energy in ($CO_2 + EAE + H_2O$) system in the temperature range 303.15 – 323.15 K at 0.1 EAE mole fractions.

Liquid Mole Fraction of CO_2	**303.15 k**	**313.15 k**	**323.15k**
0.85	0.24624	0.23577	0.2246
0.8	0.51757	0.51446	0.50951
0.75	0.75155	0.75492	0.75565
0.7	0.95116	0.96029	0.96615
0.65	1.1193	1.13367	1.14429
0.6	1.25675	1.27579	1.29073
0.55	1.36484	1.38808	1.40699
0.5	1.44452	1.47156	1.49409
0.45	1.49488	1.52528	1.55112
0.4	1.51614	1.54949	1.5783
0.35	1.50767	1.54355	1.57499
0.3	1.4685	1.50649	1.54021
0.25	1.39782	1.4375	1.47315
0.2	1.29275	1.33363	1.37082
0.15	1.15157	1.19315	1.23146
0.1	0.97131	1.01308	1.05207
0.05	0.74821	0.78961	0.82883

Table A.60: COSMO predicted EAE $\ln(\text{activity coefficient})$ in ($CO_2 + EAE + H_2O$) system in the temperature range 303.15 – 323.15 K at 0.1 EAE mole fractions.

Liquid Mole Fraction of CO_2	**303.15k**	**313.15k**	**323.15k**
0.85	-0.69509	2.3718	-0.70726
0.8	-0.9635	2.11771	-0.95625
0.75	-1.15575	1.89689	-1.132
0.7	-1.29281	1.7023	-1.25532
0.65	-1.38472	1.52817	-1.33591

0.6	-1.43979	1.3697	-1.38157
0.55	-1.4609	1.22397	-1.39493
0.5	-1.44909	1.08915	-1.37689
0.45	-1.40648	0.96259	-1.32913
0.4	-1.33137	0.84354	-1.24998
0.35	-1.22182	0.73104	-1.1374
0.3	-1.07468	0.62441	-0.9882
0.25	-0.8845	0.52344	-0.79702
0.2	-0.64703	0.42736	-0.55942
0.15	-0.35284	0.33642	-0.26619
0.1	0.00945	0.25084	0.09391
0.05	0.45554	0.17116	0.53632

Table A.61: COSMO predicted Gas phase mole fraction of CO_2 in ($CO_2 + EAE + H_2O$) system in the temperature range 303.15 – 323.15 K at 0.05 EAE mole fractions.

Liquid Mole Fraction of CO_2	**303.15k**	**313.15k**	**323.15k**
0.9	0.99948	0.9993	0.99909
0.85	0.99929	0.99904	0.99874
0.8	0.99921	0.99892	0.99856
0.75	0.99918	0.99887	0.99848
0.7	0.99917	0.99885	0.99845
0.65	0.99918	0.99885	0.99844
0.6	0.9992	0.99887	0.99846
0.55	0.99922	0.9989	0.99849
0.5	0.99925	0.99894	0.99853
0.45	0.99928	0.99898	0.99858
0.4	0.99932	0.99902	0.99864
0.35	0.99935	0.99907	0.99869
0.3	0.99939	0.99911	0.99875
0.25	0.99942	0.99915	0.99879

0.2	0.99944	0.99918	0.99883
0.15	0.99945	0.99919	0.99883
0.1	0.99942	0.99913	0.99874
0.05	0.99923	0.99884	0.99829

Table A.62: COSMO predicted Gas phase mole fraction of CO_2 in (CO_2 + EAE + H_2O) system in the temperature range 303.15 – 323.15 K at 0.1 EAE mole fractions.

Liquid Mole Fraction of CO_2	**303.15k**	**313.15k**	**323.15k**
0.85	0.99965	0.99951	0.99933
0.8	0.99945	0.99923	0.99897
0.75	0.99934	0.99907	0.99875
0.7	0.99927	0.99898	0.99861
0.65	0.99923	0.99892	0.99852
0.6	0.99921	0.99889	0.99847
0.55	0.9992	0.99887	0.99844
0.5	0.9992	0.99887	0.99843
0.45	0.99921	0.99887	0.99843
0.4	0.99921	0.99887	0.99843
0.35	0.99922	0.99888	0.99843
0.3	0.99923	0.99888	0.99842
0.25	0.99923	0.99887	0.9984
0.2	0.99921	0.99884	0.99835
0.15	0.99916	0.99876	0.99823
0.1	0.99903	0.99856	0.99791
0.05	0.99855	0.99783	0.99683